The University of Southern Mississippi
The Aquila Digital Community

Dissertations

Spring 5-2012

Genetic Variation in Potentially Virulent *Vibrio parahaemolyticus* From the Northern Gulf of Mexico

Nicholas Felix Noriea III
University of Southern Mississippi

Follow this and additional works at: https://aquila.usm.edu/dissertations

 Part of the Aquaculture and Fisheries Commons, Biology Commons, Immunology and Infectious Disease Commons, Marine Biology Commons, and the Terrestrial and Aquatic Ecology Commons

Recommended Citation

Noriea, Nicholas Felix III, "Genetic Variation in Potentially Virulent *Vibrio parahaemolyticus* From the Northern Gulf of Mexico" (2012). *Dissertations*. 799.
https://aquila.usm.edu/dissertations/799

This Dissertation is brought to you for free and open access by The Aquila Digital Community. It has been accepted for inclusion in Dissertations by an authorized administrator of The Aquila Digital Community. For more information, please contact Joshua.Cromwell@usm.edu.

The University of Southern Mississippi

GENETIC VARIATION IN POTENTIALLY VIRULENT *VIBRIO PARAHAEMOLYTICUS* FROM THE NORTHERN GULF OF MEXICO

by

Nicholas Felix Noriea III

Abstract of a Dissertation
Submitted to the Graduate School
of The University of Southern Mississippi
in Partial Fulfillment of the Requirements
for the Degree of Doctor of Philosophy

May 2012

ABSTRACT

GENETIC VARIATION IN POTENTIALLY VIRULENT *VIBRIO PARAHAEMOLYTICUS* FROM THE NORTHERN GULF OF MEXICO

By Nicholas Felix Noriea III

May 2012

Vibrio parahaemolyticus (Vp) is a gram-negative bacterium found naturally in marine and estuarine environments. *Vp* is found in oysters including those which are later consumed by the public. Sub-populations of potentially virulent *Vp* contain specific virulence factors and are relevant human pathogens capable of causing gastroenteritis, wound infection, and death. The *tdh* and *trh* genes, both encoding hemolysins, have been correlated with the majority of clinical *Vp* isolates but have not been shown to be the definitive virulence factors.

A total of 146 *Vp* isolates from the northern Gulf of Mexico were collected and probed for the presence of specific virulence factors such as *tdh, trh,* Type III secretion System (T3SS) 1, T3SS2α, T3SS2β, and *toxRS*. The most representative sub-group of potentially pathogenic *Vp* were tdh^+/trh^+. Isolates containing only *tdh* were uncommon, and tdh^-/trh^+ isolates were extremely rare.

The distribution of virulence factors in environmental *Vp* strains was compared with strain fitness through *Vp* human intestinal epithelial cell cytotoxicity assays and oyster *(Crassostrea virginica)* hemocyte bactericidal challenges. The assays were performed to determine significant differences in cytotoxicity or bactericidal survival between pathogen subgroups (tdh^+/trh^-, tdh^-/trh^+, and tdh^-/trh^+).

Significant changes in *Vp* gene expression were measured for representative clinical strains of the diametric virulence factor sub-groups tdh^{+}/trh^{-} and tdh^{-}/trh^{+}. Transcriptomic changes were measured during exposure to human intestinal epithelial cells and oyster hemocyte. Relative changes in the *Vp* transcriptome were compared both over time and between strain to give significantly regulated genes involved in cytotoxicity and oyster hemocyte bactericidal avoidance.

COPYRIGHT BY

NICHOLAS FELIX NORIEA III

2012

The University of Southern Mississippi

GENETIC VARIATION IN POTENTIALLY VIRULENT *VIBRIO PARAHAEMOLYTICUS* FROM THE NORTHERN GULF OF MEXICO

by

Nicholas Felix Noriea III

A Dissertation
Submitted to the Graduate School
of The University of Southern Mississippi
in Partial Fulfillment of the Requirements
for the Degree of Doctor of Philosophy

Approved:

_Darrell J. Grimes_____
Director

_Crystal N. Johnson_____

_Robert J. Griffitt_____

_Mohamed O. Elasri_____

_Kevin S. Dillon_____

_Susan A. Siltanen_____
Dean of the Graduate School

May 2012

ACKNOWLEDGMENTS

The author would like to thank the committee chair, Jay Grimes for providing all of the many opportunities and support to explore and conduct this project. The author would also like to thank each of the committee members, Dr. Kevin Dillon, Dr. Mohamed Elasri, Dr. Joe Griffitt, and Dr. Crystal Johnson (LSU) for their support, guidance, and assistance throughout the project. Particularly, the author would like to thank Dr. Joe Griffitt for assistance in microarray analysis and Dr. Crystal Johnson for training and access to a large collection of *Vp* isolates.

Special thanks go to Drs. Lou and Karen Burnett (NOAA) for hemocyte extraction training, Dr. Wes Burkhardt (Medical Gentics) for use of cell culturing equipment, Dr. Walt Conley (SUNY-Potsdam) for guidance, and Dr.Andy DePaola (FDA) for guidance and clinical isolates. Finally, the author would like to thank Idrissa Boube, Kim Griffitt, and Dawn Rebarchik for assistance and support throughout the project.

TABLE OF CONTENTS

LIST OF TABLES

Table

LIST OF ILLUSTRATIONS

Figure

CHAPTER I

INTRODUCTION

Vibrio parahaemolyticus (*Vp*) is a gram-negative, facultatively anaerobic motile rod-shaped bacterium. *Vp* was originally described in 1954 (*1*) after it was isolated as the causative agent of "summer diarrhea" in Japan. Due to its halophilic nature, *Vp* is ubiquitous in marine and coastal environments (*2, 3*). A characteristic member of the *Gammaproteobacteria*, *Vp* is both ecologically and medically important (*4-6*), affecting local and regional human populations including those in the northern Gulf of Mexico.

Vp is present in both the sediment and the water column (*7*) with cell densities showing significant correlation to temperature and, to a lesser extent, salinity (Johnson et al *in prep*)(*7*). Aquatic organisms can also act as a biological reservoir for these bacteria. *Vp* can accumulate in filter-feeding molluscs, including oysters in densities of over 100 times that in surrounding waters (*8*); *Vp* is also found in the hemolymph of blue crabs (*9, 10*), in shrimp homogenate (*11*), and on copepods (*4, 12*).

Vp densities may be in high enough to cause illness in humans when oysters and other seafood are eaten raw or under-cooked. The FDA estimates the infective dose to be $1x10^6$ colony forming units (cfu) (*13*).Virulent *Vp* can cause gastroenteritis, wound infections, and septicemia (*14-17*). Although the first recorded evidence of *Vp*-induced disease was in 1954, outbreaks out *Vp* are reported worldwide today (*18-21*), especially in countries where large amounts of seafood are consumed. It has been estimated that there are as many as 4,500 cases of *Vp* infections per year in the US, with 30 hospitalizations and 1-2 deaths (*22*). Although outbreaks of disease-causing *Vp* are not rare, potentially virulent *Vp* represent a minor subpopulation (<10%) of the overall *Vibrio* community in most aquatic environments (*7, 23-25*).

In 1969, clinical *Vp* isolates were tested on a newly developed specialized blood agar called Wagatsuma agar (*3*). Japanese scientists observed that some *Vp* strains exhibited hemolysis on Wagatsuma agar. The occurrence of this β –hemolysis was coined the "Kanagawa phenomenon" (KP) and was correlated with clinical strains (*3*). Specifically, *Vp* isolates from 128 dysentery patients and 308 patients with food-poisoning were plated onto Wagatsuma agar where β –hemolysis was observed in 95.3% and 88.3% of strains, respectively (*3*). In 1980, KP was shown to be caused by a novel hemolysin, Thermostable Direct Hemolysin (TDH), encoded by the *tdh* gene (*26*). In 1988, a second hemolysin was identified in a tdh^- KP^- clinical strain. The second hemolysin had extremely similar immunological characteristics to TDH, except that it was heat labile unlike TDH; it was named the TDH-related hemolysin (TRH) (*27*). Like TDH, TRH contains two subunits and the amino acid sequences encoding both hemolysins shares roughly 67% homology.

In multiple studies over several years, 90% of 784 clinical *Vp* isolates were found to contain either *tdh, trh,* or both (*3, 28, 29*), while similar studies found less than 1% of environmental isolates carried either gene (*3, 30*). A recent study done in coastal Mississippi found that between 4-5% of total environmental isolates carried either *tdh* or *trh* (*31*). The presence of both *tdh* and *trh* production has been correlated with human pathogenic *Vp*; therefore strains containing *tdh* and/or *trh* are considered 'potentially pathogenic'. Each hemolysin has been associated with pathogenicity in varying degrees. One study of 214 clinical strains showed that 52.3% were tdh^+/trh^- , while 24.3% were tdh^-/trh^+ (*29*). Another study in Calcutta, India observed that 90% of isolates taken from clinical patients were tdh^+/trh^- compared to just 0.8% for tdh^-/trh^+ strains (*32*). A study in Thailand found 76% of 317 clinical specimens to be tdh^+/trh^- (*33*).

It should be noted that *tdh* and *trh* are not present in all clinical strains (*34*) and therefore do not fully account for *Vp* pathogenicity or virulence (*35*). Studies of a *tdh*-deleted *Vp* strain revealed that even without TDH production, effects of cytotoxicity and enterotoxicity were still observed, although in reduced amounts (*36, 37*). As mentioned earlier, roughly 10% of 784 clinical isolates from several studies did not contain either the *tdh* or the *trh* gene. In 1990, an experiment was performed which examined the virulence of both tdh^+ and tdh^- *Vp* isolates in mice (*38*). The calculated LD_{50} was found to be 10^7 and 10^8 for each isolate, respectively. These findings led the researchers to conclude that although tdh^+ isolates were found predominantly in human clinical cases, lethality between *tdh* and *trh* in mice remained equal. Therefore, other factors must be responsible for the overall enteropathogenic affects of *Vp*.

Vp has several distinct pandemic serotypes. *Vp* is typed by the presence of O antigen (the lipid moiety outer membrane lipopolysaccharide) and K antigen. Prior to 1996, isolates from international clinical cases displayed a wide range of these antigens. Due to the varied nature of these serogroups, no true *Vp* pandemic serotype was identified. In a study of 86 clinical *Vp* isolates obtained in Japan and Thailand between 1962 and 1999, it was shown that before 1996 there was no predominant clinical strain of (*39*). One exception was observed in a study of clinical isolates originating in the United States from 1979 to 1987. In this study the majority of infections (71%) were shown to be urease positive. Of the urease positive isolates, 59% were associated with a single serovar, O4:K12 (*40*). All O4:K12 isolates in this study were urease positive. This was the first major report of a pandemic-like *Vp* serovar with an associated atypical virulence factor, urease.

A study in Calcutta, India monitored hospitalized patients for a period of several years, and in February of 1996 a rapid and distinct change to the antigenic pattern in clinical strains of *Vp* was seen (*32*). A single predominant serovar, O3:K6 (*32, 39*), was observed in ~65% of all cases in 1996 but not in the initial two years of observation. This O3:K6 strain was different from previously isolated O3:K6 strains as it contained *tdh* but not *trh* (*41*), and thus was termed the 'new' O3:K6. Interestingly, the new O3:K6 serovar had not been isolated previously to February of 1996, leading scientists to conclude that this O3:K6 serovar was a unique novel clone (*32*). During a high-incidence period in 1996 (from February to August), the new O3:K6 serovar comprised ~75% of all isolated strains (*42*).

The new O3:K6, the major pandemic *Vp* serovar since 1996, has prompted a tremendous amount of research into classifying both the pandemic strain and closely related strains (*21, 41-44*). Several closely related serotypes- O1:K25, O1:K26, O1:KUT and O4:K68, were discovered to also have pandemic potential and may have originated from the new O3:K6 clone (*41, 43-47*). All of the identified potentially-pandemic serotypes contained *tdh* but not the *trh* gene. A method was developed to test the pandemic-specific group of *Vp* in 2000, when it was discovered that the *toxRS* operon sequence in pandemic-causing strains had a slightly differing nucleotide sequence than non-pandemic strains (*41*). The proteins encoded by *toxRS* are trans-membrane proteins that are well documented regulators in the *Vibrio* genus (*48-50*). Investigators took advantage of the sequence divergence and developed a PCR method entitled Group-Specific PCR (GS-PCR) which only amplified pandemic-group *Vp toxRS* sequences.

Pathogenicity in *Vp* has been strongly correlated with *tdh* and *trh* but has not been shown as the sole cause of pathogenicity. Virulence factors whose presence is associated

with these two hemolysins may also contribute to the pathogenicity and virulence of *Vp*. In 2003, the sequencing of *Vp* O3:K6 strain RIMD 2210633 revealed a new virulence factor: the type III secretion system (T3SS) (*23*). The T3SS is a needle-like protein complex found on the surface of some gram-negative bacteria. The rod-shaped needle can form pores in the membrane of eukaryotic cells and inject specific proteins known as effectors into the cytosol or environment in response to certain cellular signals or environmental conditions (*51, 52*). The genes encoding the T3SS are typically found clustered together and are commonly found within mobile genetic elements such as pathogenicity islands (*52, 53*).

The RIMD2210633 genome revealed not one but two distinct T3SSs: T3SS1 and T3SS2, located in genetic clusters on chromosomes 1 and 2, respectively. Both T3SSs are genetically non-redundant and T3SS1 is associated with cytotoxicity while T3SS2 is correlated with enterotoxicity (*54*). The T3SS1 in *Vp* was found to be genetically related to the plasmid-encoded T3SS of *Yersinia pestis*, while T3SS2 has been related to the T3SS system found in *Shigella* spp. T3SS1 was found to be ubiquitous in *Vp* while T3SS2 was found only in KP^+ isolates (*34, 55*). The association of KP^+ isolates with T3SS2 was elucidated when the genes encoding T3SS2 were found residing on an 80kbp pathogenicity island (*23, 56*). This pathogenicity island also contained two copies of *tdh*, effectively flanking the T3SS (*23, 55, 57*).

In 2009, a third T3SS variant was discovered in a tdh^-/trh^+ strain (*58*) located on chromosome 2 in the location of T3SS2 in KP^+ strains. A study of environmental isolates from the northern Gulf of Mexico revealed that the new T3SS variant was found in 5/5 tdh^-/trh^+ isolates and 0/153 non- tdh^-/trh^+ isolates (*59*). After discovery of this new T3SS variant on chromosome 2, the original T3SS2 identified in 2003 was renamed T3SS2α.

The new T3SS variant was named T3SS2β. Thus T3SS2α has been associated with *tdh*$^{+}$/*trh*$^{-}$ strains while T3SS2β has been associated with *tdh*$^{-}$/*trh*$^{+}$ strains. Only a minor amount of research has been done concerning the toxicity of T3SS2β due to its recent discovery.

Little is known about the T3SS functions in regards to the ability of *Vp* to enter and survive inside oyster tissue. Several T3SS genes and their products have been characterized in *Vp* since 2003 (*60-63*), including most structural genes. Many effector genes and their products have been of particular interest to researchers seeking to understand T3SS-induced toxicity (*37, 60-65*). Conversely, there is very little information regarding which products of T3SS genes are expressed during invasion of *Vp* in oyster tissue and hemolymph.

The distribution of virulence factors in *Vp* isolated from environmental sources remains unclear. It has been shown that the fitness of Vibrios in the environment is the result of a combination of genetic factors (*66, 67*). Therefore, the presence and production of virulence factors such as the T3SS may confer some change in a strain's ability to colonize different environmental compartments such as the water column, biofilms, in sediment, and the exterior and interior of animals such as filter-feeding oysters.

Vp is widely detectable in oysters harvested from marine and estuarine environments. Studies in the northern Gulf of Mexico have shown that *Vp* is detectable in oyster meat during both warm and cool seasons (*7*). Although potentially pathogenic *Vp* is found at detectable levels in oyster meat, tissue necrosis is not a concern. Conversely, potentially pathogenic *Vp* causes both cytotoxicity and enterotoxicity in humans.

Although a large amount of research has focused on characterization of virulence factors in clinical *Vp*, little research has focused on naturally-occurring potentially

pathogenic *Vp* and their function in the environment. For instance, it is unknown whether the cytotoxicity of potentially pathogenic *Vp* varies significantly between strains carrying *tdh* or *trh*. It is also unknown how well the presence of T3SS2 variants α and β correlates with the presence of hemolysins. More research is needed to understand these rare, naturally-occurring bacteria in ecologically-relevant situations such as the colonization of oysters. The ability to understand how naturally-occurring, potentially pathogenic *Vp* function in the environment is paramount for developing more effective public health plans and seafood treatment methods.

The purpose of this study was to examine collections pathogenic and potentially virulent *Vp* from environmental sources through the accomplishment of several goals.

- First, the distribution of the virulence factorT3SS was examined in a large pool of environmental potentially pathogenic *Vp*. The distribution of virulence factors such as *tdh, trh,* TSSS1, T3SS2α, T3SS2β, and *toxRS* was correlated to help better explain their respective role in environmental *Vp* functions.
- The correlation of virulence factors and *Vp* strain fitness was accomplished through *Vp* human intestinal epithelial cell cytotoxicity assays and oyster *(Crassostrea virginica)* hemocyte bactericidal assays. These assays were performed and significant differences in cytotoxicity or bactericidal survival between virulence factor subgroups (tdh^+/trh^-, tdh^-/trh^+, tdh^-/trh^+) was examined.
- Significant changes in *Vp* gene expression was measured for representative clinical strains of the diametric virulence factor sub-groups tdh^+/trh^- and tdh^-/trh^+. Transcriptomic changes were measured during exposure to human intestinal epithelial cells and oyster hemocyte. The relative changes in the *Vp*

transcriptome were compared both over time and between strain to give significantly regulated genes involved in cytotoxicity and oyster hemocyte bactericidal avoidance.

CHAPTER II

DISTRIBUTION OF TYPE III SECRETION GENES IN *V. PARAHAEMOLYTICUS* FROM THE NORTHERN GULF OF MEXICO

One hundred and thirty potentially pathogenic environmental *Vp* were selected from roughly four thousand cultured environmental *Vp* strains. Three separate environmental sources (water, sediment, and oyster meat) from the northern Gulf of Mexico were used for sampling purposes. The 130 isolates comprised roughly 3-5% of total colonies screened from environmental samples (*7*) and were considered potentially pathogenic due to the presence of one or both of the hemolysin genes *tdh* and *trh*. Both *tdh* and *trh* were putatively identified in a preliminary colony hybridization screening process. All isolates were screened for the virulence factors *tdh, trh*, T3SS1, T3SS2α, and T3SS2β. All isolates were also examined for a group specific *toxRS* genetic sequence found in pandemic-causing strains as previously described (GS-PCR)(*18, 41*).

Materials and Methods

Sample Collection. Samples were collected in two separate sampling periods with the first sampling period occurring from October 2006 to August 2007 at sampling sites MS2, MS5, MS6, and MS8. A second sampling period occurred from February to May of 2009 at sites MS2 and MS8. No sampling occurred in 2008 and sampling was limited to two sites in 2009 for logistical purposes. Water, oyster, and sediment samples were collected from the sites in the Mississippi Sound (MS) at the following coordinates: MS2 (30^{o}17.4' N, 89^{o}17.3' W); MS5 (30^{o}37.6'N, 88^{o}83.2W); MS6 (30^{o}36.6' N, 88^{o}67.5'W); and MS8 (30^{o}38.0' N, 88^{o} 41.1' W)(Fig 1).

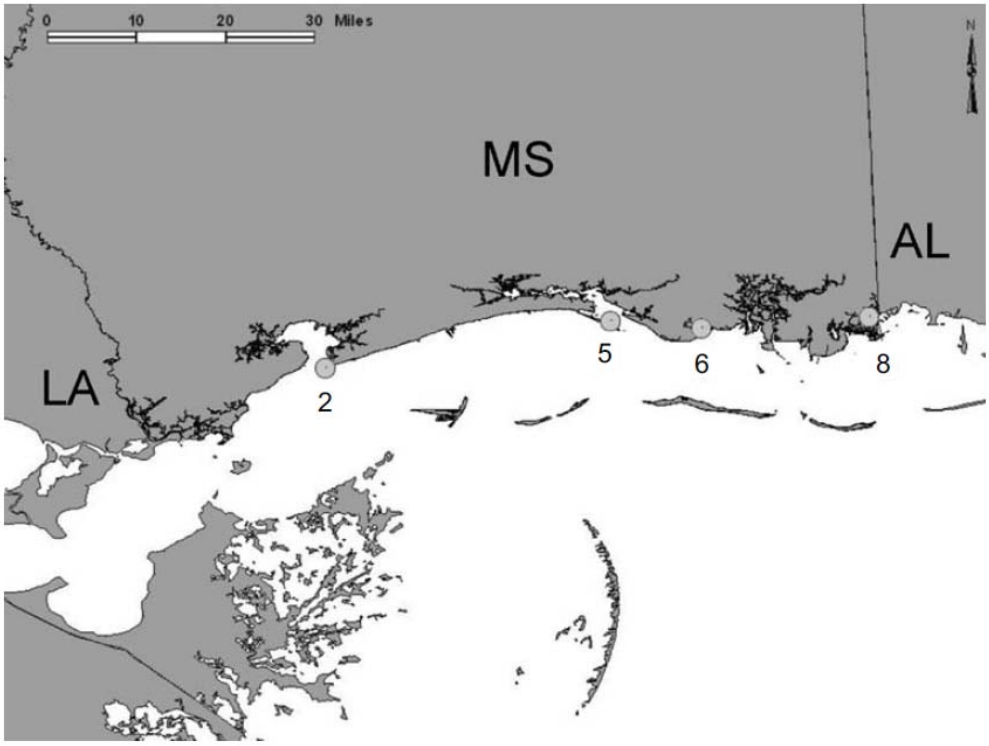

Figure 1. Locations of the four sampling sites along the Mississippi Gulf Coast. Sampling sites were designated MS-2, MS-5, MS-6, and MS-8.

Water (6- to 8- liter volumes) was collected in autoclaved plastic containers. Water conditions varied throughout the sampling period but demonstrated little inter-site variation. Specifically, the average temperature/salinity was 19.23^{o}C and 17.73ppt for site MS2, 22.6^{o}C and 22.5ppt for site MS5, 24.6^{o}C and 21.88ppt for MS6, and 20.6^{o}C and 18.1ppt for site MS8. Live oysters (8-15 each sampling trip), water, and sediment were collected as previously described (*7*). *Vp* densities were determined using a previously described direct plating/colony hybridization method (*68*), for detection of *tdh, trh*, and thermolabile hemolysin (*tlh)*.

Characterization of environmental isolates. The total collection of 130 "potentially pathogenic" *Vp* used in this study were collected over the course of two years comprising over 70 sampling trips and 210 independent enrichments. The *tlh*$^{+}$, *tdh*$^{+}$, *trh*$^{+}$, and *tdh*$^{+}$/*trh*$^{+}$ *Vp* isolates were confirmed as described previously (*7*) using a Direct Plating /

Colony Hybridization method (DPCH). In addition, *tlh*, *tdh*, and *trh* were confirmed using gene specific polymerase chain reaction (PCR) and agarose gel electrophoresis.

Genomic DNA was extracted from each isolate as described previously (*7, 69*) and confirmed isolates were stored at ambient room temperature (c.a. 23^{o}C) in soft T_1N_3 agar deeps (1% tryptone, 3% NaCl, pH 7.2, 0.7% agar). During the sampling period, 130 *tdh*$^{+}$ and/or *trh*$^{+}$ *Vp* isolates were collected for screening of additional virulence factors. Sixteen *tdh*$^{-}$/*trh*$^{-}$ isolates were chosen randomly to act as negative controls. Twelve clinical isolates were also included in the analysis and obtained from the U.S. FDA, Alaska Division of Public Health, American Type Culture Collection, or isolated locally (Table 1).

Table 1

Source of clinical isolates used in this study

Strain ID	**Origin**
BAA-238	ATCC
BAA-240	ATCC
AQ 4037	A. DePaola, FDA, Gulf Coast Seafood Lab –*tlh*$^{+}$/*tdh*$^{-}$/*trh*$^{+}$ control
FIHES 98	A. DePaola, FDA, Gulf Coast Seafood Lab –*tlh*$^{+}$/*tdh*$^{-}$/*trh*$^{-}$ control
Tx2103	A. DePaola, FDA, Gulf Coast Seafood Lab –*tlh*$^{+}$/*tdh*$^{+}$/*trh*$^{-}$ control
AK-PHL	T. Franklin, Alaska DPH; infection originated in New Orleans, LA
F11	A. DePaola, FDA, Gulf Coast Seafood Lab
CT6636	B. Tall, FDA – clinical isolate from Connecticut
KCHD 613	B. Tall, FDA – clinical isolate from Washington
Tall 901128	B. Tall, FDA – clinical isolate from Washington

Table 1 (continued).

Ny3547	B. Tall, FDA – clinical isolate from New York
Vp2007-095	Local clinical isolate

Most clinical isolates were not local and were included to represent a variety of *Vp* genotypes which have caused human illness. One clinical isolate, Vp2007-095, was the single local strain in our collection; it was acquired from a gastroenteritis patient (stool sample) who had eaten raw oysters.

Screening of environmental and clinical isolates. Three multiplex PCR screens were performed targeting T3SS1, T3SS2α, and T3SS2β. The T3SS1 multiplex screen targeted open reading frames (orfs) designated as VP1670 (*vscP*), VP1686 (*putative*), VP1689 (*vscK*), and VP1694 (*vscF*). The T3SS2α multiplex was designed to target orfs VPA1327 (*vopT*), VPA1335 (*vscS2*), VPA1339 (*vscC2*), and VPA1362 (*vopB2*). The T3SS2β multiplex targeted genes *vscS2*, *vscC2*, *vopC*, and *vopB2* specific for T3SS2β (*58*). A preliminary multiplex PCR was originally run against all 158 isolates and targeted VP1669 (*vscO*), VPA1346 (*vopJ*), VPA1354 (*vscU2*), and an internal control, VPA0226 (*tlh)*. VPA0226, encoding a thermolabile hemolysin, was chosen as an internal control due to its ubiquitous presence in *Vp*. Positive amplification of the internal control was confirmed in the preliminary multiplex before any of the 3 multiplexes were run

All multiplex PCR screenings were carried out using gene-specific primers (Appendix A). The primers used in this study targeting T3SS2β have been described previously (*58*). All other primers, with the exception of primers targeting the hemolysins and *toxRS*, are original and were designed by us using primer design software Primer3

(http://biotools.umassmed.edu/bioapps/primer3_www.cgi) and tested against self-dimerization and hairpins using the IDT OligoAnalyzer 3.1 software (http://www.idtdna.com/analyzer/Applications/OligoAnalyzer/). The primers were screened against the published sequences of chromosomes 1 and 2 of the sequenced strain RIMD 2210633 and the entire known genetic sequence for T3SS2β^+ strain TH3996 to ensure specificity and protect against cross reactivity. Primer sequences were then run through BLAST (http://blast.ncbi.nlm.nih.gov/Blast.cgi), using a modified BLASTN algorithm designed for oligonucleotide primers.

PCR cycling conditions for the *tdh, tlh,* and *trh* multiplex included an initial denaturation at 95^{o}C for 2 minutes, 33 cycles of denaturation at 95^{o}C for 45 seconds, annealing at 56^{o}C for 45 seconds, and extension at 72^{o}C for 40 seconds, and a final extension at 72^{o}C for 3 minutes. The amplification conditions for T3SS1 and T3SS2α multiplexes were set at one cycle of 95^{o}C for 5 minutes, followed by 33 cycles of amplification consisting of denaturation at 95^{o}C for 45 seconds, annealing at 60^{o}C for 40 seconds, and extension at 72^{o}C for 45 seconds, and terminated by one cycle of final extension at 72^{o}C for 3 minutes. For the T3SS2β multiplex PCR parameters were assigned as previously described (*58*). Group Specific PCR (GS-PCR), targeting a region of the *toxRS* specific to pandemic-causing groups, was performed as described previously (*41*).

After amplification, the products were resolved by gel electrophoresis using a 1.3% agarose gel run at 200 volts in sodium borate buffer (SBB) to resolve 100-600 bp amplicons. Primers were designed so that amplicon sizes were distinguishable for each multiplex set. Agarose gels were then stained using Sybr Gold (Invitrogen, Carlsbad, CA). After staining, gels were viewed in order to record presence or absence of amplicons. In the case of faint amplicon bands, PCR multiplex screens were rerun to confirm results. To

confirm amplification of the correct product, a monoplex PCR for each gene target was run with the appropriate positive control- strain Tx2103 for T3SS1 and T3SS2α genes and strain AQ4037 for T3SS2β genes. Amplicons from the monoplex were purified from agarose (Qiagen, Valencia, CA) and sent out for sequencing (McLab, San Francisco, CA).

Recognition and identification of vopB2 using fluorescence in situ hybridization. A technique known as Recognition of Individual Gene Flurescence *in-situ* Hybdridization (RING-FISH), originally documented in 2004 (*70*), was used to confirm the presence of virulence factors in specific *Vp* strains. *Vp* strains were grown overnight at 37^{o}C in 1mL of alkaline peptone water (APW) and fixed as described previously (*71*) on 4-well, 5-mm teflon printed slides (Electron Microscopy Sciences, Hatfield, PA). The *vopB2* primers used for the development of an RNA probe were identical to the T3SS2α *vopB2* primers used for the PCR screen with the exception that the forward primer contained an additional 21-bp segment encoding the binding site of the T3-RNA polymerase (Appendix A). Transcription and probing was performed as described previously (*70*) with the following changes. The *vopB2* RNA probe was fluorescently labeled via incorporation of CY3-dUTP (GE Healthcare) during transcription. Hybridization was carried out with an initial step of 80^{o}C for 20 minutes followed by 38^{o}C for 24 hours in humidity controlled chambers. After, hybridization slides were washed with deionized water and counter-stained with Fluoro Gel II with DAPI (Electron Microscopy Sciences, Hatfield, PA). Slides were then placed in storage at 4^{o}C. All slides were viewed with a Zeiss Axiostar Plus microscope (Carl Zeiss, Germany) using the appropriate filter set. *Vibrio parahaemolyticus* cells were examined in the appropriate slide well and counted. Under visualization, if no cells produced a Cy3 fluorescence the result was considered negative. Cells which were positive for RING-FISH generally resulted in cells that fluoresced

equally across the slide. Some cells on positive slides did not produce fluorescence; however these cells generally were in areas of debris which may have affected the ability for the probe to bind. Methodology and cell compatibility was first tested using the ubiquitous *Vp* gene *tlh* (K.J. Griffitt, unpublished data). Cell images were acquired using Zeiss AxioCam MR camera and AxioVision software v4.7.1.0 (Carl Zeiss).

Results

Vp isolates were screened for genes representative of T3SS1, T3SS2α, and T3SS2β (Tables 2 and 3).

Table 2

Distribution of virulence factors in environmental isolates (n=146)

	tdh$^+$/*trh*$^-$	*tdh*$^-$/*trh*$^+$	*tdh*$^+$/*trh*$^+$	*tdh*$^-$/*trh*$^-$
T3SS1	27/27	3/3	100/100	16/16
T3SS2α	27/27	0/3	0/100	0/16
T3SS2β	0/27	3/3	0/100	0/16
GS-PCR	0/27	0/3	0/100	0/16

Table 3

Distribution of virulence factors in clinical isolates (n=12)

	tdh$^+$/*trh*$^-$	*tdh*$^-$/*trh*$^+$	*tdh*$^+$/*trh*$^+$	*tdh*$^-$/*trh*$^-$
T3SS1	3/3	2/2	4/4	3/3
T3SS2α	3/3	0/2	0/4	0/3
T3SS2β	0/3	2/2	0/4	0/3

Table 3 (continued).

GS-PCR	0/3	0/2	0/4	0/3

A total of 158 strains were tested in this experiment, 146 environmental strains and 12 clinical strains. Among the 146 environmental isolates collected, 130 were considered potentially pathogenic (*tdh* and or *trh)* with 16 identified as non-pathogenic because they contained neither *tdh* nor *trh*. The 16 non-pathogenic isolates were selected at random as representative of the overall non-pathogenic *Vp* population. A total of 12 clinical isolates (three tdh^+/trh^-, two tdh^-/trh^+, four tdh^+/trh^+, and three tdh^-/trh^-) were also tested. In total, 100 (77%) of 130 potentially pathogenic *Vp* isolates were tdh^+/trh^+, 27 (21%) were tdh^+/trh^-, and 3 (2%) were tdh^-/trh^+. Of the 12 clinical isolates tested, 2 were tdh^-/trh^+, 4 were tdh^+/trh^+, 3 were tdh^+/trh^-, and 3 were tdh^-/trh^-. All 158 *Vp* isolates tested positive for all 5 T3SS1 genes selected.

Five genes associated with T3SS2α were used to screen the 158 isolates. Of the 146 environmental isolates, 27/27 tdh^+/trh^- isolates tested positive for 4 out of 5 T3SS2α genes, with all 27 testing negative for *vopB2*. All 3 $tdh^{+/}trh^-$ clinical isolates tested positive for all T3SS2α genes, including *vopB2*. No other isolate tested positive for any T3SS2α gene. The presence/absence of *vopB2* was confirmed using recognition of individual gene fluorescence *in situ* hybridization (RING-FISH) with specific gene probes as described previously (*70*). All 3 clinical tdh^+/trh^- strains exhibited the normal positive signal pattern after hybridization with a 250-bp VPA1362 RNA probe, while 27/27 environmental tdh^+/trh^- strains did not produce any positive signal after hybridization (Figure 2).

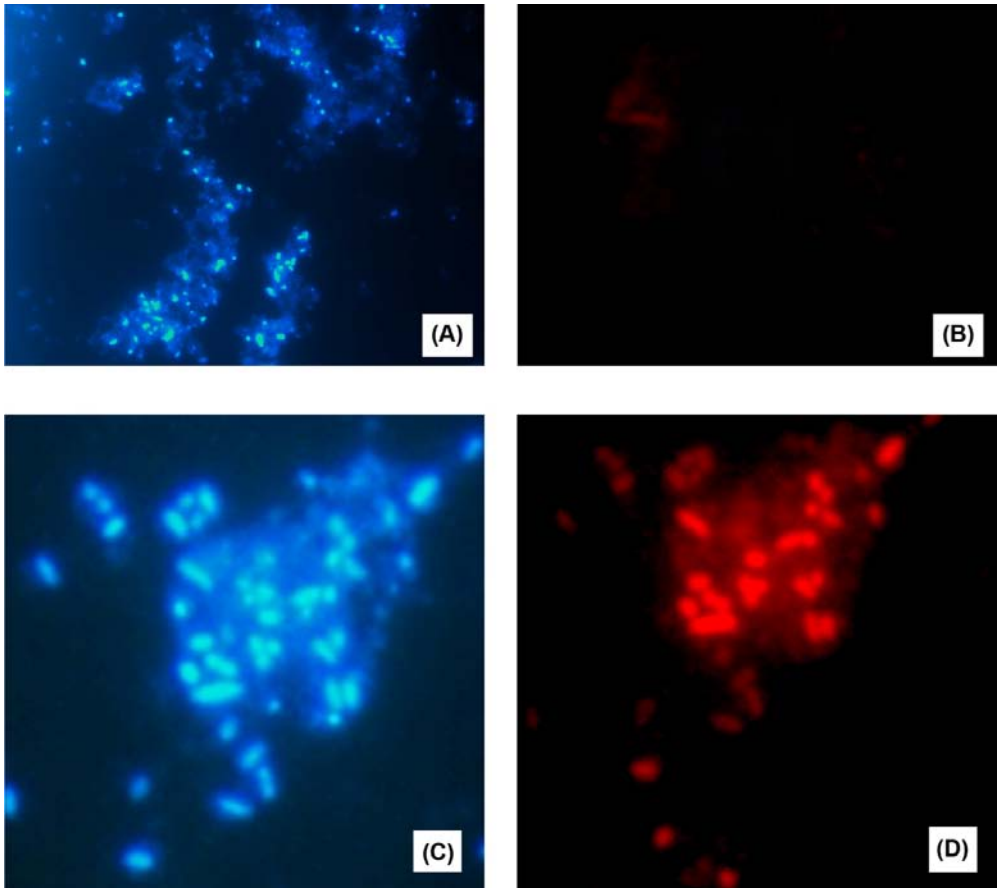

Figure 2. Representative images of *Vp* isolates tested using RING-FISH for T3SS2α gene *vopB2*. (A.) 1000X magnification DAPI image of *tdh*$^{+}$/*trh*$^{-}$ *vopB2*$^{-}$ environmental isolate 2007-103. (B.) Cy3 image of identical slide location for environmental isolate 2007-103. (C.) DAPI image of *vopB2*$^{+}$ clinical isolate Tx2103. (D.) Cy3 image of identical slide location for clinical isolate Tx2103

Aside from *vopB2*, no gene was detected differentially between clinical and environmental isolates. Therefore RING-FISH was run solely for the *vopB2* gene.

Group-specific PCR (GS-PCR), targeting a region commonly associated with *tdh*$^{+}$/*trh*$^{-}$ isolates was also used to screen all isolates. No environmental isolates were positive for GS-PCR. All 3 clinical *tdh*$^{+}$/*trh*$^{-}$ isolates positively amplified using GS-PCR. No other clinical isolates produced an amplicon.

T3SS2β genes *vscC2*, *vscS2*, *vopB2*, and *vopC* were screened against all 158 isolates. Of the 30 *tdh*$^{+}$/*trh*$^{-}$ strains, all tested negative for T3SS2β genes. All 5 *tdh*$^{-}$/*trh*$^{+}$ strains tested positive for each T3SS2β genes. No other isolate tested positive for T3SS2β genes (Table 2).

All environmental strains in this study were isolated from the water column, sediment, or oyster meat (Figs. 1, 3).

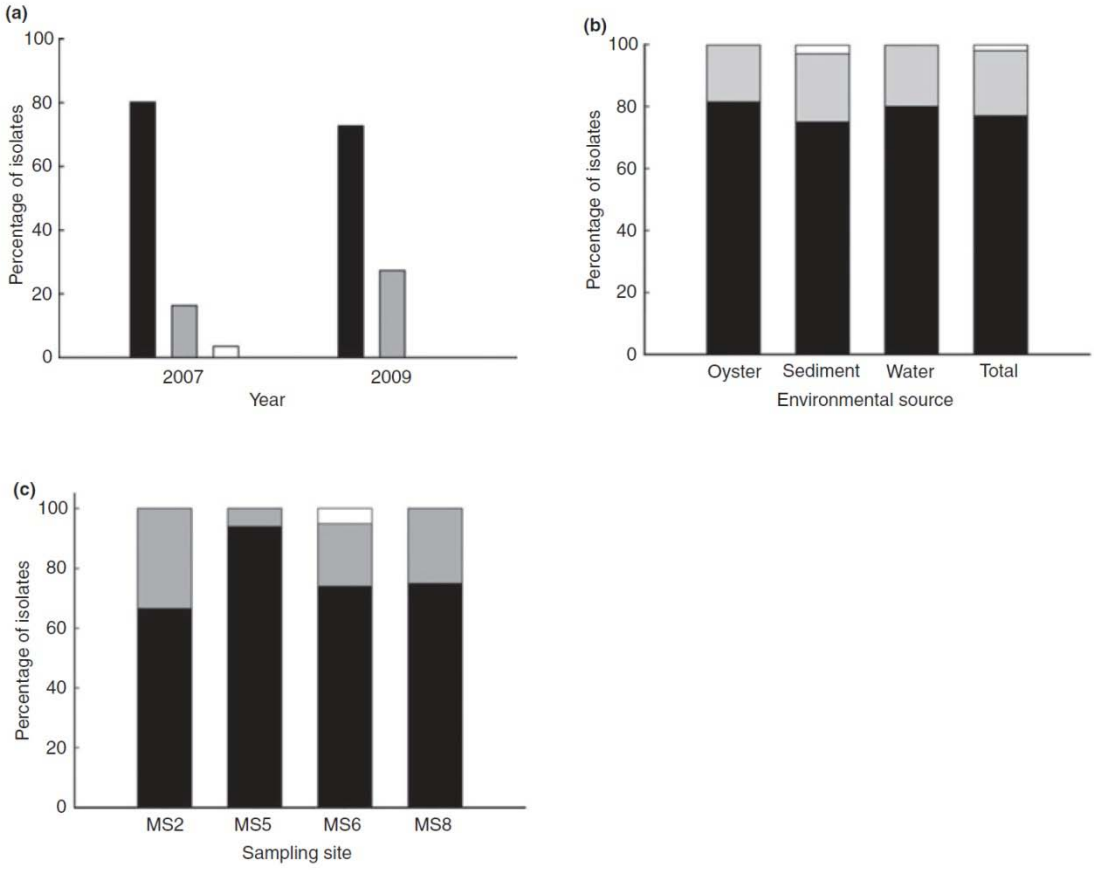

Figure 3. The percent distribution of potentially pathogenic *Vp.* (A) Distribution of isolates by hemolysin content over two separate sampling years. (B) Distribution of total isolates and of isolates in three environmental sources (oyster, water, and sediment). (C) Distribution of isolates by sampling site.

Of 130 potentially pathogenic environmental strains isolated, 73 (56%) were isolated from sediment, 27 (21%) from oyster, and 30 (23%) from water. We found 59%

of *tdh*$^+$/*trh*$^-$ isolates in sediment, 19% from oyster samples, and 22% from water. Out of 100 *tdh*$^+$/*trh*$^+$ isolates, 54% were taken from sediment samples, while 22% and 24% were isolated from oyster and water respectively. All 3 environmental *tdh*$^-$/*trh*$^+$ isolates were found in the sediment.

The single local clinical strain, VPA2007-095, tested negative for both T3SS2 and GS-PCR and tested positive for *tdh, trh*, and T3SS1. This result was also the most typical result for all 130 environmental strains that were screened.

Discussion

This study represents a rare look at the distribution of a poorly understood community of naturally-occurring bacteria from which human pathogens can arise. Although the great majority of infections come from *Vp* isolates containing *tdh* and/or *trh* and epidemiological evidence has correlated the two gene products (hemolysins) with pathogenicity (*29*), almost all naturally-occurring (environmental) isolates lack these two hemolysins (*72, 73*). Therefore, human infections most commonly arise from rare, naturally occurring *tdh*$^+$ and/or *trh*$^+$ *Vp* strains found in finfish, shellfish, coastal waters and sediment. On average, during the 2007 sampling period *tdh*- and *trh*- positive isolates represented 3% and 1% of the total (*tlh*$^+$) environmental *Vp* detected in this study, respectively (*7*). We were able to acquire a large pool of potential pathogens (*tdh*$^+$ and/or *trh*$^+$) by enriching environmental samples and isolating individual colonies that contained either *tdh* or *trh*. Each enriched sample plate yielded anywhere from 1-10 colonies containing *tdh* and/or *trh* with an average of less than 2 colonies per plate. Several colonies from the collection were analyzed for genetic diversity using REP-PCR and MLSA data (*31*) including several suspected duplicate colonies. Two sets of isolates were found to be identical by REP-PCR: Vp2007-020/Vp2007-023 along with Vp2007-043/

Vp2007-047. Interestingly, the data from this paper also showed that colonies containing *tdh* and/or *trh* from the same plate did not necessarily have the same genetic fingerprint or allelic profile, thus colonies coming from the same plate could not be dismissed as identical strains.

The genetic compliment in *Vibrio* greatly affects their function in nature (*67*). Several *Vp* pathogenicity factors have been discovered, including TDH, TRH, urease, and pili (*3, 27, 74, 75*). The presence of other pathogenicity factors such as the T3SS may alter a bacteria's fitness or ability to colonize certain environments such as host organisms including oysters. Since the Gulf of Mexico is the major producer of oysters used for raw consumption in the United States (*76*), this possibility has public health implications. However, our data shows a similar distribution between oyster, water, and sediment regardless of the presence of hemolysins or T3SSs (Figure 3). The only exception to this has been with tdh^-/trh^+ isolates which were found only in sediment.

Only three tdh^-/trh^+ isolates were identified throughout the sampling period and all three isolates were found in the sediment at sampling site MS6 (Figs 1, 3). The temperature and salinity of site MS6 at the time each of the 3 tdh^-/trh^+ isolates were collected were not significantly different from other sampling sites. Although there does indeed appear to be a bias as to at which site tdh^-/trh^+ isolates were found, temperature and salinity do not appear to be major factors; further investigation of site MS6 may better explain this isolate collection anomally.

In a separate study it was demonstrated that *Vp* outnumbered *V. vulnificus* in the sediment but not in oysters or in the water column (C.N. Johnson, *mss in prep*). Turbidity also played a large role in the densities of *Vp* and the sediment. Both suggest that sediment may play a large role in *Vp* growth and survival and introduction into the water column.

This study examined the distribution and variation of T3SS in *Vp*. Genes were selected based on relative necessity/function of the related protein in the secretion system, physical distribution in the T3SS gene cluster, and fidelity across the genome. In the case of T3SS2β, genes were chosen based on homology to T3SS2α genes that were also targeted in this screening. Three of the four T3SS2β genes screened have a homologous T3SS2α gene which was also screened: *vscC2*, *vscS2*, and *vopB2*, with 70%, 74%, and 70% homology, respectively. All 158 isolates tested positive for all 5 T3SS1 genes, confirming earlier reports of T3SS1 being ubiquitous in *Vp* (*23, 54*). T3SS2α, which has been shown to correspond with tdh^+/trh^- strains (*34, 54*), was found in all 30 tdh^+/trh^- samples, regardless of whether that isolate was GS-PCR positive. No other isolates tested positive for any of the five T3SS2α genes present in the screen. The discovery of a T3SS2 variant, T3SS2β, was made relatively recently (*58*) and has been confirmed in this study as being present in 5/5 tdh^-/trh^+ isolates. To our knowledge this is the first reported case of T3SS2β genes identified in *Vp* from the Gulf of Mexico.

While most *Vp* serotypes are noninfectious, the few infectious serotypes can become major agents of outbreaks worldwide (*24, 34*). In 1996, a pandemic strain was discovered in Calcutta and was described as a "new" O3:K6 type strain that was different from previously described clones and carried *tdh* but not *trh* (*28*). Ample evidence has linked tdh^+/trh^- strains of *Vp* with pandemic-causing serotypes (*18, 28, 41, 47, 77*). We have reported that roughly 20% of all potentially pathogenic isolates collected in this experiment were tdh^+/trh^-; we screened 158 isolates using GS-PCR (*41*) for identification of any isolates belonging to the pandemic-causing group. Out of 27 environmental tdh^+/trh^- isolates, none tested positive for GS-PCR. However, all three clinical tdh^+/trh^- isolates tested positive. The three clinical isolates that tested positive were all donated by

the FDA (Table 1). No other isolate, environmental or clinical, tested positive for the *toxRS* amplicon, including the single local clinical isolate. The non-amplification of GS-PCR on the local clinical isolate is not surprising as there have been no reported cases of the pandemic clone, O3:K6, being found in the Gulf of Mexico. Unsurprisingly all environmental isolates tested negative for GS-PCR as well.

Aside from variations between the overall T3SS2 gene cluster, not all individual genes identified as part of the *Vp* T3SS2 have been found in all isolates, allowing for some minor intra-species variation. VPA1362, an orf encoding the effector protein VopB2 in T3SS2α, was found in this study to be absent from all environmental tdh^+/trh^- isolates and present in all clinical tdh^+/trh^- strains. The gene v*opB2* was the only gene to be present differentially between environmental and clinical strains. The absence of *vopB2* in environmental strains appears to be specific to the T3SS2α variant. The T3SS2β *vopB2* gene variant (73% homology to T3SS2α VPA1362) was found in all tdh^-/trh^+ isolates, not only clinical strains.

All four T3SS2β genes targeted in this screen were positive in all five tdh^-/trh^+ isolates. This confirms the previous report of T3SS2β being found in tdh^-/trh^+ strains. The T3SS2β variant was recently discovered by Okada et al (*58*) and other T3SS2-related genes have been reported (*78*). The history of genetic transfer of T3SS in *Vp* is not well understood but the fidelity between hemolysin content and type of T3SS was observed in this experiment. Instinctively this makes sense as T3SS2β was shown to be near *trh* in the genome, while genetically T3SS2α is flanked by *tdh*.

The majority of potential pathogens we observed in this study were positive for both *tdh* and *trh*. All of these isolates tested negative for both T3SS2α and T3SS2β. This may be due to the fact that all primers targeting T3SS genes in *Vp* have been designed

using sequences solely from *tdh*$^+$/*trh*$^-$ and *tdh*$^-$/*trh*$^+$ isolates. A third T3SS2 variant may reside in *tdh*$^+$/*trh*$^+$ isolates, yet be undetected due to significant sequence divergence. A clear example of this came in 2009 when T3SS2β was discovered in strains thought to be lacking a T3SS2, although T3SS2α sequences had been known for 6 years. In order to compensate for lack of sequenced *Vp* genomes, future studies may include adapting RING-FISH to target typical T3SS2 genes in *Vp* and screening isolates using a less stringent annealing method in order to detect homologues with moderate similarity.

Currently, the pathogenicity island on chromosome 2 of *Vp* in which the T3SS2 is located has been demonstrated to contain either *tdh* and T3SS2α or *trh* and T3SS2β, but not both sets. There is currently a lack of genetic sequence data for strains containing both *tdh* and *trh*. However, understanding the genetic structure of the pathogenicity island in *tdh*$^+$/*trh*$^+$ strains may be important as we have observed these strains to make up a large portion of the environmental "potentially pathogenic" isolates.

In addition to lack of knowledge about *tdh*$^+$/*trh*$^+$ isolates, *tdh*$^-$/*trh*$^-$ isolates also have not been well characterized, although they make up the vast majority of environmental *Vp* isolates. In one report, four T3SS2-related genes were found to exist in non-toxigenic strains and were found to be actively transcribed (*78*). Although our results contradict those reported by Caburlotto et al. (*78*), it is difficult to hypothesize why these differences occurred. For instance, Caburlotto et al. examined *Vp* in the Venetian Lagoon while this study examined populations in the Gulf of Mexico, vastly separate areas with differing environmental conditions. Little is known about the genetic distribution of spatially separated *Vp* populations. Although we have not observed T3SS2 genes in any of our *tdh*$^-$/*trh*$^-$ isolates, additional strains from the northern Gulf of Mexico are being gathered for further characterization of pathogenicity factors.

In conclusion, our study has taken advantage of a unique opportunity provided by a large collection of potentially pathogenic environmental isolates to examine the presence of T3SS variation in *Vp*. We have reinforced the observation that T3SS1 is present in all *Vp* strains. Furthermore, the presence of T3SS2α, which has been most frequently associated with pathogenic *Vp*, was shown to coexist with *tdh* but was absent from all isolates containing *trh* in this study, confirming previous reports from other regions in the world. T3SS2β was detected in all tdh^-/trh^+ isolates, suggesting the two versions of T3SS are exclusive to their respective hemolysin profile and also confirmed the presence of T3SS2β in tdh^-/trh^+ isolates. As more information is discovered about the presence and distribution of pathogenicity factors like the T3SS in *Vp*, analysis of natural populations should be used to better understand the relationship between genetic content and diversity in the environment.

About This Chapter

The work in this chapter was published March 2010 in the Journal of Applied Microbiology (ISSN 1364-5072) (*59*).

CHAPTER III

VARIATION IN SURIVIVAL RATES OF POTENTIALLY VIRULENT *V. PARAHAEMOLYTICUS* EXPOSED TO OYSTER HEMOCYTE

The presence of virulence factors such as *tdh, trh*, and the T3SSs have been shown to have a significant effect on *Vp* pathogenesis in humans (*79, 80*). It remains unclear what role these factors have in host immune system avoidance for *Vp* residing in oyster tissue or in other marine animal tissues. In this experiment, we collected and typed 28 non-homologous *Vp* strains and challenged them with oyster (*C. virginica*) hemocyte bactericidal assays. Isolates were screened in parallel for the presence of *tdh, trh,* T3SS1, T3SS2α, and T3SS2β and sorted into pathogen sub-groups based on the presence of hemolysins *tdh* and *trh*. Hemocyte-induced bactericidal activity, through a calculated Hemocyte Killing Index (KI), was compared between pathogen sub-groups to determine if virulence factors have any influence.

Caco-2 cells, a human adenocarcinoma cell line, were also challenged with specific strains of *Vp* used in this experiment to determine if any relationship existed between toxicity in human intestinal epithelial cells and the presence of virulence factors. Variations in *Vp* cytotoxicity were analyzed between pathogen sub-groups and compared with *Vp* abilty to avoid killing by oyster hemocytes.

Materials and Methods

Bacterial Strain Isolation. Beginning in August 2007, water, oyster, and sediment samples were collected in four sites in the Mississippi Sound and transported on ice immediately to the laboratory for bacterial isolation. *Vp* isolates were identified using a direct plating/colony hybridization method described previously (*7*) with markers for *tlh, tdh,* and *trh*. *Vp* isolates that were positive for t*dh* and/or *trh* were picked, sub-cultured and

confirmed. Each isolate was then screened for T3SS1, T3SS2α, and T3SS2β using PCR (Appendix A). These screens were performed using three separate multiplex reactions targeting a total of 12 genes with gene-specific primers. All PCR primers, with the exception of those targeting T3SS2β, were original and designed to produce amplicons of distinct separate sizes(*59*). After each isolate was characterized for the presence of virulence factors *tdh, trh*, T3SS1, T3SS2α, and T3SS2β, they were checked on non-specific T1N3 agar plates for contamination. For long-term storage, all cultures were placed in T1N3 agar deeps with oil. For short-term use over the course of this study, cultures were taken from long-term storage, grown on T1N3 agar plates at room temperature, and placed in a 12^{o}C environment to slow growth. When needed, the agar plates were taken from 12^{o}C and allowed to warm up to room temperature.

Preparation of Vp strains, hemocytes, and Caco-2 cells for cytotoxicity challenges. A total of 28 strains were tested in oyster hemocyte bactericidal assays. All strains tested can be found in Appendix B. Individual colonies were picked and grown overnight at 37^{o}C in 15mL of APW for cytotoxicity challenges. Pure *Vp* cultures grown this way and sampled the next day contained an average density of 3-4x10^{7} cells ml^{-1} (data not shown). After overnight growth, cells were pelletted at 3000g for 5 minutes and washed twice with PBS. Cells were re-spun after wash and re-suspended in sterile PBS at the appropriate volume to achieve final seed dilution of 1x10^{5} cells per challenge. Bacterial seed densities remained constant in both oyster hemocyte and Caco-2 cytotoxicity challenges.

Eastern oysters (*Crassostrea virginica*) were gathered from the same sample sites where *Vp* was collected (Figure 1, pg 9). Oysters were transported on ice to the lab where they were immediately sacrificed for hemolymph. Specifically, a ½" notch was made with a sterile shucking knife at the ventral posterior edge of the oyster shell. Immediately, a

sterilized glass syringe fitted with a 23 gauge needle was inserted into the adductor muscle and hemolymph was drawn out and placed in polystyrene tubes on ice to prevent clumping. Care was taken not to draw mantle fluid in. The total time from oyster shell notching to hemocyte extraction was approximately 90 seconds for each oyster. The required volume of hemocyte needed for each 96-well challenge plate was pooled from 8-15 oysters. After hemocyte collection, a hemocytometer was used to determine densities and hemocyte concentration was adjusted to ~$2x10^5$ cells ml^{-1}. A dye exclusion assay was performed by diluting a subsample of hemolymph 1:5 with a 0.4% Trypan Blue solution. Hemolymph was then observed under a light microscope (Zeiss) to confirm presence and viability of hemocytes

Caco-2 cells, acquired from the American Type Culture Collection (ATCC) were grown in culture flasks (Falcon) containing Eagles Minimum Essential Media (EMEM) with 20% Fetal Bovine Serum (FBS) at 37^oC in 5% CO_2. No antibiotics were used in Caco-2 culture. Cells were passed 1-2x per week. *Vp* toxicity challenges took place between passages 8-15.

Cytotoxicity challenges. All *Vp* cytotoxicity challenges were based on previously published hemocyte and Caco-2 killing assays (*81-85*). Each *Vp* strain involved in a cytotoxicity assay was tested in triplicate. Assays were done using 96 well plate flat bottomed plates (Falcon). Each plate seeded with ~$1x10^4$ oyster hemocyte or Caco-2 cells per appropriate well. Sterile artificial seawater (ASW) was used as the media in hemocyte challenges, while EMEM was used in Caco-2 challenges. In hemocyte cytotoxicity trials, each plate was spun down at 180g for 10 minutes prior to addition of *Vp* to promote hemocyte attachment. Oyster plasma was then removed and replaced with PBS. $1x10^5$ *Vp* cells of a specific strain were added to achieve a final multiplicity of infection (MOI) of

10. This MOI was chosen based on previous *Vp* cytotoxicity work (*82-84*). After addition of both hemocyte/Caco-2 and *Vp* cells, each plate was spun down (Eppendorf 5430R) at 4^{o}C and 160g for 10 minutes to promote *Vp* attachment.

Hemocyte cytotoxicity challenges were placed at room temperature (20^{o}C) and incubated for 5 hours. Caco-2 cytotoxicity challenges were incubated at 37^{o}C and 5% CO_2 for 5 hours.

Cytotoxicity was measured via 3-(4,5-Dimethylthiazol-y-yl) (MTT) assay, which measures cell viability by assessing mitochondrial activity through colorimetric analysis of a reduced formazan dye end product. Specifically, a clear chemical product is added to the well. Active mitochondria convert this colorless product into an insoluble dye, which precipitates out to give a purple color. A relationship can be established between dye absorbance and cell density, thus providing an estimate for cell viability. Twenty five uL of APW was added to each well along with the MTT compound after incubation. An additional 2 hour grow-out/recovery period was provided after which the challenge was stopped using a solubilization solution. After dye solubilization, each plate was read at 570nm and 725nm absorbance using a SpectraMax M2 plate reader (Molecular Systems). The KI and % bacterial survival in oyster hemocyte cytotoxicity challenges were calculated using the following formulas (*85*):

$$\text{Oyster Hemocyte KI} = 1 - [\ (Abs_{HB} - Abs_{H})/\ Abs_{B}]$$

$$\%\ \textit{Vp}\ \text{Survival} = 100^{*}\ (1-\ \text{KI})$$

The cytotoxicity of *Vp* to Caco-2 cells was calculated with the following formula:

$$\text{Caco-2 Death} = 1-\ [(Abs_{CB}-Abs_{B})/\ Abs_{C}]$$

Results

A total of 29 strains of *Vp* were tested for the ability to survive exposure to oyster hemocytes. Nine tdh^+/trh^+, nine tdh^+/trh^-, four tdh^-/trh^+ , and six tdh^-/trh^+ *Vp* strains were tested. The hemocyte survival % +/- Standard Deviation (SD) was 43.6 +/- 21.8, 51.7 +/- 21.9, 47.2 +/- 10.1, and 58.7 +/- 14.6 for tdh^+/trh^+, tdh^+/trh^-, tdh^-/trh^+ , and tdh^-/trh^+ , respectively (Table 4, Figure 4).

Table 4

Vp survival in Oyster Hemocyte

tdh/trh	Sum	n	Avg Survival(%)	Std Dev	Std Error
+/+	508.161	9	43.538	21.846	7.282
+/-	435.145	9	51.651	21.864	7.288
-/+	211.173	5	47.207	10.096	5.048
-/-	248.121	6	58.647	14.643	5.978

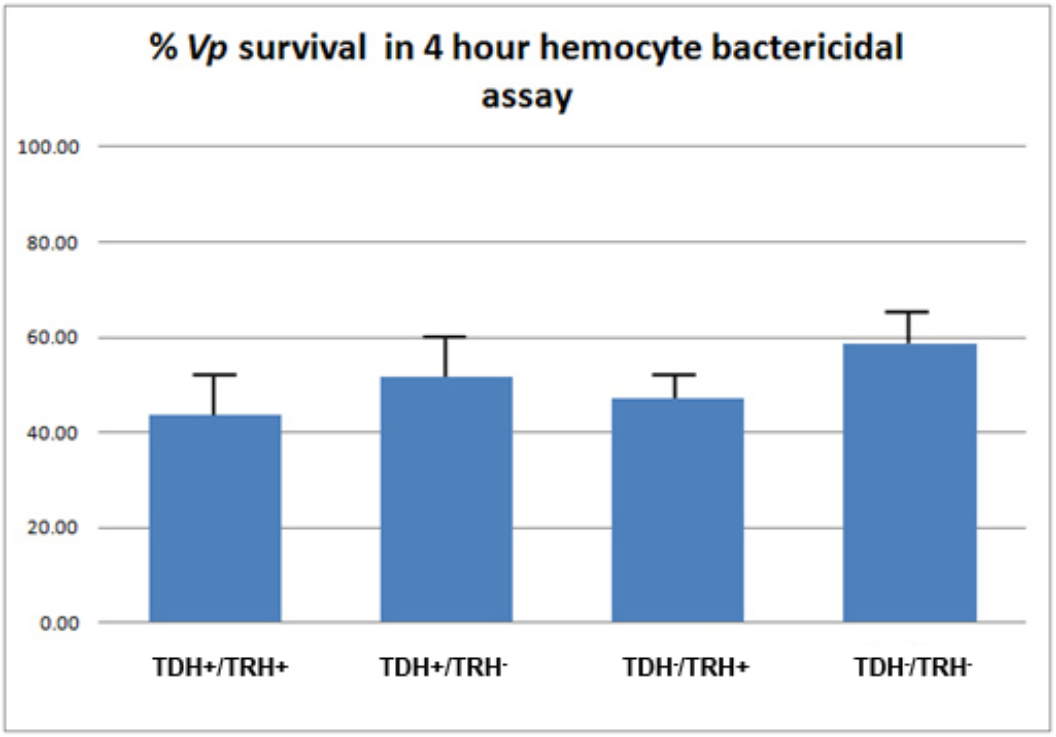

Figure 4. The percentage of *Vp* cells still viable after 4 hour oyster hemocyte bactericidal assays, separated by potential pathogen subgroup. Standard error bars are shown.

Twenty-five strains of *Vp* were additionally tested for their respective cytotoxic potential when exposed to Caco-2 cells (Table 4, Figure 5). Caco-2 Cytotoxicity was defined as the percentage of Caco-2 cells still alive after a four-hour exposure to an individual *Vp* strain. Caco-2 cytotoxicity +/- SD was measured at 56.7 +/-13.1, 56.17 +/- 29.5, 25.6 +/- 20.26, and 43 +/- 30.75 for tdh^+/trh^+, tdh^+/trh^-, tdh^-/trh^+ , and tdh^-/trh^+ isolates, respectively.

Table 5

Percentage of Caco-2 cell death after exposure to Vp

tdh / trh	Sum	n	Avg Kill %	Std Dev	Std Error
+/+	510.7	9	56.74	13.130	4.377

Tabled 4 (continued).

+/-	337.0	6	56.17	29.451	12.023
-/+	128.0	5	25.60	20.256	9.059
-/-	215.0	5	43.00	30.749	13.751

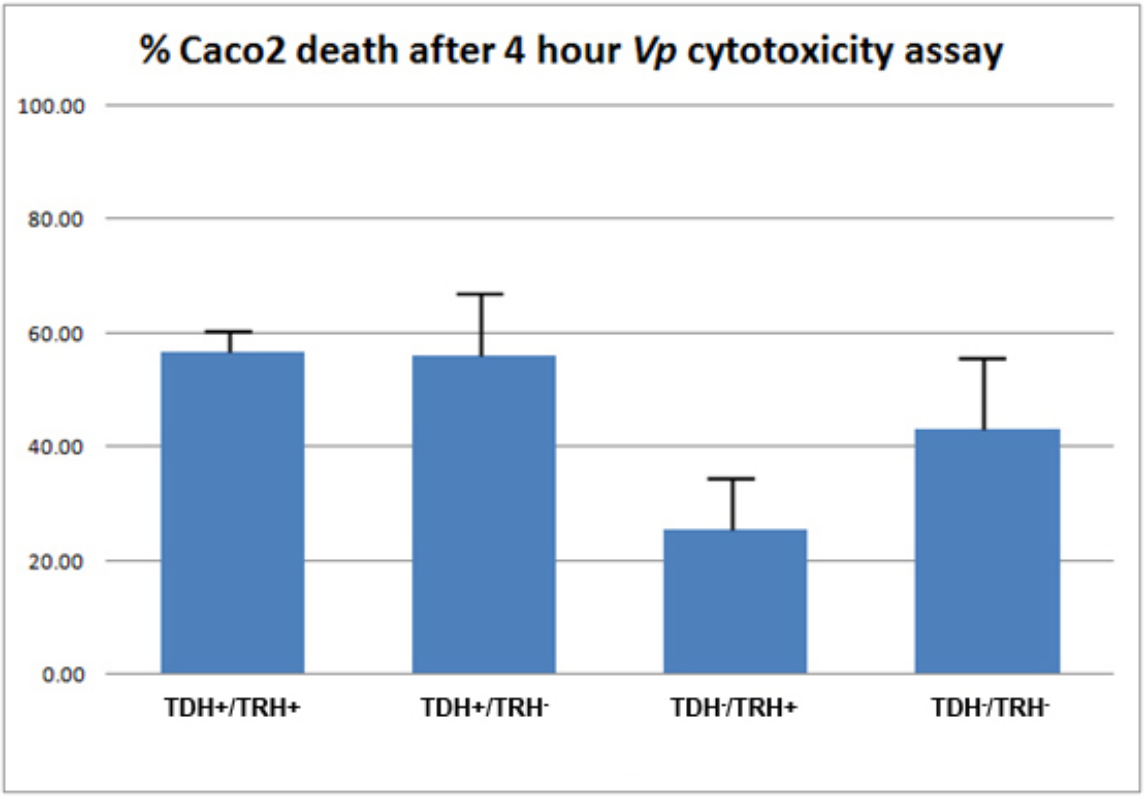

Figure 5. The percentage of Caco-2 cells killed after a 4 hour *Vp*-Caco-2 cytotoxicity assay. Standard error bars are shown.

A student's t-test ($\alpha = 0.05$) was used to evaluate any significant differences in oyster hemocyte survival between potential pathogen subgroups (Table 6). Potential pathogen subgroups were also tested for significant differences in cytotoxicity of Caco-2 cells (Table 7).

Table 6

Student t-test p values for Vp virulence factor sub-group comparisons in oyster hemocyte bactericidal assays

(tdh/trh)	***+/+***	***+/-***	***-/+***	***-/-***
+/+	-	0.539	0.929	0.471
+/-	-	-	0.538	0.972
-/+	-	-	-	0.446

Table 7

Student t-test p values for Vp virulence factor sub-group comparisons in Caco-2 cytotoxicity assays

(tdh/trh)	***+/+***	***+/-***	***-/+***	***-/-***
+/+	-	0.569	0.0119*	0.295
+/-	-	-	0.092	0.552
Table 4B (Continued).				
-/+	-	-	-	0.386

*Significant Difference at α=0.05

No meaningful relationships between presence of virulence factors and ability to survive oyster hemocyte killing were observed. There was a significant difference in *Vp* survival rates between strains of clinical and environmental sources ($p=0.028$, $\alpha = 0.05$), which is consistent with previous reports (*86*). No significant difference was found

between environmental and clinical strains of *Vp* during Caco-2 exposures ($p=0.80$ $\alpha = 0.05$).

One potential pathogen subgroup, *tdh*$^-$/*trh*$^+$, displayed significantly different cytotoxicity in Caco-2 assays than the *tdh*$^+$/*trh*$^+$ subgroup (p value 0.0119). While insignificant, a p-value of 0.092 was found in a comparison of *tdh*$^-$/*trh*$^+$ and *tdh*$^+$/*trh*$^-$ subgroups for cytotoxicity in Caco-2 assays.

Not all strains of *Vp* tested for oyster hemocyte survival were tested for Caco-2 cytotoxicity due to logistical and technical difficulties. Each of the strains tested for Caco-2 cytotoxicity had been previously tested for oyster hemocyte avoidance. No strains were tested for Caco-2 cytotoxicity that had not been previously challenged for a hemocyte KI.

There was a loose negative correlation between Caco-2 cytotoxicity and oyster hemocyte killing avoidance with an r value of -0.43. *Vp* strains with varying presence of *virulence* factors *tdh, trh*, and T3SS2 variants α and β did not contribute differently to bacteria exposed to oyster hemocyte or Caco-2 cells with one exception (*tdh*$^-$/*trh*$^+$ subgroup in Caco-2 cytotoxicity tests).

Discussion

The use of a reduced dye compound to measure *Vp* bactericidal activity in oyster hemocyte has been well documented (*82, 85*) and provides a reliable mechanism to study bacterial responses to immunological activity *in vitro*. The results of *C. virginica* hemocyte bactericidal activity in this study correlated with previous published reports of tests on some of the same clinical *Vp* strains as tested in this experiment (*82, 86*). The majority of *Vp* strains used in these challenges were environmental isolates and therefore unique to this experiment; however, some well-established clinical strains have previously been

examined. In the current experiment, Tx2103 was found to have a hemocyte KI of 55%, whereas previous reports displayed a KI of ~52% for the same strain (*86*).

The correlation of virulence factors in bacterial species and their fate after exposure to oyster hemocyte has been studied but is still not well understood (*85-88*). Reports indicated that *Vp* hemocyte bactericidal activity was correlated with season (*82*) and the nature of the strain (environmental vs clinical) (*86*). In this experiment, all oysters collected for hemocyte exposure were done between July and August of 2010. Mean water temperatures did not vary significantly to affect hemocyte activity, although the high summer temperatures could have provided an increased bactericidal activity as previously reported (*82*).

Both environmental and clinical strains were tested in this experiment, including one local clinical isolate, Vp2007-095JW. Each virulence factor subgroup tested contained at least one clinical and environmental sample. A list of all strains tested can be found in Appendix B.

Caco-2 human intestinal epithelial cells were chosen to investigate the cytotoxic ability of *Vp.* Specifically, Caco-2 cells were chosen because these cells differentiate into intestinal epithelial cells (*89*) when grown to confluence and express the appropriate intestinal epithelial membrane proteins. Previous studies of *Vp* cytotoxicity have been performed using Caco-2 cells as a reliable and practical *in vitro* cytotoxicity assay (*62, 80, 84, 90-92*). All Caco-2 cultures used in cytotoxicity assays were harvested after a minimum of 8 passes, thereby assuring the development of epithelial tight junctions and appropriate display of surface antigens (*93*) in the culture monolayer.

In both oyster and Caco-2 assays, potential pathogen sub-groups did not display any significant difference with one exception. There was a significant difference in Caco-2

cytotoxicity of *tdh*$^{-}$/*trh*$^{+}$ and *tdh*$^{+}$/*trh*$^{+}$ isolates (p= 0.012). The average Caco-2 killing capacity of strains in these two virulence factor sub-groups was 19.8% and 58.5%, respectively. These results indicate that *tdh*$^{-}$/*trh*$^{+}$ isolates could be less effective; however, even though the results were statistically significant the data set is too small to provide a conclusive association. Over a period of four years, we were only able to isolate three environmental *tdh*$^{-}$/*trh*$^{+}$ isolates. The reason behind the rarity of these isolates in the northern Gulf of Mexico is not well understood and acts as a natural limit on statistical analysis in this experiment.

The oyster hemocyte bactericidal assay data indicated that there was significant interstrain variance with regards to survival in bactericidal conditions. No differences could be seen by separating out the strains via potential pathogen sub group. Similar trends were seen in the *Vp*-Caco-2 cytotoxicity assays.

Overall, there was a weak negative correlation (r= -0.43) between *Vp* cytotoxicity in Caco-2 cells and survival in oyster hemocyte exposures. However, the significance of this correlation must take into account the experimental models. Caco-2 cytotoxicity assays, by necessity, take place in a media rich cell-culture environment widely different from the environment found in oyster hemocyte assays. Furthermore, Caco-2 assays only function as a model for cytotoxicity, the assays are significantly different from the environment of the human gut.

Interactions between tissue (hemocyte or Caco-2 monolayer) and *Vp* cells also occur in each experimental assay and may affect results. Many virulence factors in *Vp* such as T3SS1 and T3SS2 may be differentially expressed under various environmental conditions including contact with different cell types (*94, 95*).

Signaling processes controlling large genetic systems may take more time than available in these assays and is a limiting consideration for this type of experiment. For instance, *Vp* transitions between growth in a liquid medium (swimmer) and growth on a surface (swarmer) by shifting expression profiles of key genes such as the polar flagellum (*96-99*). These transcriptomic shifts are also responsible for the expression and repression of some virulence and secretion genes (*100*).

The bactericidal and cytotoxicity assays in this report were done over a four hour time course, as determined by preliminary MTT data (not shown) and previously published experiments (*82, 84, 101*). This experiment allows for good short-term standardized data to be gathered for *Vp* immune-avoidance by controlling bacterial starting densities, tissue densities, and total exposure time, but sacrifices the depth and detail of a microcosm-type experiment. Future research using microcosms and long-term (multiple week) exposures to oysters could illicit a more complete understanding of the relationship between virulence factor and bactericidal activity.

CHAPTER IV

TRANSCRIPTIONAL REGULATION IN POTENTIALLY VIRULENT *V. PARAHAEMOLYTICUS* DURING EXPOSURE TO INTESTINAL EPITHELIAL CELLS AND OYSTER HEMOLYMPH

The presence and absence of specific genes in environmental and clinical *Vp* strains have been well studied, while genetic expression studies of *Vp* are much more uncommon in the current literature. The study of gene expression can be prohibitive for a number of reasons including cost and quality of experimental design. Of the gene expression studies in *Vp* that have been reported, the majority have been performed on specific targeted subsets of genes (*94, 102-108*). Few genome-wide *Vp* studies have been done (*109, 110*).

This study examined the genetic expression differences between groups of pathogenic, potentially virulent clinical *Vp* strains using whole genome DNA microarrays. Specifically, two clinical *Vp* strains representative of distinct pathogenic subgroups were challenged with Caco-2 human intestinal epithelial cells and oyster hemolymph over a four hour exposure. The purpose of this study was to identify genes significantly differentially expressed in potentially virulent strains of *Vp* over time and between pathogenic groups.

Understanding the role of potentially virulent bacteria in the environment is a key step in discerning the relationship between these organisms and public health risk. It has been well documented that the vast majority of clinical *Vp* cases involve strains represent only a small portion of the overall *Vp* community in the environment (*7, 8, 73*). A recent survey in the northern Gulf of Mexico indicated roughly 4-5% of *Vp* isolates sampled contained relevant virulence factors (*31*). Furthermore, this study indicated that the majority of these isolates were found in sediment or oyster; tdh^-/trh^+ isolates were found

only in the sediment. Current similar studies continue to show such patterns in potentially virulent *Vp* (Johnson 2012, *mss in prep*).

We chose to study the regulation of genes involved with *Vp* exposure to oyster hemolymph by analyzing bacterial transcriptomic responses over time. *Vp* is found naturally in oyster tissue, yet the relationship between potentially virulent *Vp* and oyster colonization is unclear, if indeed they colonize oyster tissue. It is possible that *Vp* exists transiently in oysters. Multiple experiments have shown that *Vp* is depurated at varying rates in molluscs including oysters, but do not completely rid themselves of *Vp* (*111-113*). By analyzing the expression responses in potentially virulent *Vp* exposed to oyster hemolymph, a relationship between genetic capability and environmental functionality could be elucidated. Furthermore, we chose to corroborate thesis data with expression data gathered from *Vp* exposure to Caco-2 adenocarcinoma cells. Caco-2 cells, once grown to confluence, differentiate in to human intestinal epithelial cells. Both oyster hemolymph and Caco-2 exposure designs provide basic *in-vitro* mechanisms for understanding complex *in-vivo* functions.

Materials and Methods

Bacterial Strains. Two *Vp* strains, TX2103 and AQ4037 were chosen for this study as representatives of the pathogen subgroups *tdh*$^{+}$/*trh*$^{-}$/*T3SS2*α^{+} and *tdh*$^{-}$/*trh*$^{+}$/*T3SS2*β^{+}. The two *Vp* strains chosen are the FDA reference strains used for potentially virulent subgroups. AQ4037 is the strain in which TRH was originally discovered (*27*). It should also be noted that Tx2103 belongs to the pandemic O3:K6 serovar, while AQ4037 is of the non-pandemic (or pre-pandemic) O3:K6 serovar. The presence of *tdh, trh*, and T3SS genes was confirmed using gene-specific PCR (Table 2, pg 14). All strains were acquired from the FDA (Appendix B).

Strains were kept on T_1N_3 agar deeps at room temperature for long term storage and T_1N_3 plates at 15^{o}C for short-term storage. Cultures were re-plated every four weeks and examined for contamination. For microarray analysis, cultures were removed from short-term storage and individual colonies were plated onto Thio-Citrate-Bile-Salt (TCBS) agar plates and incubated at 37^{o}C overnight. After confirmation on TCBS plates, colonies for each strain were placed into 15mL 10X Alkaline Peptone Water (APW) and grown for 18 hours at 37^{o}C. Cultures were then enumerated using both plate count and hemocytometer. The procedure of inoculating in APW through enumeration was repeated multiple times to ensure consistent and reproducible bacterial concentrations for each strain.

Prior to gene expression challenges, each strain was grown overnight in 10X APW at 37^{o}C. Afterwards, the cultures were pelletted by centrifugation at 2200g for 10 minutes followed by removal of the growth media. Cells were then washed with Phosphate Buffered Saline (PBS) and respun. After this, *Vp* pellets were resuspended in PBS and diluted 1:5 for a final concentration of $1.1x10^{6}ml^{-1}$. This concentration was chosen to give a Multiplicity of Infection (MOI) of 10 in the challenges.

Caco-2 culture. For genetic expression analysis *Vp* was challenged with both Caco-2 colorectal adenocarcinoma cells and oyster hemocyte. Caco-2 cells display characteristics of enterocytic differentiation once they have reached confluence and were acquired from the American Type Culture Collection (ATCC). The cells were grown in Eagles Minimum Essential Media (EMEM) (ATCC) with 20% Fetal Bovine Serum (FBS)(ATCC) at 37^{o}C in 5% CO^2. Cells were passed two times per week at roughly 80% confluence. All *Vp* toxicity challenges took place between passages 8-15. For *Vp* challenges, Caco-2 cells were passed and 16 additional flasks (Falcon) were inoculated

with trypsinized Caco-2 cells. The doubling time for Caco-2 cells is approximately 62 hours; prior to inoculation, the cell concentration was checked with a hemocytometer. Once the concentration was known, each flask was seeded with an initial concentration of ~$2.5x10^4 mL^{-1}$ cells per flask with the objective of reaching a final concentration of $1x10^5 mL^{-1}$ cells in a confluent layer, thus achieving the stated MOI of 10.

Collection of oyster hemolymph. Acquisition of a large volume of oyster hemolymph was accomplished by harvesting *Crassostrea virginica* oysters directly from the environment. Specifically, all oysters were collected locally in areas identical to where local *Vp* were acquired (see Chapter 2). Once oysters were collected, oyster hemolymph was pooled from multiple oysters and placed immediately on ice to prevent cell aggregation. Specifically, oyster hemolymph was extracted as previously described (*81*)(K. Burnette, *personal correspondence*) with some modifications. Specifically, oysters were notched on the posterior edge with a pair of sterilized pliers. Next, a sterile glass syringe with a 23gauge sterile needle was inserted through the cavity and into the adductor muscle. Hemolymph was drawn directly from the adductor muscle, with great care taken not to extract mantle fluid as well. Consistent with previous reports, roughly 1-5 ml of hemolymph were collected per oyster (*81, 82*). After hemolymph was collected and pooled together on ice, hemolymph concentrations were measured using a hemocytometer and diluted with sterile ASW to 1×10^5 ml^{-1}. Cell enumeration was performed as described previously (*114*) using hemocytometry to determine viable cells using dye exclusion. Trypan blue, chosen for dye exclusion, was combined with hemolymph suspension and injected into a hemocytometer. All stained and unstained cells were counted in the four corner chambers of the hemocytometer and cell number determined.

Bacterial Challenges. To determine levels of *Vp* gene expression during exposure to various tissue types, two representative *Vp* strains were challenged with two differing tissue types: oyster hemolymph and Caco-2 cells. The experiment was comprised of 32 separate challenges; each bacterial strain was challenged with each tissue type at two separate time points, 1 hour and 4 hours. These time points were chosen based on preliminary growth data with media only (Figure 6 and 7).

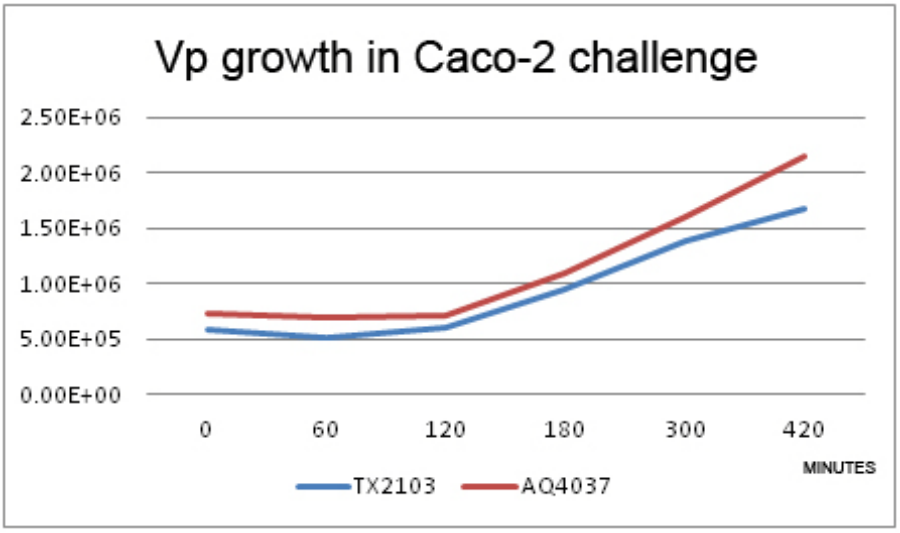

Figure 6. Vp growth over time (minutes) when exposed to Caco-2 cells in EMEM with 10%FBS.

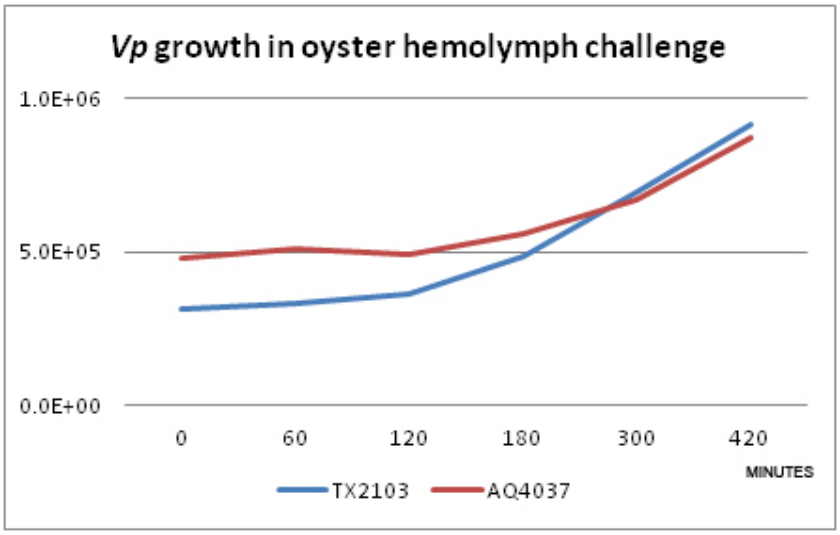

Figure 7. Vp growth over time (minutes) in oyster hemolymph assays.

Each challenge (specific time point, strain, and tissue type) was repeated in quadruplicate to ensure reproducibility and to identify any irregularities in individual arrays. In oyster hemolymph challenges, the pooled and iced oyster hemolymph was enumerated and seeded into 6 well culture plates (BD Falcon) as previously described (*82*) with slight modification. Specifically, 3 x 10^5 hemocyte cells (3mL of $1x10^5$) were seeded per well and spun down for 10 minutes at 180g. Next the serous fluid was removed, the wells were washed with ASW, and the culture plates were respun. Finally, the ASW was removed and the correct volume of bacteria (3mL of $1x10^6$) was added to achieve a final MOI of 10. The culture plates were respun a final time for 5 minutes at 180g to promote bacterial adhesion. At each time point (1 and 4 hours), half of the sample was carefully removed via pipette and immediately purified for RNA.

Caco-2 challenges were performed with identical time points and MOI as the oyster hemocyte challenges to allow for inter-tissue time-point gene expression comparisons. Each of the 16 separate Caco-2 challenges was done in individual flasks where the human intestinal epithelial cells had reached confluence. Specifically, after flasks had reached confluence, *Vp* was added at the correction concentration and the flasks were spun down at 180g for 5 minutes and placed back in 37^{o}C 5% CO_2 incubators. At each time point *Vp*/Caco-2 suspension was removed by pipette and immediately purified for RNA.

RNA Extraction and Labeling. RNA taken from bacterial challenges was immediately stabilized with Qiagen RNAprotect and purified with Qiagen RNeasy mini kit as per the manufacturer's suggested protocol (QIAGEN). After purification, RNA was checked on a NanoDrop 1000 (ThermoSci) for concentration and contaminants. Once each RNA sample passed NanoDrop analysis, the sample was then loaded and run on a Bioanalyzer 2100 (Agilent) to confirm that there was no degradation.

After quality confirmation, each RNA sample was labeled for microarray analysis. RNA was labeled as per Pathogenic Functional Genomics Resource Center (PFGRC) instruction. Specifically, RNA was reverse transcribed using PowerScript RT (Invitrogen) in the presence of random hexamers and 25mM dNTP/aa-UTP labeling mix. The ratio of aa-UTP to dTTP was set at 2:1. Amino-allyl labeled cDNA was then purified using Qiagen MinElute (QIAGEN) kit, substituted a specific phosphate wash and elution buffer. After purification, the aa-cDNA was chemically labeled with a Cy3 dye ester and then repurified using the MinElute kit. Final analysis of the Cy3-labeled cDNA probe was done on a NanoDrop1000. Total dye incorporation and incorporation ratio was calculated. Probes were pelleted using a Vacu-fuge (Eppendorf) and stored short-term in the dark at -80^{o}C until hybridization.

DNA microarrays. The microarrays used were designed and produced by the J Craig Venter Institute (JCVI) http://pfgrc.jcvi.org/index.php/microarray/array_description/vibrio_parahaemolyticus/version1.html). The JCVI produced these microarrays in the Pathogen Functional Genomics Resource Center (PFGRC) which was awarded to them by the National Institute of Health (NIH) National Institute of Allergy and Infectious Disease (http://www.niaid.nih.gov/Pages/default.aspx). The *Vp* microarray plates were awarded to this project after an application was submitted to the PFGRC.

The PFGRC microarrays used in this study correspond to the *Vibrio parahaemolyticus* v1 arrays. The design of the microarray is a standard glass slide with an aminosaline coating, printed with 21,168 spots distributed in 48 grids. The spots account for double-coverage of each of the 9,442 70mer oligonucleotides, along with controls. *Vp* oligonucleotide probe sequences were designed from *Vp* strains RIMD2210633, AQ3810,

and plasmid pO3K6, and from *V. cholera* El Tor N16961. Annotation files are available for viewing at http://pfgrc.jcvi.org/index.php/microarray/array_description/vibrio_parahaemolyticus/version1.html.

Microarrays were hybridized with Cy3 cDNA probes as per PFGRC instructions. Arrays were prehybridized with a 20xSSC/10%SDS/1%BSA solution at 42^{o}C for one hour. Prehybridized slides were then washed, placed in alcohol, and dried extremely carefully to prevent streaks or spots on the array. The hybridization buffer used was a 40% formamide, 5xSSC, 0.1%SDS solution with 0.6ug/ul Salmon Sperm DNA added as a blocking agent. The hybridization buffer was then combined with the lyophilized probe and heated at 95^{o}C for 10 minutes. Next, microarrays were hybridized using a a-Hyb hybridization station (Miltenyi) at 42^{o}C for 20 hours. Array hybridization was limited to 4 at one time. After hybridization, microarrays were washed and scanned using a VersArray scanner (BioRad).

Expression Analysis. Analyses of scanned microarray images were done using the TM4 Microarray Software Suite (http://www.TM4.org). Specifically, Spotfinder v3.2.1 was used for initial image analysis. Hybridized microarray images were received in dual layer TIFF format after scanning and loaded into Spotfinder. Next, grids were created semi-automatically using the listed PFGRC parameters and manually aligned to the array images. Spot intensities were determined using the Otsu segmentation method to subtract background noise. Annotation files were added, with the final Spotfinder analysis providing calculated intensities, background values, spot position/gene identifiers, and quality control flags.

Statistical analysis was accomplished using JMP Genomics software (SAS). After image analysis, data from Spotfinder was saved and loaded into JMP Genomics. Distribution analysis was accomplished for all 32 microarray files. After distribution analysis the data was standardized and a Correlation and Principal Components analysis was done. Normalization was then confirmed and significant differentially expressed genes were discovered using two-way Analysis of Variance (ANOVA). ANOVA was used to compare microarray data through inter-strain, inter-tissue, and time point comparison.

Minimizing the variance and noise of expression in microarray data sets is pivotal to making meaningful predictions. PFGRC *Vp* microarrays were designed with double coverage of all available probes. In this experiment, significant differentially expressed genes were recorded on a per-spot, not per-gene, basis. This was chosen to prevent under-representation of significantly expressed genes through mechanisms such as physical sources of variation that occur spatially on the microarray. PFGRC arrays are spotted glass slides and therefore subject to variation from both the slide and printing apparatus. The application of a per-spot analysis along with quadruplicate biological replicates allows for the normalization of several sources of variance while at the same time emphasizing the identification of significant genes.

Results

The expression of the 9,442 genes gathered from each of the 32 *Vp* microarrays was analyzed using TM4 Microarray Suite and SAS JMP Genomics software. Each experimental sample was performed in quadruplicate to increase robustness of the results. The spot intensity levels for each array was normalized, grouped, and compared using a two-way ANOVA statistical test to predict up and down regulation of genes. Statistical tests were run comparing expression of individual *Vp* strains over time for each tissue

types, as well as comparing the expression of genes between strains at identical time points and tissue type. No analysis was done to compare genetic expression between Caco-2 and oyster hemocyte challenge groups.

In each strain, genes were identified as significantly up or down-regulated based on changes in levels of expression between the chosen time points of 1 to 4 hours. These time points were chosen after preliminary growth data (Figures 5A/B) demonstrated that once *Vp* cultures were seeded in their respective tissue type, *Vp* maintained a lag phase for roughly two hours before entering the exponential phase of growth. The initial time point of one hour was chosen to allow time for the bacteria to acclimate and gene expression reflect the environmental. The time point at 4 hours was chosen to prevent rising culture densities from shifting the MOI greatly and to also prevent the over-accumulation of degraded cells from having an effect on environmental chemistry such as pH, $[CO_2]$, $[O_2]$, etc.

Regulation of genes in individual strains. A total of 475 genes were found to be significantly differentially expressed between time points for each strain in similar tissue challenges (Table 8).

Table 8

Summary of all genes significantly up or down-regulated in each Vp challenge group

Strain	Caco-2		Oyster Hemolymph	
	Up	Down	Up	Down
Tx2103	39	24	80	72
AQ4037	35	31	120	74

A list of all significant up or down-regulated genes can be found in (Appendix C). Over the course of the experiment in hemolymph tissue challenges Tx2103 significantly up-regulated 39 genes and down-regulated 24. AQ4037 regulated (up/down) 35/31 genes. In Caco-2 tissue, Tx2103 significantly regulated (up/down) 80/72 genes over time, while AQ4037 contained 120/74 significantly regulated genes.

Following identification of significant genes, functional categories for each of the significantly expressed genes was determined and genes were grouped according to specific function. The total number of genes in each category can be found in Figures 8 and 9.

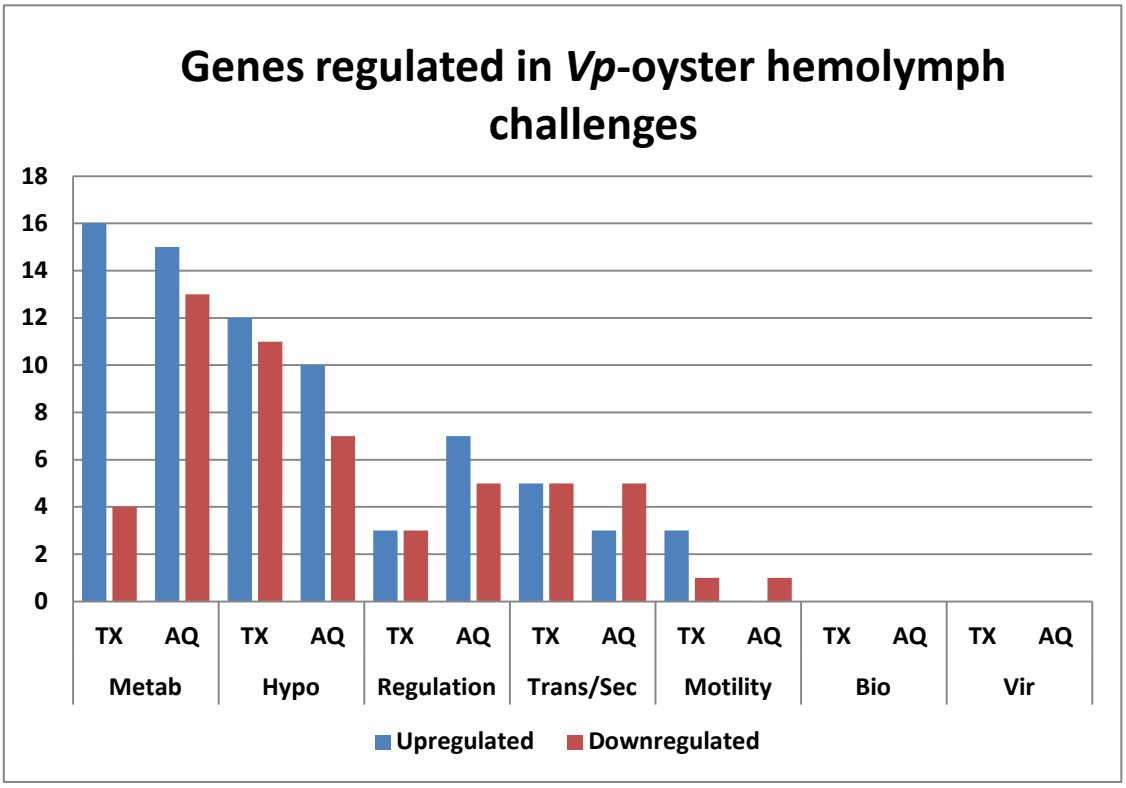

Figure 8. Total genes regulated in *Vp*-oyster hemolymph challenges. Genes are separated into categories: Meta-Metabolism, Hypo-Hypothetical, Regulation, Trans/Sec- Transport and secretion related, Motility and Chemotaxis, Bio-Biofilm/attachment related, Vir-virulence related genes.

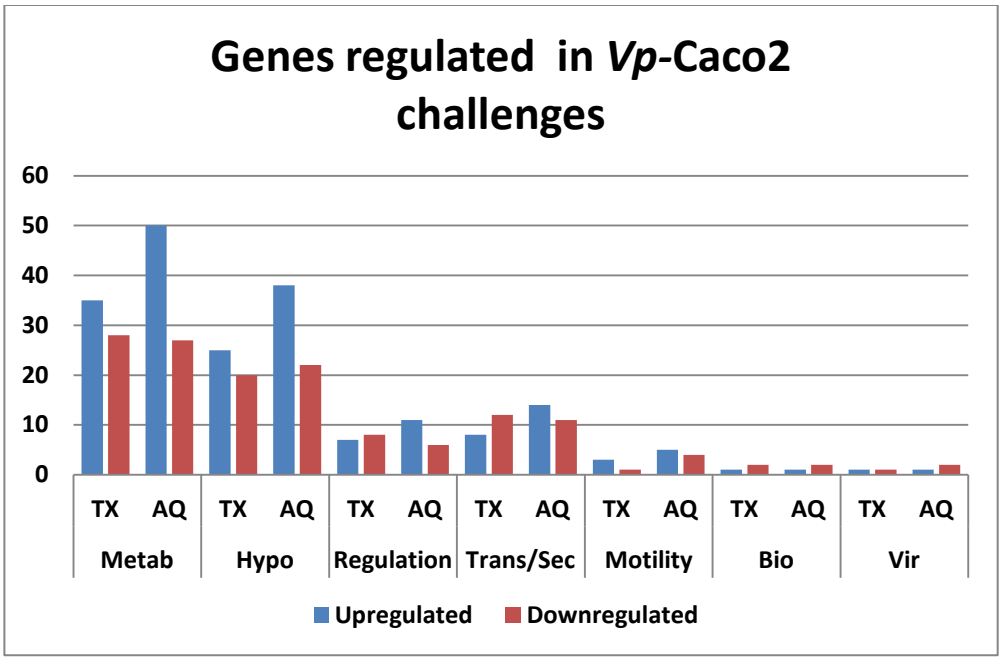

Figure 9. Total genes regulated in *Vp*-Caco-2 challenges. Genes are separated into categories: Meta-Metabolism, Hypo-Hypothetical, Regulation, Trans/Sec- Transport and secretion related, Motility and Chemotaxis, Bio-Biofilm/attachment related, Vir-virulence related genes.

Functional categories consisted of metabolism (carbohydrate, lipid, amino acid, and nucleic acid), transport/secretion, motility/chemotaxis, regulatory proteins, hypothetical and conserved proteins, biofilm/attachment, and virulence-related genes. Generally, the number of genes up and down regulated over time in each category for individual strains was similar, with some exceptions. The ratio at which Tx2103 up-regulated to down-regulated metabolic genes was 4.0 (16/4) in oyster tissue compared to AQ4037, which regulated metabolic genes at a ratio of 1.15 (15/13). This pattern was not observed in Caco-2 challenges where the ratio of up to down-regulated genes was 1.25 for Tx2103 and 1.85 for AQ4037.

The majority of significant genes expressed over time for each strain took place in Caco-2 challenges (346) compared to oyster hemolymph (129). When separated by category, the ratios of genes regulated (# up-regulated genes / # down-regulated genes) in

Caco-2 challenges compared to oyster hemolymph challenges were 2.92, 2.625, 1.8, and 2.5 for metabolism, hypothetical, regulation, transport/secretion, and chemotaxis, respectively. The ratio of total genes regulated in each tissue type was also separated by strain and category (Figures 10-12).

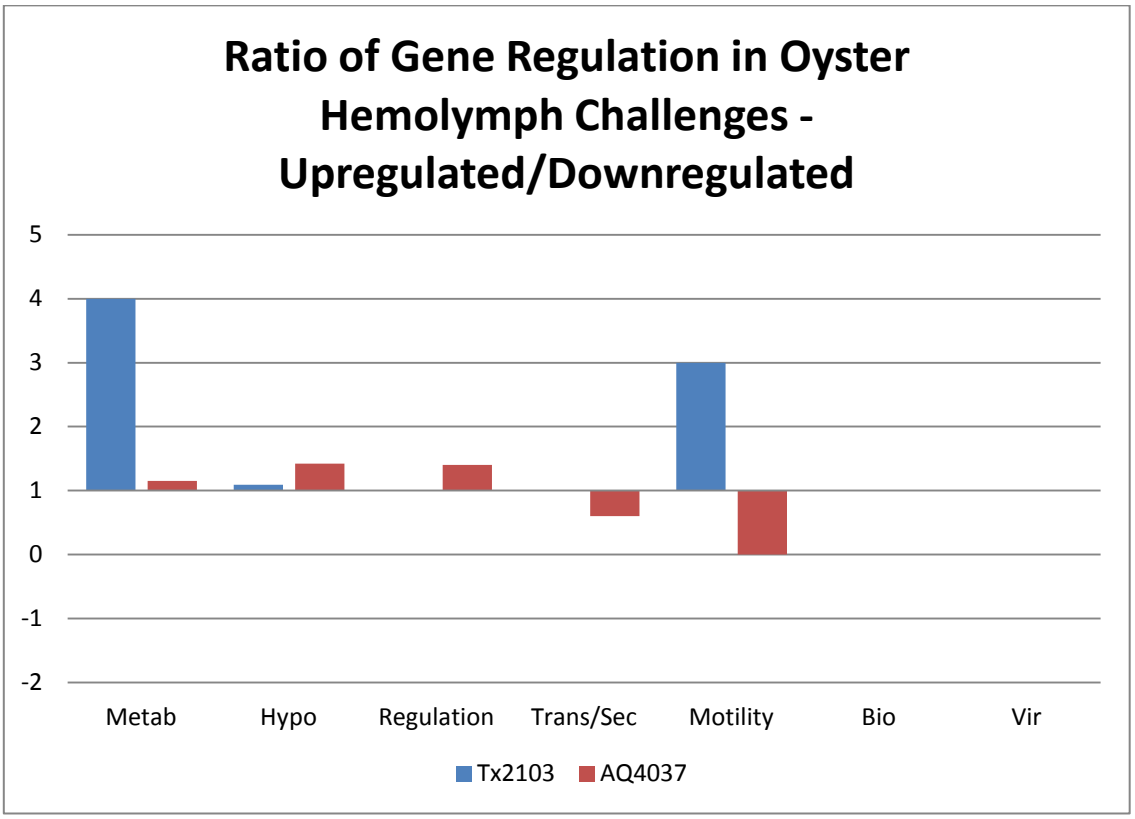

Figure 10. Ratio of significantly up-regulated to down-regulated genes in oyster hemolymph challenges for each functional gene category and challenge type. Ratios are separated for each strain and gene functional group. Numbers greater than one indicate more up-regulated genes, numbers less than one indicate more down-regulated genes.

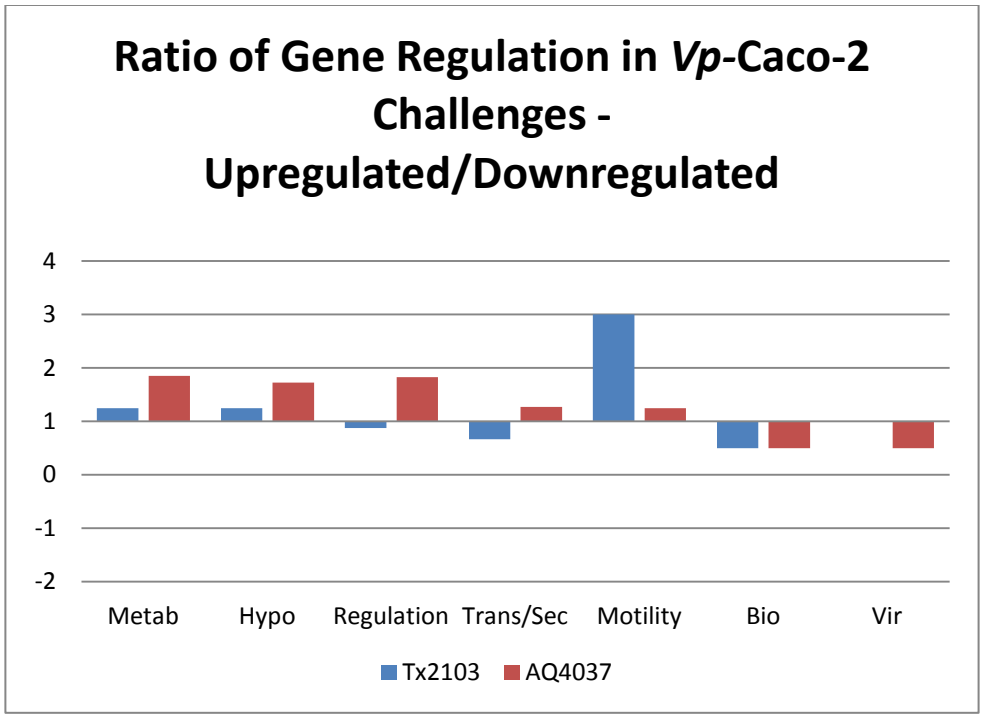

Figure 11. Ratio of significantly up-regulated to down-regulated genes in Caco-2 cytotoxicity challenges for each functional gene category and challenge type. Ratios are separated for each strain and gene functional group. Numbers greater than one indicate more up-regulated genes, numbers less than one indicate more down-regulated genes.

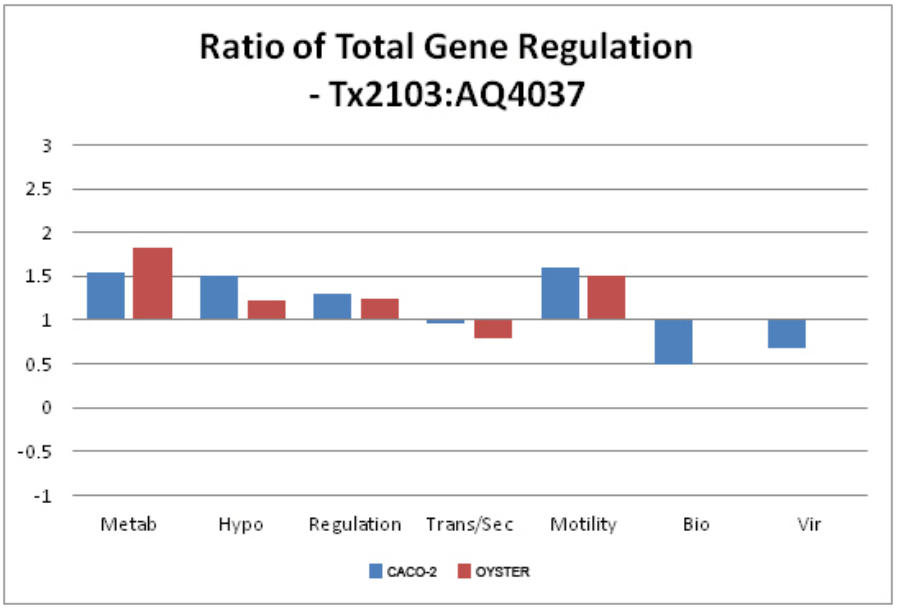

Figure 12. Ratio of total number of genes expressed by strain (Tx2103/AQ4037). Numbers greater than one demonstrate more regulated genes in Tx2103, 1 means equal number of regulated genes between strains, and numbers less than one reveal more regulated genes in AQ4037.

Notably, in AQ4037 nine chemotaxis genes were regulated in Caco-2 challenges, while only one was regulated in oyster challenges. This is in contrast to the four genes regulated by Tx2103 in both oyster and Caco-2 challenges.

The number of genes regulated in the hypothetical protein gene category varied significantly between challenge groups and strains. A ratio was determined by totaling the number of genes both up and down-regulated in each *Vp* strain for both challenge groups (Caco-2 and oyster hemocyte). The total number of significantly regulated genes in Caco-2 challenge groups was divided by the total number of significantly regulated genes in oyster hemocyte challenge groups. The ratio of regulated genes in Caco-2 challenges to oyster hemolymph challenges was markedly in the hypothetical protein gene category. Specifically, the ratio in Tx2103 was 1.96 compared to 3.53 in AQ4037. In other terms, Tx2103 regulated twice as many hypothetical proteins in Caco-2 challenges, while AQ4037 significantly regulated almost four times the number of hypothetical genes in Caco-2 challenges than in oyster hemocyte challenges. The proportion of regulated hypothetical genes compared in all significantly regulated genes remained consistent between challenge groups, 31.0% and 30.3% for oyster and Caco-2 challenges respectively.

No biofilm/attachment or virulence genes were detected as being significantly differentially expressed in oyster hemolymph challenges, however 11 total genes from these categories were found to be significantly regulated in Caco-2 challenges (Table 9).

Table 9

Total genes up or down-regulated by category. O – Oyster, C – Caco-2

	Metab		**Hypo**		**Regulat**		**Trans**		**Chemo**		**Bio**		**Vir**	
	Up	*Dw*	*Up*	*Dw*	*Up*	*Dw*	*Up*	*Dw*	*Up*	*Dw*	*Up*	*Dw*	*Up*	*Dw*
Tx-O	16	4	12	11	3	3	5	5	3	1	0	0	0	0
AQ-O	15	13	10	7	7	5	3	5	0	1	0	0	0	0
Tx-C	35	28	25	20	7	8	8	12	3	1	1	2	1	1
AQ-C	50	27	38	22	11	6	14	11	5	4	1	2	1	2

Interstrain variation in expression of genes. A total of 523 genes were found to have significant interstrain variation at corresponding time points and tissue types (Table 10).

Table 10

Total summary of genes displayed significant expression variation between strains at equal time points/challenge groups

	Metab		**Hypo**		**Regul**		**Trans**		**Chemo**		**Bio**		**Vir**	
	AQ	*TX*	*AQ*	*TX*	*AQ*	*TX*	*AQ*	*TX*	*AQ*	*TX*	*AQ*	*TX*	*AQ*	*TX*
Oys- 1h	5	23	2	9	0	1	1	4	2	0	0	0	0	0
Oys - 4h	4	41	12	7	2	2	1	7	0	1	0	0	0	0
Caco - 1h	19	34	21	19	5	10	5	8	3	2	2	0	3	5
Caco - 4h	73	44	36	38	13	8	18	11	6	4	1	3	7	1

A total of 241 genes were expressed at a higher level in AQ 4037 across all time points and challenge groups while 282 genes were expressed at a significantly higher level in Tx2103. In oyster tissue challenges, Tx2103 contained 95 genes significantly higher expressed than AQ4037,while AQ4037 only expressed 29 genes at higher rates than Tx2103. These results are markedly different from the Caco-2 challenge where Tx2103 displayed 187 genes at higher levels than AQ4037 and AQ4037 contained 212 genes that were expressed at significantly higher levels than Tx2103(Figure 13 and 14).

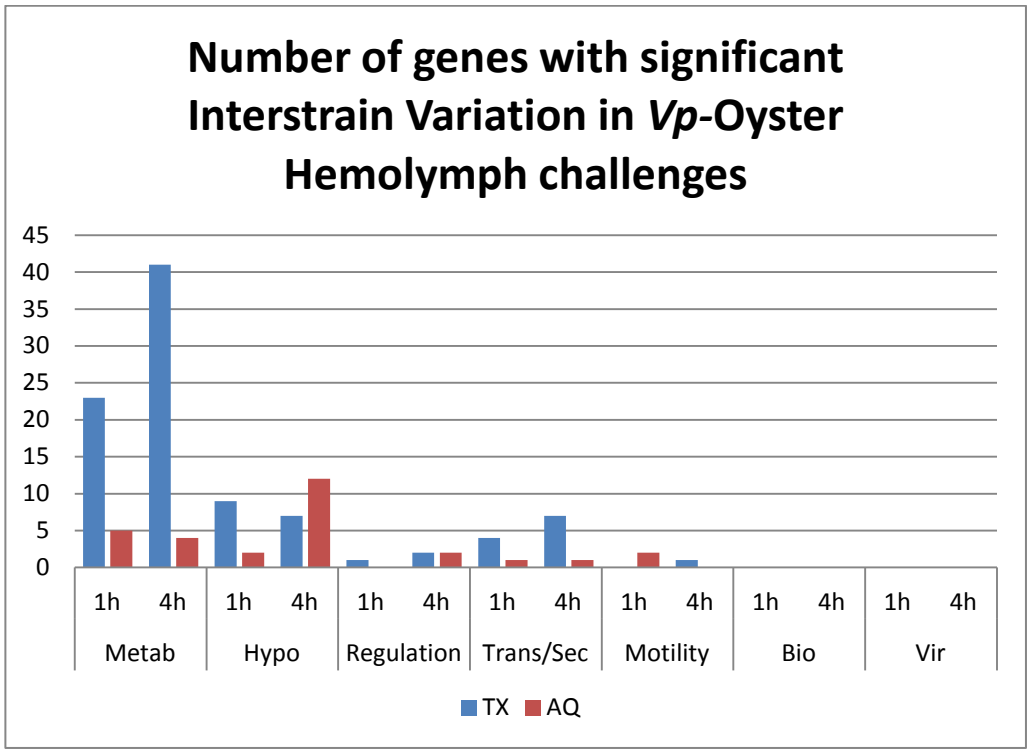

Figure 13. Total number of genes significantly differentially expressed between strains at equal time points in *Vp*-oyster hemocyte challenges.

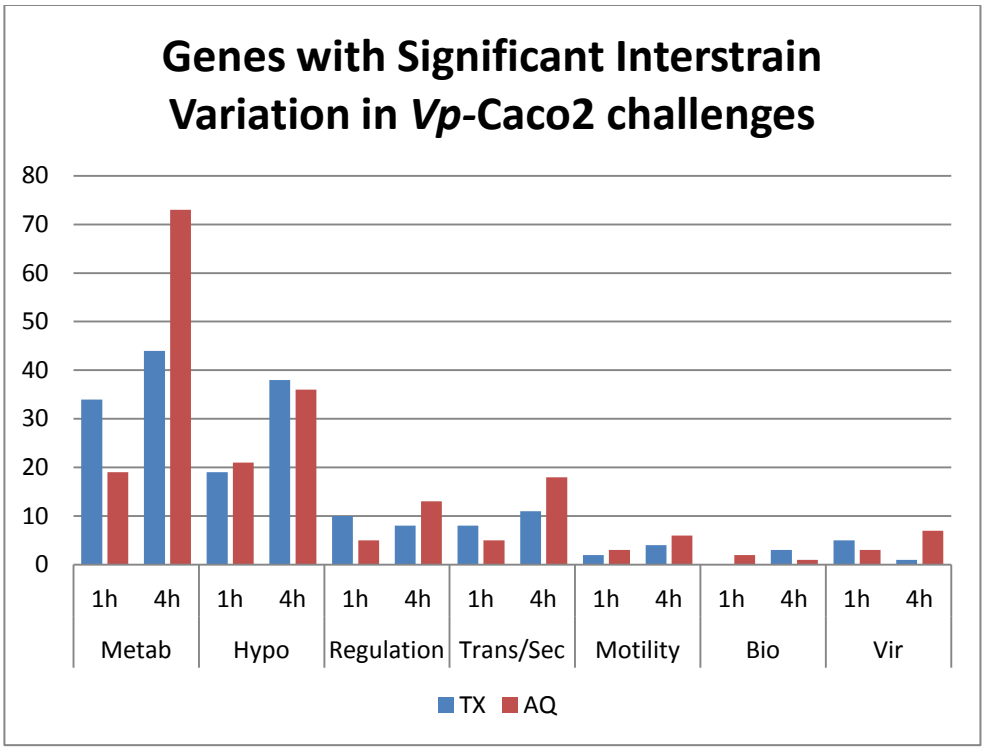

Figure 14. Total number of genes significantly differentially expressed between strains at equal time points in *Vp*-Caco-2 challenges.

Of the 241 genes expressed in higher amounts in AQ 4037, the vast majority (88%) came from the Caco-2 challenge group, while Tx2103 had only 66% (187) of genes from the Caco-2 challenge group. This discrepancy is most visible in the metabolism gene category. The ratio of metabolic genes expressed higher in Tx2103 to AQ4037 was 7.1 and 0.85 in oyster hemolymph and Caco-2 challenge groups, respectively. The large discrepancy of genes expressed to higher degrees in Tx2103 to AQ4037 in oyster hemolymph can be further broken down by time point- at one hour the ratio was 4.6 while at four hours the ratiowas 10.25. The time point ratios in the Caco-2 challenge groups give almost the exact opposite effect, with the ratios of 1.79 and 0.60 for the one hour and four hour time points, respectively (Figure 15-17).

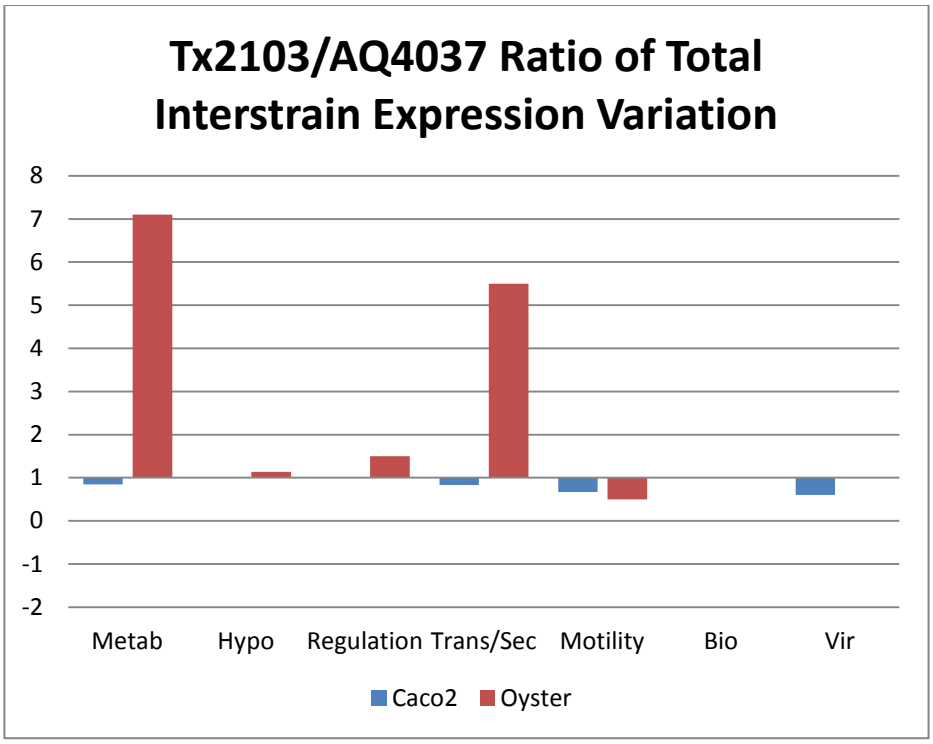

Figure 15. Ratio of Tx2103 differentially up-regulated genes to AQ4037 differentially up-regulated genes across all time points for each gene functional category. The challenge groups are separated.

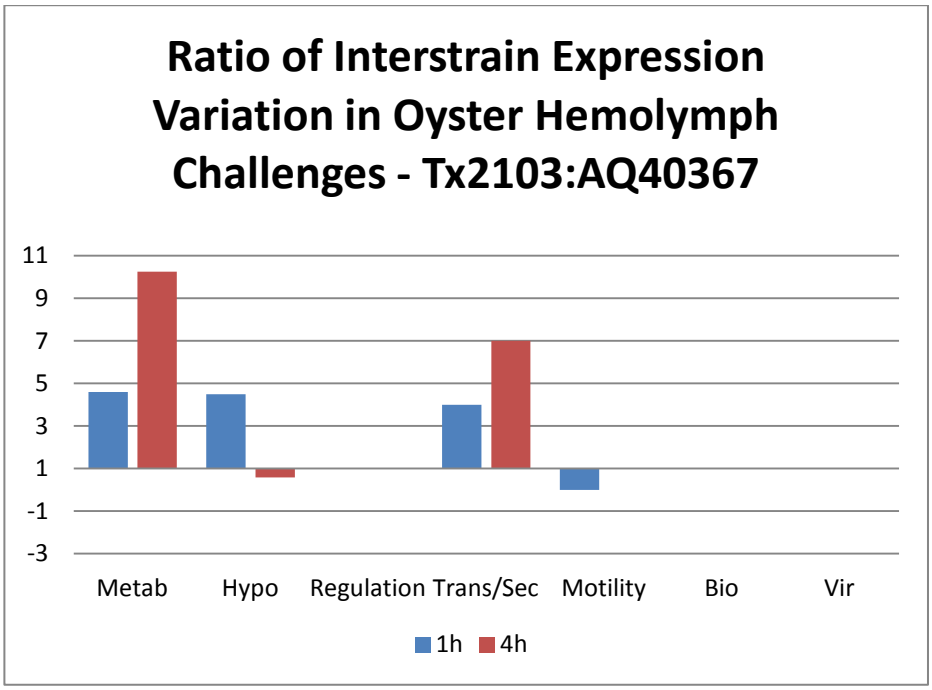

Figure 16. Ratio of Tx2103 differentially up-regulated genes to AQ4037 differentially up-regulated genes for each gene functional category in oyster hemocyte bactericidal assays.

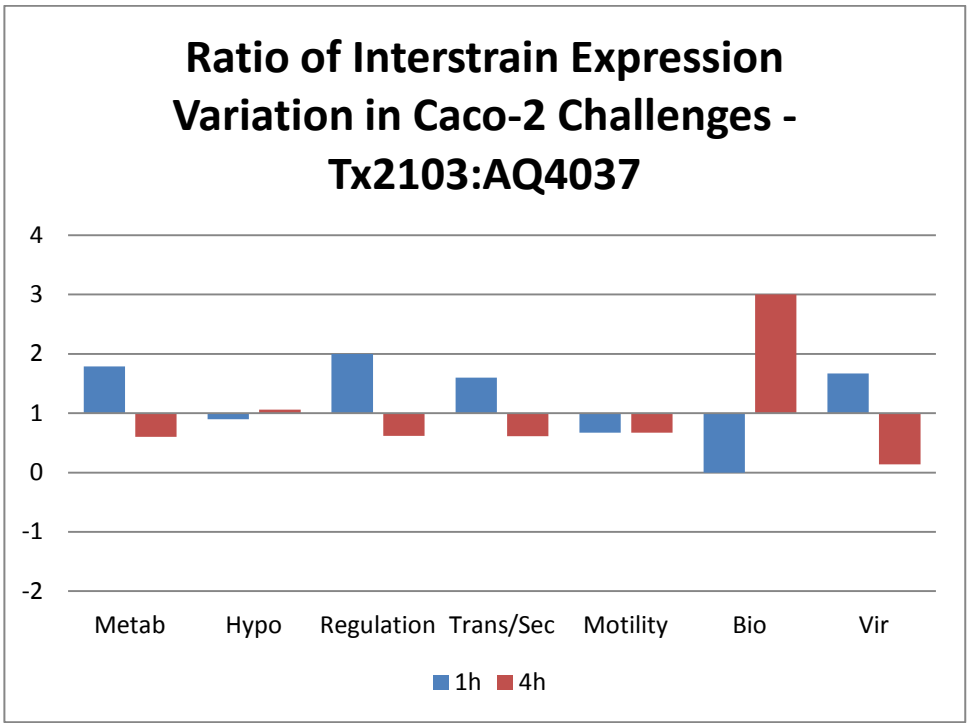

Figure 17. Ratio of Tx2103 differentially up-regulated genes to AQ4037 differentially up-regulated genes for each gene functional category in Caco-2 cytotoxicity assays.

The disparity of strain expression ratios can be further seen in the transport/secretion gene category. In the oyster hemolymph challenge group, the ratio of transport and secretion genes expressed higher in Tx2103 compared to AQ4037 is 5.5, with ratios of 4.0 and 7.0 for the one and four hour time points, respectively. In the Caco-2 challenge group, the ratio is 0.83 with one hour and four hour time points corresponding to the ratios 1.6 and 0.61.

The largest disparities in significant gene expression between strains can be found in metabolism genes at the four hour oyster challenge time point (10.25) and virulence genes at the four hour Caco-2 challenge time point (7.0). Virulence genes were not significantly expressed between strains in any oyster challenge. In Caco-2 challenges, Tx2103 significantly expressed more virulence genes at the early time point (1.67 ratio) than at the late time point (0.14 ratio).

Discussion

This project was designed to gain a deeper understanding of how *Vp* differentially expresses genes between potential pathogen subgroups in a naturally- occurring extreme environment such as exposure to oyster hemocyte. The experimental design to acquire the RNA samples for analysis was based on previous oyster hemocyte bactericidal assays (Chapter III). There is currently little data available on *Vp* transcriptomic responses to oyster hemocyte.

An identical experimental design to the oyster hemocyte bactericidal assay was set up based on *Vp*-Caco-2 cytotoxicity assays. The transcriptomic data gathered from Caco-2 cytotoxicity experiments were used as points of comparison for hemocyte assays. Transcriptomic data from *Vp* in cytotoxicity assays is extremely useful when utilized as a comparison tool, but becomes much weaker as a stand-alone model when assessing *Vp* responses to environmental conditions. The Caco-2 models provide an excellent method for *in vitro* studies of bacterial cytotoxic potential but are not designed as a proxy for the human gut environment.

The genetic cross-talk of tissues and bacteria must be taken into account when analyzing the *Vp* transcriptomic response in these assays. Mussel hemocytes regulate defense and immune-related genes at varying rates for different bacteria (*115, 116*). For instance, it has been demonstrated that hemocytes contribute to bactericidal activity through phagocytosis (*117*). Phagocytosis can be enhanced through the production of enzymes such as integrin and are well regulated in oyster hemocytes (*118*). It has also been demonstrated that different *Vibrio* species can cause different gene regulatory responses in mussel hemocyte (*116, 119*); however, the degree to which strains of a single species differentially affect hemocyte gene expression is unknown. The analysis of the

transcriptomic response of *Vp* in oyster hemocyte bactericidal assays was done recognizing the environmental variability caused by tissue 'cross-talk'. The genetic regulation of oyster hemocyte was not studied in this experiment. Care was taken to normalize all hemocyte tissue samples. All hemolymph was pooled and maintained at an identical cold temperature to reduce clumping and promote uniformity during attachment. Oysters collected for hemocyte extraction were done on the same reef within a specific range of temperature and salinity.

Caco-2 cells express genes which have a profound effect on *Vibrio* pathogenicity and virulence. Caco-2 cells differentiate into intestinal epithelial cells when grown to confluence in a monolayer and display multiple surface antigens. Several virulence factors, such as the T3SS, can cause multiple changes in gene regulation in target cells such as Caco-2 (*37, 61, 62, 120-124*). It has been previously reported that different potential pathogen subgroups contain differing T3SS (among other virulence factors) in *Vp (59)*, therefore there may be differing pathways of contribution to overall cytotoxicity. Mechanisms used by the T3SS can cause different and complex signaling cascades in Caco-2 cells, altering Caco-2 gene expression (*120, 125, 126*). Therefore, variance in genetic 'feedback' must be taken into account when interpreting interstrain *Vp* expression in Caco-2 cytotoxicity assays.

Gene expression was measured by examining the differences in gene expression as opposed to analyzing the absolute transcriptomic response at each time point. Emphasis could be placed on those genes most likely effecting current environmental conditions by focusing on only genes which were up or down-regulated during an exposure. As such, there were a total of 475 genes identified as significantly up or down regulated in a combination of both strains and challenge groups (Appendix A), with 58% total genes

being up-regulated. Neither strain was directly favored in identification of regulated genes over time, 45% of all regulated genes came from Tx2103 while AQ4037 comprised 55%. We found that the PFGRC *Vp* microarrays performed without showing bias. The JCVI PFGRC microarrays used in this experiment contained 70mer probes based on sequence data from available *Vp* genomes, which is limited and comprised mainly of the tdh^{+}/trh^{-} O3:K6 pandemic clone and variants thereof. Inherently, this could favor the Tx2103 strain. While both Tx2103 and AQ4037 are of the O3:K6 serovar, Tx2103 bears a closer genetic relationship to the pandemic clone RIMD2210633, as both are $tdh^{+}/trh^{-}/T3SS2a^{+}$, while AQ4037 is $tdh^{-}/trh^{+}/T3SS2B^{+}$. We found no evidence of this through analysis of available expression data.

Metabolic differences in strains exposed to oyster hemocyte. The functional gene group Metabolic Processes contained the most number of genes in the oyster hemocyte bactericidal challenge groups with 37% of all regulated genes. In the hemocyte assays, Tx2103 and AQ4037 up-regulated a similar number of genes, 16 and 15 respectively. AQ4037 repressed metabolic genes at a significantly greater number of genes than Tx2103- 13 genes compared to 4.

Tx2103 down-regulated a quinone and putative oxidoreductase, a DNA helicase ruvB, and a murein transglycolase. Quinone reductase has been demonstrated in *Vp* to be part of a respiration-driven sodium pump (*127*) that responds under alkaline conditions. Murein transglycolases alter the peptidoglycan layer of the cell during growth and development (*128*). AQ4037 down-regulated several genes involved in amino acid metabolism and synthesis, glycolysis, and DNA synthesis. The majority of metabolic genes down-regulated were involved in protein metabolism (46%).

Genes up-regulated by AQ4037 in the oyster hemolymph challenges included lipid metabolism and biosynthesis, ribosomal biosynthesis, electron transport, and several stress-related genes. Two siderophore synthesis genes were up-regulated, *pvsA* and an *acsD* homologue, suggesting *Vp* AQ4037 was operating under iron limiting conditions. PvsA is a vibrioferrin biosynthesis compound synthesized under iron limiting conditions, while the *acsD* gene contains conserved domain sequences akin to the *Erwinia* acrhomobactin biosynthesis protein (*129*). A general stress resistance gene in *E. coli*, *rpoS* was up-regulated which induces a variety of genes including starvation genes (*130*). Carbon starvation is considered one of the primary inducers of RpoS (*131, 132*).

Tx2103 up-regulated several metabolic genes involved in fatty acid metabolism and biosynthesis, lipid biosynthesis, and oxidative phosphorylation, but did not up-regulate any stress-related or starvation-induced genes. The discrepancy between down-regulated metabolic genes in Tx2103 and AQ4037 could be due to an increased level of fitness of tdh^{+}/trh^{-} potentially virulent *Vp* in oyster tissue. AQ4037 up-regulated several stress-induced genes and siderophores. The majority of genes up-regulated by Tx2103 corresponded to biosynthesis and metabolism. In a separate study of over four years, the presence of potentially virulent *Vp* in oysters from the northern Gulf of Mexico was examined. While several tdh^{+}/trh^{+} and tdh^{+}/trh^{-} were cultured from oyster meat, no tdh^{-}/trh^{+} isolate was cultured from oyster tissue (*31, 59*).

While *Vp* growth in preliminary experiments was very similar for each challenge group, we hypothesize that the diluted EMEM media in Caco-2 experiments could have provided nutrients and compounds unavailable to the *Vp* strains in the oyster hemolymph challenges. The cellular content of Caco-2 cells also differs from oyster hemocytes which could affect the available resources for *Vp* if these cells were lysed. Furthermore, the Caco-

2 and hemolymph challenges were run in separate distinct environmental conditions: Caco-2 challenges were done at 37°C with 5% CO_2 in diluted EMEM while oyster hemolymph challenges were done at 22°C in 18 ppt ASW with no media supplementation. For these reasons, there was no examination of differences in gene expression between tissue groups.

The Caco-2 challenges presented contrasting metabolic expression data to the oyster hemolymph challenges. The *Vp* strain AQ4037 up-regulated twice as many metabolic genes as down-regulated. Tx2103 up-regulated several metabolic genes involved in DNA/RNA synthesis, stabilization, and repair as well as two genes coding for proteins involved in the breakdown of peptidoglycan. Alcohol dehydrogenase and glutathione peroxidase were also up-regulated, suggesting oxidative stress. Conversely, Tx2103 down-regulated several genes involved in carbohydrate metabolism, biosynthesis, and electron transport.

AQ4037 up-regulated a wide variety of metabolic genes including fatty acid synthesis and metabolism, sugar metabolism, RNA synthesis, and electron transport. Down-regulated genes included amino acid metabolism and biosynthesis, DNA repair and synthesis, sugar biosynthesis and metabolism, and a single heat-shock protein, related to DnaJ.

Shifts in Patterns of Localized Hypothetical Gene Expression in Vp-Oyster Hemocyte Assays. A total of 145 hypothetical and conserved genes were significantly up or down-regulated over time in both Caco-2 and oyster hemocyte assays. Combining data from both strains, more hypothetical genes were up-regulated in Caco-2 challenges (72%) than in oyster challenges. Some of the hypothetical genes were found to have metabolism-related conserved domains which could partly explain why hypothetical genes were regulated at greater frequency in Caco-2 challenge groups than in oyster hemolymph.

Vp contains two chromosomes of 3.29Mbp (I) and 1.88Mbp (II). Both chromosomes contain an identical percentage of protein coding regions with nearly identical average coding length (*23*). Chromosome I contains most of the essential growth and viability genes including copies of each tRNA gene; chromosome II contains some essential genes and genes related to regulation and transport. Chromosome II is considered to have a role in environmental adaptation (*23*).

In the oyster hemolymph challenges, Tx2103 significantly regulated more genes on chromosome II than AQ4037 in oyster hemolymph (13 to 2), but not in Caco-2 cells (23 to 34). Since chromosome II has been related more to environmental adaptation, these hypothetical proteins could be involved in pathways which helps Tx2103 adapt to the oyster environment. Both strains regulated a similar relative number of genes on chromosome I in both challenge groups. While many regulated hypothetical genes contain putative conserved domain sequences such as permeases, ATPases, and Rf2 transcriptional regulator, multiple hypothetical genes with no predicted function were seen regulated across both strains. Specifically, in oyster hemolymph challenges DUF-family motif hypothetical genes VP0752 and VP0836 were up-regulated, while DUF-motif containing hypothetical gene VPA1284 was down-regulated. It should be noted that VPA1284 was the only hypothetical gene on chromosome II which AQ4037 significantly down-regulated in oyster hemolymph challenges.

Transport, Attachment, and Virulence expression in oyster hemocyte and Caco-2 cytotoxicity assays. Tx2103 up-regulated several sodium symporter genes in oyster hemolymph challenges, which is intuitive when taking into account the both the halophilic nature of the bacterium and high sodium environment. Vibrios can produce ATP with a sodium motive force (*127*). Also, in *Vp* the polar flagella are driven via a sodium pump

while lateral flagella are driven with a proton pump (*133*). In the oyster hemocyte assays Tx2103 up-regulated flagellar proteins including the hook protein and motor flagellum-specific ATP synthase. Tx2103 down-regulated genes involved in potassium uptake and macrolide-specific efflux proteins. These results suggest that Tx2103 was able to take advantage of the halophilic environment of the hemolymph challenge. AQ4037 up-regulated only 3 transport/secretion genes in oyster hemolymph. All up-regulated genes were ABC transporters, including one hemin transporter. The up-regulation of the hemin transporter corresponds with the increase in siderophore gene transcription seen in AQ4037 oyster hemolymph challenges. AQ4037 also down-regulated few transport/secretion genes, of note the outer membrane protein *ompV* was down-regulated, which functions in NaCl regulation in *Vp* (*134*).

The general functions of transport/secretion genes regulated in Caco-2 trials were different from hemolymph trials in both strains. Tx2103 up-regulated a single sodium/proline symporter along with multiple outer membrane proteins, secretion proteins, and a sodium-type flagellar protein precursor. Down-regulated genes included multiple ABC transporters, a sodium/glutamate symporter, MSHA-related attachment proteins, and *ExbD2*, a TonB system transport protein. The TonB system in gram-negative bacteria helps to transmit the proton motive force from the cytoplasmic membrane to the outer membrane, where it can be used to fuel multiple functions (*135*).

In Caco-2 challenges, AQ4037 preferred motility to attachment. AQ4037 up-regulated several motility-related genes including *flhB, flhF, CheZ, flgE*, and two flagellar and biofilm-related proteins. 42% of all down-regulated genes in AQ4037 were adhesion related proteins, including *pilZ*, a type IV pilus assembly protein.

Very few virulence factors were detected as being significantly regulated in any strain or challenge group. These results can be explained by the relationship between quorum-sensing, nutrient density, and virulence. It has been shown that surface sensing in *Vp* promotes genetic expression of colonization and virulence genes (*106, 136, 137*). Furthermore, virulence factors such as the T3SS can be induced by the limitation of certain nutrients such as iron and calcium (*136*) and under certain cell densities (*100*). Specifically, *Vp* and *V. harveyi* have been shown to secrete virulence factors under low-density conditions through an auto-inducing signaling cascade. This has been demonstrated in an opposite manner to Enterohemarrogenic *E. coli*, which secrete T3SS proteins at high cell densities (*138*). Experiments showing virulence production under low-density conditions occurred over a 14 hour time frame, while the short nature of these tissue exposures could have not provided the time necessary to promote observable changes in genetic expression. It should also be noted that while limited calcium is a proven promoter of T3SS gene expression, both challenges took place in calcium rich environments.

Overall, many significant differences in genetic expression were found between *Vp* strains in oyster hemocyte bactericidal assays. These differences were further illustrated by analyzing the transcriptomic response of *Vp* in a cytotoxic-inducing environment and comparing the results to *Vp*-hemocyte gene regulation. This study has demonstrated that tdh^{+}/trh^{-} and tdh^{-}/trh^{+} strains of *Vp* significantly differ in many functional categories when exposed to oyster hemocyte.

CHAPTER V

CONCLUSIONS AND FUTURE DIRECTIONS

Potential pathogen *Vp* subgroups displayed unique and separate characteristics throughout this project. Only 130 potentially pathogenic *Vp* strains out of thousands isolated from the northern Gulf of Mexico were found to contain *tdh* and/or *trh*. Approximately half of these strains came from sediment, the remaining strains were isolated evenly between water and oyster tissue. Only three *tdh*$^-$/*trh*$^+$ isolates were found over four years of sampling, and all occurred in sediment at one site. REP and ERIC-PCR showed that these strains shared strong homology but were not identical. Thesis data suggest that in the northern Gulf of Mexico the environment may be more favorable to potentially pathogenic *Vp* that carry *tdh*.

A representative *tdh*$^+$/*trh*$^-$ *Vp* strain up-regulated metabolic, hypothetical, transport, and secretion-related genes at a significantly higher frequency than a representative *tdh*$^-$/*trh*$^+$ strain in oyster hemocyte bactericidal assays. Furthermore, the *tdh*$^-$/*trh*$^+$ strain induced multiple stress response genes. These same expression patterns were not seen in Caco-2 cytotoxicity assays. The oyster bactericidal assay contained lower nutrients and were more indicative of natural conditions compared to the Caco-2 cytotoxicity assays. It is unsure if the differences in genetic expression were due to the lower nutrient environment or the presence of hemocytes or both.

The potential pathogen subgroups of *Vp* did not display any significant difference in bacterial oyster hemocyte assays. This suggests that neither *tdh*$^+$/*trh*$^-$ nor *tdh*$^-$/*trh*$^+$ subgroups are better equipped to deal with hemocyte exposure. Differences in regulated genes between subgroups is therefore slightly more likely due to be a response of environmental conditions, not the presence of hemocytes.

The results of these experiments indicate that metabolism plays a strong role in how potentially pathogenic *Vp* isolates are distributed in the environment and that metabolic factors may be useful indicator of potentially pathogenic strains. Future research should acknowledge that this data used representative clinical strains for expression studies. The rarity of *tdh*$^{-}$/*trh*$^{+}$ isolates in the northern Gulf of Mexico is a double-edged sword- it is both an interesting discovery and a limitation to the significance that can be placed on data acquired from potential pathogen subgroup analysis. An experiment which is able to test a large collection of environmental and clinical *tdh*$^{-}$/*trh*$^{+}$ isolates could help increase the significance of these findings.

The functions of all organisms are extremely complex at the molecular level. A strong assessment of relevant genetic characteristics, such as transcriptomics, in *Vp* provides a good framework for additional research but cannot be generalized. Environment, time, and cell densities are some of many variables which affect *Vp.* The combination of genetic and organism-level experiments help to ensure a lucid understanding of potentially pathogenic *Vp* and their role in the environment.

APPENDIX A

OLIGONUCLEOTIDE PRIMERS USED IN THIS STUDY

Name	Sequence	Reference
tdh_89F	TCCCTTTTCCTGCCCCC	(*139*)
tdh_321R	CGCTGCCATTGTATAGTCTTTATC	(*139*)
trh_20F	TTGCTTTCAGTTTGCTATTGGCT	(*139*)
trh_292R	TGTTTACCGTCATATAGGCGCTT	(*139*)
tl_884F	ACTCAACACAAGAAGAGATCGACAA	(*139*)
tl_1091R	GATGAGCGGTTGATGTCCAAA	(*139*)
VP1669F	TACCGAGTTGCCAACGTG	This Study
VP1669R	GATTGTTCCGCGATTTCTTG	This Study
VP1670F	ACCGATTACTCAAGGCGATG	This Study
VP1670R	TACGTTGTTGGCGTGATTGT	This Study
VP1686F	CAAAAGCGATCACAAAAGCA	This Study
VP1686R	AGCGACTTAACGGCATCATC	This Study
VP1689F	AAGGTTGGCAAAAAGCGTTA	This Study
VP1689R	GCTCTTCAACGAGCCAAGAG	This Study
VP1694F	ACGATGCGACCAACAGTGTA	This Study
VP1694R	TTTTAATTGCATCGGTGACG	This Study
VPA1327F	TGGCGAAAGAGCCATTAGAT	This Study
VPA1327R	TCAACTCCAAATTCGCCTTC	This Study
VPA1335F	ATGTAACGGCGGCTAGCTTA	This Study
VPA1335R	CAAACTGTGTCAGTAGCACCA	This Study

VPA1339F	GATTCGCGGAACTCAAGAAG	This Study
VPA1339R	CTTGTCCGAGATCAACGTCA	This Study
VPA1346F	GGCTCTGATCTTCGTGAA	This Study
VPA1346R	GATGTTTCAGGCAACTCTC	This Study
VPA1354F	AATTGGCCGAGCCAACTTT	This Study
VPA1354R	GTCATCCGGTTCTTGTGTAA	This Study
VPA1362F	CTGCAGGTATCGCATCTTCA	This Study
VPA1362R	TTAGAACCAACCGACGAAGC	This Study
Beta_vscC2_F	GTACTTTGCTGTCTAACC	(*58*)
Beta_vscC2_R	CTTACTCTTAACTTCCGACG	(*58*)
Beta_vscS2_F	TTGATGTTGTTTCGGCTAGC	(*58*)
Beta_vscS2_R	CCACCGCCGAACTCGGCTAACAAG	(*58*)
Beta_vopB2_F	GAGCCTGTTGCTCTATGGAGCCAGG	(*58*)
Beta_vopB2_R	CGACACAGAACGCAATGCTTGCTCG	(*58*)
Beta_vopC_F	AACCAACTTGCGACTAAATC	(*58*)
Beta_vopC_R	TCCCGACAGTTTTTCTGCAC	(*58*)
GS-PCR_F	TAATGAGGTAGAAACA	(*43*)
GS-PCR_R	ACGTAACGGGCCTACA	(*43*)

APPENDIX B

VIBRIO PARAHAEMOLYTICUS ISOLATES USED IN CYTOTOXICITY AND HEMOCYTE BACTERICIDAL ASSAYS

Isolate Storage Code	*tlh*	*tdh*	*trh*	*environmental/clinical*
AK strain	+	+	+	clinical
BAA-238	+	+	+	clinical
F11	+	+	+	clinical
Vp2007-095	+	+	+	clinical
Vp2006-016	+	+	+	environmental
Vp2007-023	+	+	+	environmental
Vp2007-052	+	+	+	environmental
Vp2007-057	+	+	+	environmental
Vp2009-015	+	+	+	environmental
Vp2009-026	+	+	+	environmental
Tx2103	+	+	-	clinical
CT6636	+	+	-	clinical
Vp2006-001	+	+	-	environmental
Vp2006-004	+	+	-	environmental
Vp2006-008	+	+	-	environmental
Vp2006-041	+	+	-	environmental
Vp2007-064	+	+	-	environmental
Vp2007-070	+	+	-	environmental
Vp2007-106	+	+	-	environmental
Vp2009-027	+	+	-	environmental

AQ4037	+	-	+	clinical
KCHD 613	+	-	+	clinical
Vp2007-005	+	-	+	environmental
Vp2007-007	+	-	+	environmental
Vp2007-025	+	-	+	environmental
FIHES	+	-	-	clinical
901128	+	-	-	clinical
NY3547	+	-	-	clinical
Vp2006-009	+	-	-	environmental
Vp2007-004	+	-	-	environmental
Vp2007-017	+	-	-	environmental
Vp2007-026	+	-	-	environmental

APPENDIX C

GENES SIGNIFICANTLY UP OR DOWN-REGULATED IN *VP* OYSTER HEMOCYTE AND CACO-2 CHALLENGES

Locus	Gene Name	Description
		Tx2103 – Oyster – Down-regulated
VPA0478		putative oxidoreductase
VP2542		quinone oxidoreductase
A79_5812	ruvB	holliday junction DNA helicase RuvB
VP2628		membrane-bound lytic murein transglycosylase C
VPA0223		putative HlyD family secretion protein
VPA0223		putative HlyD family secretion protein
VP0535	lspA	signal peptidase II
A79_0503		potassium uptake protein, TrkH family
VPA0409		plasma membrane protein involved in salt tolerance
A79_4324		Flp pilus assembly protein
A79_5698		RDD family, putative
VP0728		hypothetical protein
VPA0370		hypothetical protein
VPA0393		hypothetical protein
VPA0557		hypothetical protein
VPA0945		hypothetical protein
VPA0946		hypothetical protein
VPA0946		hypothetical protein
VPA1284		hypothetical protein
VPA1470		hypothetical protein
VPA1711		hypothetical protein
A79_3171		protein YgiW
VP1211		sensor histidine kinase
A79_2580	proB	glutamate 5-kinase
		Tx2103 – Oyster – Up-regulated
A79_5012		glycerol-3-phosphate dehydrogenase [NAD(P)+] (NAD(P)H-dependent glycerol-3-phosphate dehydrogenase)
A79_5726		ribosomal protein L13
VP0442		ubiquinol-cytochrome c reductase, cytochrome b
VP0739		ribose-phosphate pyrophosphokinase
VP1143		imidazole glycerol phosphate synthase subunit HisF
VP1591		3-hydroxydecanoyl-ACP dehydratase
VP2269		succinyl-diaminopimelate desuccinylase
VP2433		purine nucleoside phosphorylase
VP2550	recA	recombinase A

VP2832	gpsA	NAD(P)H-dependent glycerol-3-phosphate dehydrogenase
VP2880		acetyl-CoA carboxylase
VP3027		thiamine biosynthesis protein ThiC
VPA1012		cytochrome c554
VPA1121		putative acyl-CoA dehydrogenase
VPA1122		putative aldehyde dehydrogenase
VPA1122		putative aldehyde dehydrogenase
A79_0469		conserved hypothetical protein
VP0474		hypothetical protein
VP0752		hypothetical protein
VP0836		hypothetical protein
VP1131		hypothetical protein
VP1377		hypothetical protein
VP1415		hypothetical protein
VP1714		hypothetical protein
VP2025		hypothetical protein
VP2161		hypothetical protein
VPA1149		hypothetical protein
VPA1465		hypothetical protein
A79_3585		cyclic nucleotide binding protein/2 CBS domains
VC1273		extracellular solute-binding protein, family 7
VP1597		putative N6-adenine-specific DNA methylase
A79_3591		sodium/solute symporter, putative
A79_3591		sodium/solute symporter, putative
VP2869		sodium/solute symporter
VP2869		sodium/solute symporter
VPA0166		putative outer membrane protein
VP0778		flagellar hook protein
VP0778		flagellar hook protein
VPA1533		putative flagellum-specific ATP synthase

Tx2103 – Caco-2 – Down-regulated

A79_0634		lactaldehyde reductase
A79_0994	ectA	L-2,4-diaminobutyric acid acetyltransferase
A79_1067		citrate synthase
A79_1166		sulfatase
A79_1298		probable 6-phospho-beta-glucosidase
A79_1741		endonuclease/exonuclease/phosphatase family
A79_1923		deCa-heme c-type cytochrome
A79_2025		translation elongation factor
A79_2026		mandelate racemase
A79_3791	oadA	oxaloacetate decarboxylase alpha subunit
A79_4400		Zn-dependent protease

A79_4475	cydB	cytochrome D ubiquinol oxidase, subunit II
A79_4818		chromosome partition protein MukB
A79_4898		acetyltransferase, gnat family
A79_5364		endochitinase
A79_6218		NADP-dependent fatty aldehyde dehydrogenase
VCA0859		oxidoreductase, aldo/keto reductase 2 family
VP0028		zinc-binding alcohol dehydrogenase
VP0482		glutamate synthase, large subunit
VP0748		5'-nucleotidase precursor
VP2444		putative acetyltransferase
VP2461		phosphoglucomutase/phosphomannomutase family protein MrsA
VPA0102		putative isomerase
VPA0958		putative NADH oxidase
VPA0984		uroporphyrin-III C-methyltransferase
VPA1129		putative hydroxymethylglutaryl-CoA lyase
VPA1147		putative phenylacetate-CoA ligase
VPA1411		putative glycosyltransferase
A79_1306		conserved hypothetical protein
A79_1516		conserved hypothetical protein
A79_1943		conserved hypothetical protein
A79_4920		conserved hypothetical protein
A79_5405		conserved hypothetical protein
A79_6125		conserved hypothetical protein
VP0474		hypothetical protein
VP0625		hypothetical protein
VP0626		hypothetical protein
VP0989		hypothetical protein
VP1223		hypothetical protein
VP1939		hypothetical protein
VP2341		hypothetical protein
VP2421		hypothetical protein
VPA0137		hypothetical protein
VPA0140		hypothetical protein
VPA0837		hypothetical protein
VPA1031		hypothetical protein
VPA1074		hypothetical protein
VPA1146		hypothetical protein
A79_2291		transmembrane regulatory protein ToxS
A79_3690		transcriptional regulator
A79_4210	pcm	protein-L-isoaspartate O-methyltransferase
A79_4578		methyltransferase
VP0122		BipA protein
VPA0335		SoxR protein

VPA1497		transcriptional regulator, LysR family
VPA1655		putative FecB
A79_1508		ABC transporter, permease/ATP-binding protein
A79_2318		putative sugar transport system
A79_3700		multidrug resistance protein A
VP0415		putative general secretion pathway protein A
VP0660		putative type IV pilin
VP0702		SecY interacting protein Syd
VP1218		putative outer membrane protein precursor
VP1435		putative sodium/glutamate symporter
VP2702		MSHA biogenesis protein MshN
VPA0154		TonB system transport protein ExbD2
VPA0604		ABC transporter, periplasmic substrate-binding protein
VPA1166		chloride channel protein
A79_2667		polar flagellin A
A79_3151		putative biofilm-associated surface protein
VPA1329		putative traA protein

Tx2103 – Caco-2 – Up-regulated

A79_0026		chitobiase
A79_0678		ABC transporter, ATP-binding protein
A79_1359	argG	argininosuccinate synthase
A79_1778		UTP--glucose-1-phosphate uridylyltransferase
A79_1855		glutaredoxin
A79_2942		translation initiation factor IF-2
A79_3490		ImcF-related family
A79_3675		glutathione peroxidase
A79_4878		amidohydrolase 3
A79_5231		prolipoprotein diacylglyceryl transferase
A79_5242		thiol:disulfide interchange protein DsbC
A79_5484		conserved hypothetical protein
A79_6050		cell wall-associated hydrolase
A79_6198	hmgA	homogentisate 1,2-dioxygenase
VP0041		ATP-dependent DNA helicase Rep
VP0157		ATP-dependent DNA helicase RecG
VP0481		glutamate synthase, small subunit
VP0513	lysS	lysyl-tRNA synthetase
VP0665		transglycosylase, Slt family
VP0716		lipoyl synthase
VP0722		penicillin-binding protein 2
VP1255		GGDEF family protein
VP1301		exodeoxyribonuclease I
VP2322		pseudouridine synthase Rlu family protein
VP2400		UDP-glucose 4-epimerase

VP2861		rRNA methylase, SpoU family
VP2911		DNA-binding protein HU-2
VP2942		soluble pyridine nucleotide transhydrogenase
VP3000	rho	transcription termination factor Rho
VPA0123		putative hydrolase
VPA0124		putative acetyltransferase
VPA0436		putative resolvase
VPA0474		spermidine n1-acetyltransferase
VPA0566		alcohol dehydrogenase
VPA1201		periplasmic nitrate reductase, cytochrome c-type protein
A79_0571		hypothetical protein
A79_0584		conserved hypothetical protein
A79_0604		conserved hypothetical protein
A79_1952		conserved hypothetical protein
A79_3581		conserved hypothetical protein
A79_3692		conserved hypothetical protein
A79_4983		conserved hypothetical protein
VCA0645		hypothetical protein
VP0473		hypothetical protein
VP1559		hypothetical protein
VP1683		hypothetical protein
VP2085		hypothetical protein
VP2172		hypothetical protein
VP2774		hypothetical protein
VP2905		hypothetical protein
VPA0005		hypothetical protein
VPA0056		hypothetical protein
VPA0418		hypothetical protein
VPA0749		hypothetical protein
VPA0787		hypothetical protein
VPA0933		hypothetical protein
VPA0933		hypothetical protein
VPA1344		hypothetical protein
VPA1426		hypothetical protein
VPA1743		hypothetical protein
A79_0525		CpsF
A79_1659		protein YhgF
A79_5786		sensory box/ggdef family protein
VP0569		DNA-binding response regulator PhoB
VP0833	fur	ferric uptake regulator
VP2574		GTP-binding protein LepA
VP2857		putative periplasmic protein CpxP
A79_0499		ABC-type multidrug efflux pump
A79_1271		outer membrane protein

A79_1552		putative msha pilin protein msha
A79_1627		amino-acid abc transporter binding protein
A79_1684	putP	sodium/proline symporter
A79_2015		outer membrane protein
VPA0721		rough colony protein RcpA
VPA0856		putative transmembrane transport protein
A79_1849		methyl-accepting chemotaxis protein
VPA1539		putative sodium-type flagellar protein MotY precursor
VPA1541		flagellar motor switch protein
A79_3703		autoinducer 2 sensor kinase/phosphatase LuxQ
VPA1218		putative secretion protein

AQ4037 – Oyster – Down-regulated

A79_0425	kbl	2-amino-3-ketobutyrate coenzyme A ligase
A79_2680		lipoprotein-34 NlpB
A79_3664		sulfatase
A79_4129		PhoH family protein
A79_4272		protein ThiJ
A79_5966	pyk	pyruvate kinase
A79_5966	pyk	pyruvate kinase
VP1103		alanine dehydrogenase
VP2428		elongation factor EF-2
VP2434		phosphopentomutase
VP2948		4-hydroxybenzoate octaprenyltransferase
VP2953		RNA polymerase sigma factor 32
VPA0169		agmatinase
VP0187		putative Dca
VP0219		hypothetical protein
VP0254		hypothetical protein
VP1041		gonadoliberin III-related protein
VP2469		hypothetical protein
VP3030		hypothetical protein
VPA1284		hypothetical protein
A79_2408		GTP-binding protein Obg/CgtA
A79_4778		transcriptional regulatory protein FixJ
VP2577	rseA	sigma-E factor negative regulatory protein RseA
VP2772	rpsG	30S ribosomal protein S7
VPA1538		putative two-component response regulator
VP0535	lspA	signal peptidase II
VP1194		putative ABC transporter, ATP-binding protein
VP2676		PmbA protein
VPA0318		putative outer membrane protein OmpV
VPA0318		putative outer membrane protein OmpV
VPA1533		putative flagellum-specific ATP synthase

AQ4037 – Oyster – Up-regulated

A79_3197		vibrioferrin biosynthesis protein PvsA
A79_4687		redoxin domain protein
A79_6044		smr/muts family protein
VC1144		ATP-dependent Clp protease, ATP-binding subunit ClpA
VC2260		30S ribosomal protein S2
VP0237		UTP-glucose-1-phosphate uridylyltransferase
VP0263	rpsC	30S ribosomal protein S3
VP1181		lactonizing lipase
VP1591		3-hydroxydecanoyl-ACP dehydratase
VP2053		acyl carrier protein
VP2873	fumC	fumarate hydratase
VP2873	fumC	fumarate hydratase
VPA0454		putative DNA-binding stress protein
VPA1510		2-amino-3-ketobutyrate coenzyme A ligase
VPA1661		putative AcsD
A79_4798		conserved hypothetical protein
VC1778		hypothetical protein
VP0595		hypothetical protein
VP0752		hypothetical protein
VP0752		hypothetical protein
VP0836		hypothetical protein
VP1322		putative LicD1 protein
VP2328		hypothetical protein
VP2424		hypothetical protein
VPA1330		hypothetical protein
A79_0955		transcriptional regulator, MarR family
A79_3059		YheO domain protein
A79_3585		cyclic nucleotide binding protein/2 CBS domains
A79_4208		RNA polymerase sigma factor 32 (RpoS)
A79_4376		putative LysR-family transcriptional regulator
VC0415		rod shape-determining protein MreB
VP2632		transcriptional regulator, LacI family
A79_0162		peptide transport system ATP-binding protein SapF
VPA0133		putative ABC transporter substrate-binding protein
VPA0423		hemin ABC transporter, periplasmic hemin-binding protein HutB

AQ4037 – Caco-2 – Down-regulated

A79_0177	metC	cystathionine beta-lyase
A79_0319		RNA pseudouridine synthase family protein
A79_0891		acetyltransferase
A79_1711		phospholipase, patatin family

A79_1845		efflux ABC transporter, permease protein
A79_2269		glycosyl transferase, family 39
A79_2810		4-aminobutyrate aminotransferase
A79_3146		oxidoreductase alpha (molybdopterin) subunit
A79_3363		khg/kdpg aldolase
A79_4285		tellurite resistance protein
A79_4432		ferredoxin-dependent glutamate synthase 1
VC0305		ATP-dependent RNA helicase
VP0033		protoporphyrinogen oxidase
VP0735		2-octaprenyl-3-methyl-6-methoxy-1,4-benzoquinol hydroxylase
VP0829		N-acetylglucosamine-6-phosphate deacetylase
VP1048	ruvC	Holliday junction resolvase
VP1301		exodeoxyribonuclease I
VP1646		aconitate hydratase
VP2186		bacteriocin production protein
VP2316		uridylate kinase
VP2552		DNA mismatch repair protein
VP2885		DNA-binding protein Fis
VP3035		Sua5/YciO/YrdC family protein
VPA0278		isopentenyl pyrophosphate isomerase
VPA0867		DnaJ-related protein
VPA1158		acetyl-CoA synthase
VPA1201		periplasmic nitrate reductase, cytochrome c-type protein
A79_0377		YjqA
A79_0876		conserved hypothetical protein
A79_1669		conserved hypothetical protein
A79_1851		hypothetical protein
A79_2215		hypothetical protein
A79_2446		hypothetical protein
A79_2553		conserved hypothetical protein
A79_4489		hypothetical protein
A79_4496		hypothetical protein
A79_4782		hypothetical protein
A79_5417		conserved hypothetical protein
A79_5997		conserved hypothetical protein
VCA1065		hypothetical protein
VP0913		hypothetical protein
VPA0443		hypothetical protein
VPA0720		hypothetical protein
VPA0748		hypothetical protein
VPA0772		hypothetical protein
VPA1027		hypothetical protein
VPA1092		hypothetical protein

VPA1599		hypothetical protein
VPA1692		hypothetical protein
A79_0638		transcriptional regulator, AraC family
A79_1285		protein in PtsN-ptsO intergenic region
A79_4639		two-component response regulator
A79_5987		twin-arginine translocation pathway signal
VCA0682		transcriptional regulator UhpA
VP1755		putative histidine kinase
A79_1439		permease of the drug/metabolite transporter
A79_3159		cation efflux system
A79_3605		MadN protein
A79_3675		glutathione peroxidase
A79_3727	napD	NapD protein
A79_4966		permease of the major facilitator superfamily
VP3066		putative amino acid ABC transporter, permease protein
VPA0153		TonB system transport protein ExbB2
VPA0650		heat shock protein 70 family protein
VPA0721	rcpA	rough colony protein RcpA
VPA1131		putative periplasmic binding protein-related protein
VP1535	uspE	putative stress protein
VP2159		putative methyl-accepting chemotaxis transmembrane protein
VP2254		flagellar protein FliS
VPA1554		LafF
VPA0939		putative adhesin
VPA1307		putative adhesion protein
A79_0585		VcsR2
A79_2095		type IV pilus assembly protein PilZ

AQ4037 – Caco-2 – Up-regulated

A79_0426	tdh	L-threonine 3-dehydrogenase
A79_1191	moaD	molybdopterin converting factor, subunit 1
A79_1643	pfkA	6-phosphofructokinase
A79_2228		polyribonucleotide nucleotidyltransferase
A79_2276		DNA gyrase/topoisomerase IV, A subunit
A79_3168		ATP-dependent Zn protease
A79_4292	glpK	glycerol kinase
A79_4687		redoxin domain protein
A79_5041	menB	naphthoate synthase
A79_5105	mobA	molybdopterin-guanine dinucleotide biosynthesis protein A
A79_5288		soluble lytic murein transglycosylase
A79_5815	ruvC	crossover junction endodeoxyribonuclease RuvC
A79_5816	aspS	aspartyl-tRNA synthetase
A79_6062		isocitrate dehydrogenase, NADP-dependent

A79_6250	purT	phosphoribosylglycinamide formyltransferase 2
A79_6262		endonuclease 4
VC2260		30S ribosomal protein S2
VP0152	greB	transcription elongation factor GreB
VP0202		putative sugar-phosphate nucleotide transferase
VP0231		putative UDP-galactose phosphate transferase
VP0507		branched chain amino acid transport system II carrier protein
VP0846	sdhB	succinate dehydrogenase catalytic subunit
VP1533		putative ATPase
VP1542		cytochrome c oxidase, subunit CcoQ
VP1591		3-hydroxydecanoyl-ACP dehydratase
VP1591		3-hydroxydecanoyl-ACP dehydratase
VP1724		DNA polymerase III subunit epsilon
VP2055		acyl carrier protein S-malonyltransferase
VP2055		acyl carrier protein S-malonyltransferase
VP2056		3-oxoacyl-(acyl carrier protein) synthase
VP2071		fatty acid metabolism regulator
VP2096		molybdenum cofactor biosynthesis protein A
VP2194		3-oxoacyl-[acyl-carrier-protein] synthase I
VP2273	dapA	dihydrodipicolinate synthase
VP2326		acetyltransferase-related protein
VP2326		acetyltransferase-related protein
VP2342		DNA polymerase IV
VP2355		peptidyl-prolyl cis-trans isomerase A
VP2437		NupC family protein
VP2599		fructose-bisphosphate aldolase
VP2676	tldE	PmbA protein (peptidase)
VPA0263		flagellar basal body P-ring biosynthesis protein
VPA0436		putative resolvase
VPA0452		putative cytochrome b561
VPA0466		universal stress protein A
VPA0611		acetate/propionate kinase
VPA0618		putative acyl-CoA dehydrogenase
VPA0648		putative DOPA-dioxygenase-related protein
VPA1157		electron transfer flavoprotein, alpha-subunit
VPA1498		putative L-lactate permease
A79_0469		conserved hypothetical protein
A79_0469		conserved hypothetical protein
A79_0903		conserved hypothetical protein
A79_1374		Hypothetical - FOG ggdef domain
A79_1810		conserved hypothetical protein
A79_2007		conserved hypothetical protein
A79_4386		conserved hypothetical protein
A79_4827		Hypothetical - gonadoliberin III-related protein

VC1685		hypothetical protein
VCA0645		hypothetical protein
VCA0967		hypothetical protein
VP0039		hypothetical protein
VP0595		hypothetical protein
VP0749		hypothetical protein
VP0898		hypothetical lipoprotein
VP0901		hypothetical protein
VP0937		hypothetical protein
VP0943		hypothetical protein
VP1518		hypothetical protein
VP1659		hypothetical protein
VP1803		hypothetical protein
VP2421		hypothetical protein
VP2789		hypothetical protein
VP2850		hypothetical protein
VP2905		hypothetical protein
VP3049		SpoOM-related protein
VPA0039		hypothetical protein
VPA0156		hypothetical protein
VPA0206		hypothetical protein
VPA0219		hypothetical protein
VPA0324		hypothetical protein
VPA0406		hypothetical protein
VPA0451		hypothetical protein
VPA0499		hypothetical protein
VPA0521		hypothetical protein
VPA0652		hypothetical protein
VPA0934		hypothetical protein
VPA1352		hypothetical protein
A79_2612		hypothetical adenine-specific methylase YfcB
A79_4974		AraC-type DNA-binding domain-containing protein
VP0899		putative O-methyltransferase
VP1101	cysB	transcriptional regulator for cysteine regulon
VP1130		tRNA (5-methylaminomethyl-2-thiouridylate)-methyltransferase
VP1734		DNA-binding response regulator
VP2793		cyclic AMP receptor protein
VP2824		ribosome-associated GTPase
VP3067	glmU	bifunctional N-acetylglucosamine-1-phosphate uridyltransferase/glucosamine-1-phosphate acetyltransferase
VPA1276		putative DNA-binding response regulator
VPA1655		putative FecB
A79_0144		ABC-type multidrug efflux pump
A79_2413		ApaG protein

A79_2622		long-chain fatty acid transport protein
A79_2788		magnesium and cobalt efflux protein CorC
A79_3241		putative alkylphosphonate ABC tranporter
A79_4905	brnQ	branched-chain amino acid transport system II carrier protein
VC1361		amino acid ABC transporter, permease protein
VP0507		branched chain amino acid transport system II carrier protein
VP1180		lipase chaperone
VP1879		serine transporter
VP1998		putative outer membrane protein TolC
VP2091		oligopeptide ABC transporter, periplasmic oligopeptide-binding protein
VP3069		ATP synthase subunit B
VPA0150		putative ferrichrome-iron receptor
A79_1856		putative protein F-related protein
A79_2645	flhB	flagellar biosynthetic protein FlhB
A79_3959		FlgE
A79_6092		flagellar biosynthesis protein FlhF
VP2230		chemotaxis protein CheZ
A79_0745		putative biofilm-associated surface protein
VP1656		putative translocator protein PopD

APPENDIX D

GENES DISPLAYING SIGNIFICANT INTERSTRAIN VARIATION IN GENE EXPRESSION AT IDENTICAL TIME POINTS AND CHALLENGE GROUPS

Higher in Tx2103 – 1h – Oys

VPA1419		putative 3-hydroxyisobutyrate dehydrogenase
VPA1510		2-amino-3-ketobutyrate coenzyme A ligase
VP2542		quinone oxidoreductase
VPA1152		putative long-chain-fatty-acid-CoA ligase
VP3027		thiamine biosynthesis protein ThiC
VP0540	cstA	putative carbon starvation protein A
VP3019		putative multidrug resistance protein
VP0540	cstA	putative carbon starvation protein A
A79_2779	thiF	thiazole biosynthesis adenylyltransferase ThiF
VP3027		thiamine biosynthesis protein ThiC
A79_2782	thiH	thiazole biosynthesis protein ThiH
VP3023	thiG	thiazole synthase
A79_2777	thiC	thiamine biosynthesis protein ThiC
A79_2779	thiF	thiazole biosynthesis adenylyltransferase ThiF
A79_2782	thiH	thiazole biosynthesis protein ThiH
VP3022		thiamine biosynthesis protein ThiH
VP3022		thiamine biosynthesis protein ThiH
A79_2777	thiC	thiamine biosynthesis protein ThiC
VP3023	thiG	thiazole synthase
VP3025		ThiF protein
VP3025		ThiF protein
VP3024		sulfur carrier protein ThiS
VP3024		sulfur carrier protein ThiS
VPA0223		putative HlyD family secretion protein
VC1565		outer membrane protein TolC, putative
VP3019		putative multidrug resistance protein
A79_2785		permease of the major facilitator superfamily
VPA1303		hypothetical protein
VPA0945		hypothetical protein
A79_4386		conserved hypothetical protein
VP1581		hypothetical protein
VP1076		hypothetical protein
VPA0438		hypothetical protein
VPA0946		hypothetical protein
VPA0946		hypothetical protein
VPA0960		hypothetical protein
VPA0947		transcriptional regulator, ArsR family

		Higher in AQ4037 – 1h – Oys
A79_0425	kbl	2-amino-3-ketobutyrate coenzyme A ligase
A79_4236		putative efflux pump component MtrF
A79_4181		outer membrane phospholipase, chain A
A79_0278		helicase IV
VP3054		thiol:disulfide interchange protein
A79_1369	cadA	cadmium-translocating P-type ATPase
VPA1533		putative flagellum-specific ATP synthase
A79_3632		polar flagellin
VPA0339		hypothetical protein
VP0474		hypothetical protein

	Higher in Tx2103 – 4h – Oys
A79_5012	glycerol-3-phosphate dehydrogenase [NAD(P)+] (NAD(P)H-dependent glycerol-3-phosphate dehydrogenase)
A79_3065	lactoylglutathione lyase
VP2434	phosphopentomutase
A79_4272	protein ThiJ
VPA1163	oxidoreductase, aldo/keto reductase 2 family
VC0067	aminopeptidase P
VP0442	ubiquinol-cytochrome c reductase, cytochrome b
VP2880	acetyl-CoA carboxylase
A79_5726	ribosomal protein L13
VP0739	ribose-phosphate pyrophosphokinase
VPA1126	putative acyl-CoA carboxyltransferase beta chain
VPA1122	putative aldehyde dehydrogenase
VPA0301	methionine sulfoxide reductase A
VPA1419	putative 3-hydroxyisobutyrate dehydrogenase
VP3026	thiamine-phosphate pyrophosphorylase
VP2869	sodium/solute symporter
VPA1121	putative acyl-CoA dehydrogenase
VPA1122	putative aldehyde dehydrogenase
A79_3591	sodium/solute symporter, putative
VPA1157	electron transfer flavoprotein, alpha-subunit
VPA1230	glyceraldehyde-3-phosphate dehydrogenase
VPA1121	putative acyl-CoA dehydrogenase
VP3026	thiamine-phosphate pyrophosphorylase
VP1281	rpmI 50S ribosomal protein L35
VP2030	30S ribosomal protein S1
VPA1152	putative long-chain-fatty-acid-CoA ligase
VP3027	thiamine biosynthesis protein ThiC
VP3027	thiamine biosynthesis protein ThiC

VPA1120		enoyl-CoA hydratase
A79_2782	thiH	thiazole biosynthesis protein ThiH
VP3023	thiG	thiazole synthase
VP3023	thiG	thiazole synthase
VP3022		thiamine biosynthesis protein ThiH
VP0540		putative carbon starvation protein A
VP3022		thiamine biosynthesis protein ThiH
A79_2782	thiH	thiazole biosynthesis protein ThiH
VP0540		putative carbon starvation protein A
VP3025		ThiF protein
A79_2777	thiC	thiamine biosynthesis protein ThiC
VP3025		ThiF protein
A79_2777	thiC	thiamine biosynthesis protein ThiC
A79_3579	treP	pts system, trehalose-specific iibc component
A79_6073		amino acid ABC transporter, permease protein
VP2867		cell volume regulation protein CvrA
VP1966		proton/glutamate symporter
VP1194		putative ABC transporter, ATP-binding protein
VP3019		putative multidrug resistance protein
VPA0166		putative outer membrane protein
VPA1542		putative flagellar assembly protein
VP2161		hypothetical protein
VP0304		hypothetical protein
A79_3629		single-strand binding protein family
VP0304		hypothetical protein
VP1795		hypothetical protein
VPA0960		hypothetical protein
VPA0960		hypothetical protein
A79_4778		transcriptional regulatory protein FixJ
VP2386		glycerol kinase

Higher in AQ4037 – 4h – Oys

VCA0563	pntA	NAD(P) transhydrogenase subunit alpha
VPA0453		catalase/peroxidase
VPA0454		putative DNA-binding stress protein
VP1181		lactonizing lipase
VP2704		MSHA biogenesis protein MshL
VPA0793		hypothetical protein
A79_2118		conserved hypothetical protein
VC1530		hypothetical protein
A79_5433		conserved hypothetical protein
A79_4798		conserved hypothetical protein
VP0761		hypothetical protein
A79_2478		ParA family protein

VPA0345		hypothetical protein
VPA0690		hypothetical protein
VPA0397		hypothetical protein
VP1870		hypothetical protein
VPA0036		hypothetical protein
A79_4381		transcriptional regulator
A79_2580	proB	glutamate 5-kinase

Higher in Tx2103 – 1h – Caco-2

VP3061		dihydroxy-acid dehydratase
A79_0698		STM-proteaseA
A79_4609	ilvB	acetolactate synthase, large subunit, biosynthetic type
A79_2276		DNA gyrase/topoisomerase IV, A subunit
VPA1055		nitrite reductase
A79_2318		putative sugar transport system
VP1903		DNA polymerase III subunit epsilon
VP0710		PTS system, trehalose-specific IIBC component
VP1450		putative component of anaerobic dehydrogenase
A79_4818		chromosome partition protein MukB
A79_4475	cydB	cytochrome D ubiquinol oxidase, subunit II
A79_5288		soluble lytic murein transglycosylase
VP1468		putative hexosyltransferase
A79_6250	purT	phosphoribosylglycinamide formyltransferase 2
A79_6218		NADP-dependent fatty aldehyde dehydrogenase
VPA0452		putative cytochrome b561
VP3007		ATP-dependent DNA helicase RecQ
VPA1155		electron transfer flavoprotein-ubiquinone oxidoreductase
VP1112		adenosylmethionine--8-amino-7-oxononanoate transaminase
A79_6250	purT	phosphoribosylglycinamide formyltransferase 2
VP1724		DNA polymerase III subunit epsilon
VPA0192		tryptophanase
VPA1674		ribulokinase
A79_1169	nhaB	Na+/H+ antiporter NhaB
VP0088		hypothetical protein
VPA0691		putative riboflavin deaminase
VPA1157		electron transfer flavoprotein, alpha-subunit
VP3022		thiamine biosynthesis protein ThiH
VP0260		50S ribosomal protein L2
VP3022		thiamine biosynthesis protein ThiH
VP3027		thiamine biosynthesis protein ThiC
VP3025		ThiF protein
VP3027		thiamine biosynthesis protein ThiC
VP3025		ThiF protein
VPA0489		putative ATP-binding component of a transport system

VPA0488		putative transmembrane protein
VP2310		surface antigen (outer membrane protein assembly factor YaeT)
VP1526		spermidine/putrescine ABC transporter, periplasmic spermidine/putrescine-binding protein
VPA0352		putative permease of ABC transporter
A79_5938		drug resistance transporter, EmrB/QacA family
A79_0269		transporter
VCA0758		arginine ABC transporter, permease protein
A79_2667		polar flagellin A
VP2693		putative MshP protein
VP0122		BipA protein
VPA1349		putative Type III secretion protein Spa33
VP0660	pilV	putative type IV pilin
A79_0729	pilP	type IV pilus
A79_2291		transmembrane regulatory protein ToxS
VP2024		hypothetical protein
VPA0137		hypothetical protein
VP1571		hypothetical protein
A79_2830		conserved hypothetical protein
VPA0652		hypothetical protein
VPA0850		hypothetical protein
VPA0165		hypothetical protein
VP1733		hypothetical protein
VP2376		hypothetical protein
A79_5479		hypothetical protein
VPA1305		hypothetical protein
VC1685		hypothetical protein
VPA1655		putative FecB
A79_3927		conserved hypothetical protein
VP0586		hypothetical protein
VP1533		putative ATPase (bacteriophage f237 ORF3)
VP2278		hypothetical protein
VP0595		hypothetical protein
VP0554		hypothetical protein
A79_2612		hypothetical adenine-specific methylase YfcB
A79_4974		AraC-type DNA-binding domain-containing protein
A79_4210	pcm	protein-L-isoaspartate O-methyltransferase
VP0428		cyclic AMP phosphodiesterase
A79_4578		methyltransferase
VPA1279		diacylglycerol kinase
VP1786		hypothetical protein
A79_0458		transposase
VP1939		hypothetical protein
VP0368		mannitol operon repressor

VP2927	nusG	transcription antitermination protein NusG
VP2294		putative SAM-dependent methyltransferase
		Higher in AQ4037 – 1h - Caco-2
A79_4492		acyl-CoA dehydrogenase
VP1036	mukE	condesin subunit E
A79_1684	putP	sodium/proline symporter
A79_3675		glutathione peroxidase
VP1771		4-aminobutyrate aminotransferase
VPA0642		putative glutathione S-transferase
VPA1201	napC	periplasmic nitrate reductase, cytochrome c-type protein
A79_6380		ferredoxin
VP1348		peptidase, M20A family
VC0305	RhlB	ATP-dependent RNA helicase
VP1142		1-(5-phosphoribosyl)-5-[(5- phosphoribosylamino)methylideneamino] imidazole-4-carboxamide isomerase
A79_2711		nuclease
VP2032	sohB	sohB protein, peptidase U7 family
VP0665		transglycosylase, Slt family
A79_3669		oxidoreductase, short-chain dehydrogenase/reductase family
A79_2292		adenylosuccinate synthetase
A79_1359	argG	argininosuccinate synthase
VP0722		penicillin-binding protein 2
A79_1372		ferredoxin-1
A79_1694		permease of the drug/metabolite transporter
A79_1439		permease of the drug/metabolite transporter
VP1216		multidrug resistance protein (bicyclomycin/multidrug efflux pump)
VP2411		putative tight adherence TadB-related transmembrane protein
VP0706		ABC transporter, ATP-binding protein
A79_3190		methyl-accepting chemotaxis protein
VPA1541		flagellar motor switch protein
VP2811		sodium-type polar flagellar protein MotX
A79_3703		autoinducer 2 sensor kinase/phosphatase LuxQ
A79_1552		putative msha pilin protein msha
VP1657		putative translocator protein PopB
A79_3165		putative adhesin
VPA1218		putative secretion protein
VPA0442		hypothetical protein
VPA0061		hypothetical membrane protein
VPA0772		hypothetical protein
A79_0377		YjqA
VP0668		hypothetical protein
A79_5572		conserved hypothetical protein
A79_0244		conserved hypothetical protein

VPA0787		hypothetical protein
A79_0876		conserved hypothetical protein
VPA0749		hypothetical protein
A79_5417		conserved hypothetical protein
VC1530		hypothetical protein
VP1509		hypothetical protein
A79_4782		hypothetical protein
VP2085		hypothetical protein
A79_4983		conserved hypothetical protein
VP1918		hypothetical protein
A79_5484		conserved hypothetical protein
A79_1374		FOG ggdef domain
VPA1426		hypothetical protein
A79_5997		conserved hypothetical protein
A79_2935	rpoN	RNA polymerase sigma-54 factor
VPA0619		putative transcriptional regulator
VP2450		transcriptional regulator, MarR family
A79_5786		sensory box/ggdef family protein
VP1016	infA	translation initiation factor IF-1
A79_5987		twin-arginine translocation pathway signal
A79_1855		glutaredoxin
VP3000	rho	transcription termination factor Rho

Higher in Tx2103 – 4h – Caco-2

VP2109		lactoylglutathione lyase
VP1468		putative hexosyltransferase
A79_0891		acetyltransferase
A79_4217	pyrG	CTP synthase
VP1719		aspartate kinase
VP2431		phosphoserine phosphatase
A79_1778		UTP--glucose-1-phosphate uridylyltransferase
A79_0698		STM-proteaseA
A79_1659		protein YhgF
VP1781		putative glutamine synthetase
VP0596		cysteine desulfurase
VP2316		uridylate kinase
VP2322		pseudouridine synthase Rlu family protein
A79_4485		enoyl-CoA hydratase/carnithine racemase
VP0826	asnB	asparagine synthetase B
VP1215		ribosomal small subunit pseudouridine synthase A
VC2090		succinate dehydrogenase, hydrophobic membrane anchor protein
A79_5302	pdhA	pyruvate dehydrogenase E1 component, alpha subunit
A79_2854	fni	isopentenyl-diphosphate delta-isomerase, type 2

VP3059		acetolactate synthase II, small subunit
VPA1201		periplasmic nitrate reductase, cytochrome c-type protein
VP0408		O-sialoglycoprotein endopeptidase
VCA1060	ribB	3,4-dihydroxy-2-butanone 4-phosphate synthase
A79_1193	moaB	molybdenum cofactor biosynthesis protein B
VPA0409		plasma membrane protein involved in salt tolerance
A79_3171		protein YgiW
A79_1946		phosphotransferase family protein
VP1916		putative amidase
VPA0305		catalase
VC2402		cell division protein FtsW
VP1646		aconitate hydratase
A79_0795		collagenase PrtC
VP1275		formimidoylglutamase
VP1646		aconitate hydratase
VP1301		exodeoxyribonuclease I
A79_0865		stability protein StbD, putative
A79_6240		bifunctional adenosylcobalamin biosynthesis protein CobP
A79_6198	hmgA	homogentisate 1,2-dioxygenase
VP3022		thiamine biosynthesis protein ThiH
A79_2782	thiH	thiazole biosynthesis protein ThiH
VP3022		thiamine biosynthesis protein ThiH
VP3025		ThiF protein
VP3025		ThiF protein
VP3024		sulfur carrier protein ThiS
VC1273		extracellular solute-binding protein, family 7
A79_2015		outer membrane protein
A79_1549	rarD	RarD protein
A79_3159		cation efflux system
A79_2430	tolQ	protein TolQ
VP1511		putative formate dehydrogenase-specific chaperone
VP2329		efflux pump component MtrF
VP3066		putative amino acid ABC transporter, permease protein
VP1474		putative capsule transport protein, OtnA protein
VPA0721		rough colony protein RcpA
VP0170		putative transmembrane ABC transporter protein
VP2746		fimbrial assembly protein
VP2247		flagellar assembly protein
VPA1492		methyl-accepting chemotaxis protein
VPA1539		putative sodium-type flagellar protein MotY precursor
VPA0939		putative adhesin
A79_6356		msha biogenesis protein mshe
A79_1885		ggdef family protein
A79_0585		VcsR2

A79_5997	conserved hypothetical protein
A79_0481	conserved hypothetical protein
A79_2427	hypothetical protein
A79_3927	conserved hypothetical protein
VPA0204	hypothetical protein
A79_4496	hypothetical protein
A79_2032	conserved hypothetical protein
VCA1065	hypothetical protein
VCA1076	hypothetical protein
VCA1076	hypothetical protein
A79_4782	hypothetical protein
A79_1851	hypothetical protein
VP2647	hypothetical protein
A79_6072	conserved hypothetical protein
VPA0095	hypothetical protein
VPA0704	hypothetical protein
A79_4489	hypothetical protein
VP0888	hypothetical protein
VPA1305	hypothetical protein
VP1845	hypothetical protein
VP1836	hypothetical protein
VP0670	hypothetical protein
VP1886	hypothetical protein
VP0913	hypothetical protein
VPA1599	hypothetical protein
A79_1669	conserved hypothetical protein
VC1530	hypothetical protein
VP2853	hypothetical protein
A79_3581	conserved hypothetical protein
VPA1692	hypothetical protein
VPA0926	hypothetical protein
VPA1246	hypothetical protein
VPA0720	hypothetical protein
VCA0126	hypothetical protein
VPA1068	hypothetical protein
VP2494	hypothetical protein
VPA0815	hypothetical protein
VPA1743	hypothetical protein
A79_0768	Rrf2 family protein
A79_2942	translation initiation factor IF-2
VPA0974	putative AraC-family transcriptional regulatory protein
VPA0249	putative transcription activator
A79_0684	signal transduction histidine kinase
A79_1151	methyltransferase

VPA0988		nucleoside diphosphate kinase regulator
VPA1214		putative transcriptional regulator
		Higher in AQ4037 – 4h – Caco-2
VP2770	tuf	elongation factor Tu
VP0580		antioxidant, AhpC/Tsa family
VP0920		DNA-binding protein HU-beta
VP1879		serine transporter
VP3069		ATP synthase subunit B
VP0251		putative cell division protein FtsN
VP0580		antioxidant, AhpC/Tsa family
A79_4292	glpK	glycerol kinase
VP2863		aspartate ammonia-lyase
VP1591		3-hydroxydecanoyl-ACP dehydratase
VP3074		ATP synthase subunit C
VP2863		aspartate ammonia-lyase
VP3070		ATP synthase subunit C
A79_0927		putative transposase B
A79_1499	gcvP	glycine dehydrogenase
VP1116	bioD	dithiobiotin synthetase
VP0202		putative sugar-phosphate nucleotide transferase
VP2437		NupC family protein
A79_4687		redoxin domain protein
A79_3791	oadA	oxaloacetate decarboxylase alpha subunit
VPA0611		acetate/propionate kinase
VP0129		phosphoenolpyruvate carboxykinase
VP1438		DnaK-related protein
VP1944		excinuclease ABC subunit C
A79_3896		T-protein
VP0479		5'-methylthioadenosine/S-adenosylhomocysteine nucleosidase
A79_1971		succinate dehydrogenase flavoprotein subunit
A79_5522		3-oxoacyl-[acyl-carrier-protein] synthase 1
VPA0936		aspartate aminotransferase
A79_6218		NADP-dependent fatty aldehyde dehydrogenase
A79_3257	add	adenosine deaminase
A79_3588		fumarate hydratase class II 1
VP2188		folylpolyglutamate synthase/dihydrofolate synthase
VPA0784	def	peptide deformylase
A79_1741		endonuclease/exonuclease/phosphatase family
A79_6062		isocitrate dehydrogenase, NADP-dependent
A79_5522		3-oxoacyl-[acyl-carrier-protein] synthase 1
A79_1298		probable 6-phospho-beta-glucosidase
A79_2811	phnW	2-aminoethylphosphonate--pyruvate transaminase
A79_0634		lactaldehyde reductase

A79_3374		ATP-dependent DNA helicase rep
VP1730		putative long-chain-fatty-acid-CoA ligase
VP1229		Na+/H+-antiporter protein
VP0395		type I restriction enzyme R protein
VP2351		Na(+)-translocating NADH-quinone reductase subunit A
VPA0102		putative isomerase
A79_4898		acetyltransferase, gnat family
VP2355		peptidyl-prolyl cis-trans isomerase A
A79_6262		endonuclease 4
A79_2364		radical SAM protein, family
A79_0627		6-phospho-beta-glucosidase BglA
A79_4262	ppiB	peptidyl-prolyl cis-trans isomerase B
VP1542		cytochrome c oxidase, subunit CcoQ
VP2032		sohB protein, peptidase U7 family
A79_0994	ectA	L-2,4-diaminobutyric acid acetyltransferase
VPA0618		putative acyl-CoA dehydrogenase
VP1543		cytochrome c oxidase, subunit CcoO
VP1878		MutT/nudix family protein
VP0483		glutamate synthase, small subunit
VP1542		cytochrome c oxidase, subunit CcoQ
A79_2026		mandelate racemase
A79_1272		copper/silver resistance periplasmic protein
VP1010		pseudouridine synthase family 1 protein
VP1586		putative phage protein, Vpf148 [bacteriophage VfO3K6]
VPA1395		putative transposase
VPA0813		PTS system, fructose-specific IIA/FPR component
VPA0060		lysis protein - phage PP7
A79_3232	spoT	guanosine-3,5-bis(diphosphate) 3-pyrophosphohydrolase
VP1933		3-demethylubiquinone-9 3-methyltransferase
A79_3653	leuA	2-isopropylmalate synthase
VPA1498		putative L-lactate permease
A79_5581		cytosol aminopeptidase
VP1163		putative alpha-1,6-galactosidase
VP2091		oligopeptide ABC transporter, periplasmic oligopeptide-binding protein
VP1879		serine transporter
VP0507		branched chain amino acid transport system II carrier protein
VP2642		putative permease
VPA1704		putative integral membrane protein, possible transporter
VP2091		oligopeptide ABC transporter, periplasmic oligopeptide-binding protein
VP1435		putative sodium/glutamate symporter
A79_4067		anaerobic C4-dicarboxylate transporter DcuA
A79_2416		chaperone SurA

A79_4385	low-affinity zinc transport protein
VP0591	protein export protein SecF
VP1995	ABC transporter, ATP-binding protein
VP2437	NupC family protein
A79_3700	multidrug resistance protein A
VPA0604	ABC transporter, periplasmic substrate-binding protein
VPA0424	TonB system transport protein ExbD1
VP2705	MSHA biogenesis protein MshK
VPA0807	putative multidrug resistance protein
VP2258	flagellin
VP1184	putative sodium-dependent transporter
VP2259	flagellin
VPA0266	flagellar basal body rod modification protein
A79_1856	putative protein F-related protein
VP0773	chemotaxis CheV
VP1656	putative translocator protein PopD
VP1665	putative type III secretion protein
A79_1019	type III secretion outer membrane pore, YscC/HrcC family
VPA1329	putative traA protein
VP1656	putative translocator protein PopD
VP1660	putative regulator in type III secretion
A79_0582	outer protein J
VP1801	hypothetical protein
A79_3606	conserved hypothetical protein
VPA0451	hypothetical protein
VP1257	SanA protein
VPA0196	hypothetical protein
A79_0600	hypothetical protein
VPA0371	hypothetical protein
VPA0837	hypothetical protein
VP1495	hypothetical protein
VP2278	hypothetical protein
VPA1245	hypothetical protein
VPA0156	hypothetical protein
VP1269	hypothetical protein
VP2469	hypothetical protein
A79_4827	gonadoliberin III-related protein
A79_1374	FOG ggdef domain
VPA0935	hypothetical protein
A79_0245	conserved hypothetical protein
VP2421	hypothetical protein
A79_1306	conserved hypothetical protein
VPA1735	hypothetical protein
VP1238	hypothetical protein

VP0054	hypothetical protein
VP2624	hypothetical protein
VP1518	hypothetical protein
VP1516	hypothetical protein
VP2789	hypothetical protein
VC0038	hypothetical protein
VPA0324	hypothetical protein
VPA0206	hypothetical protein
VP1107	hypothetical protein
VPA0521	hypothetical protein
VP0474	hypothetical protein
VPA1337	hypothetical protein
VP1803	hypothetical protein
A79_5484	conserved hypothetical protein
VC0464	transcriptional regulator, LuxR family
VP2294	putative SAM-dependent methyltransferase
VP2951	GlpG protein
A79_4762	transcriptional regulator, AraC family
VC0464	transcriptional regulator, LuxR family
VP2793	cyclic AMP receptor protein
VPA1276	putative DNA-binding response regulator
VPA1655	putative FecB
A79_4578	methyltransferase
VP2387	transcriptional regulator, DeoR family
A79_0232	heme receptor HupA
A79_5856	transcriptional regulator
A79_3690	transcriptional regulator

REFERENCES

1. T. Fujino *et al.*, On the bacteriological examination of shirasu-food poisoning. *Med. J. Osaka Univ.*, 299 (1953).

2. S. W. Joseph, R. R. Colwell, J. B. Kaper, Vibrio parahaemolyticus and related halophilic Vibrios. *Crit. Rev. Microbiol.* **10**, 77 (1982).

3. Y. Miyamoto *et al.*, In vitro hemolytic characteristic of Vibrio parahaemolyticus: its close correlation with human pathogenicity. *J. Bacteriol.* **100**, 1147 (1969).

4. T. Kaneko, R. R. Colwell, Ecology of Vibrio parahaemolyticus in Chesapeake Bay. *J. Bacteriol.* **113**, 24 (1973).

5. T. A. Dadisman, Jr., R. Nelson, J. R. Molenda, H. J. Garber, Vibrio parahaemolyticus gastroenteritis in Maryland. I. Clinical and epidemiologic aspects. *Am. J. Epidemiol.* **96**, 414 (1972).

6. J. R. Bonner, A. S. Coker, C. R. Berryman, H. M. Pollock, Spectrum of Vibrio infections in a Gulf Coast community. *Ann. Intern. Med.* **99**, 464 (1983).

7. C. N. Johnson *et al.*, Relationships between environmental factors and pathogenic vibrios in the northern Gulf of Mexico. *Appl. Environ. Microbiol.*, (2009).

8. A. DePaola, L. H. Hopkins, J. T. Peeler, B. Wentz, R. M. McPhearson, Incidence of Vibrio parahaemolyticus in U.S. coastal waters and oysters. *Appl. Environ. Microbiol.* **56**, 2299 (1990).

9. J. W. Davis, R. K. Sizemore, Incidence of Vibrio species associated with blue crabs (Callinectes sapidus) collected from Galveston Bay, Texas. *Appl. Environ. Microbiol.* **43**, 1092 (1982).

10. R. K. Sizemore, R. R. Colwell, H. S. Tubiash, T. E. Lovelace, Bacterial flora of the hemolymph of the blue crab, Callinectes sapidus: numerical taxonomy. *Appl. Microbiol.***29**, 393 (1975).

11. C. Vanderzant, R. Nickelson, Survival of Vibrio parahaemolyticus in shrimp tissue under various environmental conditions. *Appl. Microbiol.***23**, 34 (1972).

12. T. Kaneko, R. R. Colwell, Adsorption of Vibrio parahaemolyticus onto chitin and copepods. *Appl. Microbiol.***29**, 269 (1975).

13. U.S. Department of Health and Human Sevices, *Quantitative Risk Assessment on the Public Health Impact of Pathogenic Vibrio parahaemolyticus in Raw Oysters; Risk Assessment*. (Federal Register 2005, vol. 70, pp. 41772-41773).

14. N. A. Daniels *et al.*, Vibrio parahaemolyticus infections in the United States, 1973-1998. *J. Infect. Dis.* **181**, 1661 (2000).

15. N. A. Daniels *et al.*, Emergence of a new Vibrio parahaemolyticus serotype in raw oysters: A prevention quandary. *J.A.M.A.* **284**, 1541 (2000).

16. U.S. Center for Disease Control, *Outbreak of Vibrio parahaemolyticus infections associated with eating raw oysters--Pacific Northwest,* (M.M.W.R. 1997, 0098-7484).

17. U.S. Center for Disease Control, *Outbreak of Vibrio parahaemolyticus infection associated with eating raw oysters and clams harvested from Long Island Sound--Connecticut, New Jersey, and New York, 1998,* (M.M.W.R., 1999, 0098-7484).

18. A. Chowdhury *et al.*, Emergence and serovar transition of Vibrio parahaemolyticus pandemic strains isolated during a diarrhea outbreak in Vietnam between 1997 and 1999. *Microbiol. Immunol.* **48**, 319 (2004).

19. K. Garcia *et al.*, Dynamics of clinical and environmental Vibrio parahaemolyticus strains during seafood-related summer diarrhea outbreaks in southern Chile. *Appl. Environ. Microbiol.* **75**, 7482 (2009).

20. U.S. Center for Diease Control, *Disease, Control, And, Prevention*, (M.M.W.R , 2006, **55**, 1-42).

21. V. Vuddhakul *et al.*, Isolation of a pandemic O3:K6 clone of a Vibrio parahaemolyticus strain from environmental and clinical sources in Thailand. *Appl. Environ. Microbiol.* **66**, 2685 (2000).

22. U.S. Center for Diease Control, *Vibrio parahaemolyticus infections associated with consumption of raw shellfish--three states, 2006*, (M.M.W.R 2006, **55**, 854).

23. K. Makino *et al.*, Genome sequence of Vibrio parahaemolyticus: a pathogenic mechanism distinct from that of V cholerae. *Lancet* **361**, 743 (2003).

24. J. Martinez-Urtaza *et al.*, Characterization of pathogenic Vibrio parahaemolyticus isolates from clinical sources in Spain and comparison with Asian and North American pandemic isolates. *J. Clin. Microbiol.* **42**, 4672 (2004).

25. J. Martinez-Urtaza *et al.*, Environmental determinants of the occurrence and distribution of Vibrio parahaemolyticus in the rias of Galicia, Spain. *Appl. Environ. Microbiol.* **74**, 265 (2008).

26. Y. Miyamoto *et al.*, Simplified purification and biophysicochemical characteristics of Kanagawa phenomenon-associated hemolysin of Vibrio parahaemolyticus. *Infect. Immun.* **28**, 567 (1980).

27. T. Honda, Y. X. Ni, T. Miwatani, Purification and characterization of a hemolysin produced by a clinical isolate of Kanagawa phenomenon-negative Vibrio parahaemolyticus and related to the thermostable direct hemolysin. *Infect. Immun.* **56**, 961 (1988).

28. J. Okuda, M. Ishibashi, S. L. Abbott, J. M. Janda, M. Nishibuchi, Analysis of the thermostable direct hemolysin (tdh) gene and the tdh-related hemolysin (trh) genes in urease-positive strains of Vibrio parahaemolyticus isolated on the West Coast of the United States. *J. Clin. Microbiol.* **35**, 1965 (1997).

29. H. Shirai *et al.*, Molecular epidemiologic evidence for association of thermostable direct hemolysin (TDH) and TDH-related hemolysin of Vibrio parahaemolyticus with gastroenteritis. *Infect. Immun.* **58**, 3568 (1990).

30. M. Nishibuchi, M. Ishibashi, Y. Takeda, J. B. Kaper, Detection of the thermostable direct hemolysin gene and related DNA sequences in Vibrio parahaemolyticus and other vibrio species by the DNA colony hybridization test. *Infect. Immun.* **49**, 481 (1985).

31. C. N. Johnson *et al.*, Genetic relatedness among tdh+ and trh+ Vibrio parahaemolyticus cultured from Gulf of Mexico oysters (Crassostrea virginica) and surrounding water and sediment. *Microb. Ecol.* **57**, 437 (2009).

32. J. Okuda *et al.*, Emergence of a unique O3:K6 clone of Vibrio parahaemolyticus in Calcutta, India, and isolation of strains from the same clonal group from Southeast Asian travelers arriving in Japan. *J. Clin. Microbiol.* **35**, 3150 (1997).

33. V. Laohaprertthisan *et al.*, Prevalence and serodiversity of the pandemic clone among the clinical strains of Vibrio parahaemolyticus isolated in southern Thailand. *Epidemiol. Infect.* **130**, 395 (2003).

34. C. E. Meador *et al.*, Virulence gene- and pandemic group-specific marker profiling of clinical Vibrio parahaemolyticus isolates. *J. Clin. Microbiol.* **45**, 1133 (2007).

35. T. Lynch *et al.*, Vibrio parahaemolyticus disruption of epithelial cell tight junctions occurs independently of toxin production. *Infect. Immun.* **73**, 1275 (2005).

36. K. S. Park *et al.*, Cytotoxicity and enterotoxicity of the thermostable direct hemolysin-deletion mutants of Vibrio parahaemolyticus. *Microbiol. Immunol.* **48**, 313 (2004).

37. R. N. Bhattacharjee *et al.*, Microarray analysis identifies apoptosis regulatory gene expression in HCT116 cells infected with thermostable direct hemolysin-deletion mutant of Vibrio parahaemolyticus. *Biochem. Biophys. Res. Commun.* **335**, 328 (2005).

38. K. Hoashi *et al.*, Pathogenesis of Vibrio parahaemolyticus: intraperitoneal and orogastric challenge experiments in mice. *Microbiol. Immunol.* **34**, 355 (1990).

39. E. Arakawa *et al.*, Emergence and prevalence of a novel Vibrio parahaemolyticus O3:K6 clone in Japan. *Jpn. J. Infect. Dis.* **52**, 246 (1999).

40. S. L. Abbott *et al.*, Emergence of a restricted bioserovar of Vibrio parahaemolyticus as the predominant cause of Vibrio-associated gastroenteritis on the West Coast of the United States and Mexico. *J. Clin. Microbiol.* **27**, 2891 (1989).

41. C. Matsumoto *et al.*, Pandemic spread of an O3:K6 clone of Vibrio parahaemolyticus and emergence of related strains evidenced by arbitrarily primed PCR and toxRS sequence analyses. *J. Clin. Microbiol.* **38**, 578 (2000).

42. P. K. Bag *et al.*, Clonal diversity among recently emerged strains of Vibrio parahaemolyticus O3:K6 associated with pandemic spread. *J. Clin. Microbiol.* **37**, 2354 (1999).

43. N. R. Chowdhury *et al.*, Clonal dissemination of Vibrio parahaemolyticus displaying similar DNA fingerprint but belonging to two different serovars (O3:K6 and O4:K68) in Thailand and India. *Epidemiol. Infect.* **125**, 17 (2000).

44. N. R. Chowdhury *et al.*, Molecular evidence of clonal Vibrio parahaemolyticus pandemic strains. *Emerg. Infect. Dis.* **6**, 631 (2000).

45. M. Okura *et al.*, Genetic analyses of the putative O and K antigen gene clusters of pandemic Vibrio parahaemolyticus. *Microbiol. Immunol.* **52**, 251 (2008).

46. M. Okura *et al.*, PCR-based identification of pandemic group Vibrio parahaemolyticus with a novel group-specific primer pair. *Microbiol. Immunol.* **48**, 787 (2004).

47. M. Okura *et al.*, Genotypic analyses of Vibrio parahaemolyticus and development of a pandemic group-specific multiplex PCR assay. *J. Clin. Microbiol.* **41**, 4676 (2003).

48. Z. Lin, K. Kumagai, K. Baba, J. J. Mekalanos, M. Nishibuchi, Vibrio parahaemolyticus has a homolog of the Vibrio cholerae toxRS operon that mediates environmentally induced regulation of the thermostable direct hemolysin gene. *J. Bacteriol.* **175**, 3844 (1993).

49. E. S. Krukonis, R. R. Yu, V. J. Dirita, The Vibrio cholerae ToxR/TcpP/ToxT virulence cascade: distinct roles for two membrane-localized transcriptional activators on a single promoter. *Mol. Microbiol.* **38**, 67 (2000).

50. S. E. Lee *et al.*, Vibrio vulnificus has the transmembrane transcription activator ToxRS stimulating the expression of the hemolysin gene vvhA. *J. Bacteriol.* **182**, 3405 (2000).

51. C. J. Hueck, Type III protein secretion systems in bacterial pathogens of animals and plants. *Microbiol. Mol. Biol. Rev.* **62**, 379 (1998).

52. G. R. Cornelis, F. Van Gijsegem, Assembly and function of type III secretory systems. *Annu. Rev. Microbiol.* **54**, 735 (2000).

53. P. Troisfontaines, G. R. Cornelis, Type III secretion: more systems than you think. *Physiology.* **20**, 326 (2005).

54. K. S. Park *et al.*, Functional characterization of two type III secretion systems of Vibrio parahaemolyticus. *Infect. Immun.* **72**, 6659 (2004).

55. K. Izutsu *et al.*, Comparative genomic analysis using microarray demonstrates a strong correlation between the presence of the 80-kilobase pathogenicity island and pathogenicity in Kanagawa phenomenon-positive Vibrio parahaemolyticus strains. *Infect. Immun.* **76**, 1016 (2008).

56. T. Sugiyama, T. Iida, K. Izutsu, K. S. Park, T. Honda, Precise region and the character of the pathogenicity island in clinical Vibrio parahaemolyticus strains. *J. Bacteriol.* **190**, 1835 (2008).

57. T. Iida *et al.*, Close proximity of the tdh, trh and ure genes on the chromosome of Vibrio parahaemolyticus. *Microbiology* **144**, 2517 (1998).

58. N. Okada *et al.*, Identification and characterization of a novel type III secretion system in trh-positive Vibrio parahaemolyticus strain TH3996 reveal genetic lineage and diversity of pathogenic machinery beyond the species level. *Infect. Immun.* **77**, 904 (2009).

59. N. F. Noriea, 3rd, C. N. Johnson, K. J. Griffitt, D. J. Grimes, Distribution of type III secretion systems in Vibrio parahaemolyticus from the northern Gulf of Mexico. *J Appl. Microbiol.***109**, 953 (2010).

60. T. Ono, K. S. Park, M. Ueta, T. Iida, T. Honda, Identification of proteins secreted via Vibrio parahaemolyticus type III secretion system 1. *Infect. Immun.* **74**, 1032 (2006).

61. T. Kodama *et al.*, Identification of two translocon proteins of Vibrio parahaemolyticus type III secretion system 2. *Infect. Immun.* **76**, 4282 (2008).

62. T. Kodama *et al.*, Identification and characterization of VopT, a novel ADP-ribosyltransferase effector protein secreted via the Vibrio parahaemolyticus type III secretion system 2. *Cell. Microbiol.* **9**, 2598 (2007).

63. Y. Akeda *et al.*, Identification and characterization of a type III secretion-associated chaperone in the type III secretion system 1 of Vibrio parahaemolyticus. *FEMS Microbiol. Lett.* **296**, 18 (2009).

64. I. Adkins, S. Schulz, S. Borgmann, I. B. Autenrieth, S. Grobner, Differential roles of Yersinia outer protein P-mediated inhibition of nuclear factor-kappa B in the induction of cell death in dendritic cells and macrophages. *J. Med. Microbiol.* **57**, 139 (2008).

65. A. D. Liverman *et al.*, Arp2/3-independent assembly of actin by Vibrio type III effector VopL. *Proc. Natl. Acad. Sci. U.S.A.* **104**, 17117 (2007).

66. M. D. Gamble, C. R. Lovell, Infaunal burrows are enrichment zones for Vibrio parahaemolyticus. *Appl. Environ. Microbiol.* **77**, 3703 (2011).

67. D. J. Grimes *et al.*, What genomic sequence information has revealed about Vibrio ecology in the ocean--a review. *Microb. Ecol.* **58**, 447 (2009).

68. A. M. Zimmerman *et al.*, Variability of total and pathogenic Vibrio parahaemolyticus densities in northern Gulf of Mexico water and oysters. *Appl. Environ. Microbiol.* **73**, 7589 (2007).

69. A. K. Bej *et al.*, Detection of total and hemolysin-producing Vibrio parahaemolyticus in shellfish using multiplex PCR amplification of tl, tdh and trh. *J. Microbiol. Methods.* **36**, 215 (1999).

70. K. Zwirglmaier, W. Ludwig, K. H. Schleifer, Recognition of individual genes in a single bacterial cell by fluorescence in situ hybridization--RING-FISH. *Mol. Microbiol.* **51**, 89 (2004).

71. M. Stoffels, W. Ludwig, K. H. Schleifer, rRNA probe-based cell fishing of bacteria. *Environ. Microbiol.* **1**, 259 (1999).

72. A. DePaola, C. A. Kaysner, J. Bowers, D. W. Cook, Environmental investigations of Vibrio parahaemolyticus in oysters after outbreaks in Washington, Texas, and New York (1997 and 1998). *Appl. Environ. Microbiol.* **66**, 4649 (2000).

73. A. DePaola, J. L. Nordstrom, J. C. Bowers, J. G. Wells, D. W. Cook, Seasonal abundance of total and pathogenic Vibrio parahaemolyticus in Alabama oysters. *Appl. Environ. Microbiol.* **69**, 1521 (2003).

74. N. Nakasone, M. Iwanaga, The role of pili in colonization of the rabbit intestine by Vibrio parahaemolyticus Na2. *Microbiol. Immunol.* **36**, 123 (1992).

75. M. Nishibuchi, J. Kaper, Thermostable Direct Hemolysin Gene of Vibrio parahaemolyticus: a Virulence gene Aquired by a marine bacterium. *Infection and Immunity* **63**, 2093 (1995).

76. T. M. Minton, A Review of the Market Structure of the Louisiana Oyster Industry: A Microcosm of the United States Oyster Industry. *Journal of Shellfish Research* (2004).

77. N. R. Chowdhury, O. C. Stine, J. G. Morris, G. B. Nair, Assessment of evolution of pandemic Vibrio parahaemolyticus by multilocus sequence typing. *J. Clin. Microbiol.* **42**, 1280 (2004).

78. G. Caburlotto, M. Gennari, V. Ghidini, M. Tafi, M. M. Lleo, Presence of T3SS2 and other virulence-related genes in tdh-negative Vibrio parahaemolyticus environmental strains isolated from marine samples in the area of the Venetian Lagoon, Italy. *FEMS Microbiol. Ecol.* **70**, 506 (2009).

79. T. Kodama, [Functional analysis of type III secretion system 2 of Vibrio parahaemolyticus]. *Nihon saikingaku zasshi. Japanese Journal of Bacteriology* **64**, 303 (2009).

80. T. Kodama *et al.*, Two regulators of Vibrio parahaemolyticus play important roles in enterotoxicity by controlling the expression of genes in the Vp-PAI region. *PLoS One* **5** (2010).

81. S. M. Allen, L. E. Burnett, The effects of intertidal air exposure on the respiratory physiology and the killing activity of hemocytes in the pacific oyster, *Crassostrea gigas* (Thunberg). *Journal of Experimental Marine Biology and Ecology*, 165 (2008).

82. F. J. Genthner, A. K. Volety, L. M. Oliver, W. S. Fisher, Factors influencing in vitro killing of bacteria by hemocytes of the eastern oyster (Crassostrea virginica). *Appl. Environ. Microbiol.* **65**, 3015 (1999).

83. G. Caburlotto *et al.*, Effect on human cells of environmental Vibrio parahaemolyticus strains carrying type III secretion system 2. *Infect. Immun.* **78**, 3280 (2010).

84. F. Raimondi *et al.*, Enterotoxicity and cytotoxicity of Vibrio parahaemolyticus thermostable direct hemolysin in in vitro systems. *Infect. Immun.* **68**, 3180 (2000).

85. A. K. Volety, L. M. Oliver, F. J. Genthner, W. S. Fisher, A rapid tetrazolium dye reduction assay to assess the bactericidal activity of oyster (*Crassostrea virginica*) hemocytes against *Vibrio parahaemolyticus*. *Aquaculture* **172**, 18 (1999).

86. A. K. Volety *et al.*, Responses of oyster *Crassostrea virginica* hemocytes to environmental and clinical isolates of *Vibrio parahaemolyticus*. *Aquatic Microbial Ecology* **25**, 10 (2001).

87. L. Harris-Young, M. L. Tamplin, J. W. Mason, H. C. Aldrich, J. K. Jackson, Viability of Vibrio vulnificus in Association with Hemocytes of the American Oyster (Crassostrea virginica). *Appl. Environ. Microbiol.* **61**, 52 (1995).

88. S. Yoshida, M. Ogawa, Y. Mizuguchi, Relation of capsular materials and colony opacity to virulence of Vibrio vulnificus. *Infect. Immun.* **47**, 446 (1985).

89. L. Smetanova, V. Stetinova, Z. Svoboda, J. Kvetina, Caco-2 Cells, Biopharmaceutics Classification System (BCS) and Biowaiver. *Acta Medica* **54**, 6 (2011).

90. A. Takahashi, T. Iida, R. Naim, Y. Naykaya, T. Honda, Chloride secretion induced by thermostable direct haemolysin of Vibrio parahaemolyticus depends on colonic cell maturation. *J. Med. Microbiol.* **50**, 870 (2001).

91. A. Takahashi, N. Kenjyo, K. Imura, Y. Myonsun, T. Honda, Cl(-) secretion in colonic epithelial cells induced by the vibrio parahaemolyticus hemolytic toxin related to thermostable direct hemolysin. *Infect. Immun.* **68**, 5435 (Sep, 2000).

92. A. Takahashi *et al.*, Haemolysin produced by Vibrio mimicus activates two Cl-secretory pathways in cultured intestinal-like Caco-2 cells. *Cell Microbiology* **9**, 583 (2007).

93. M. Heyman, A. M. Crain-Denoyelle, S. K. Nath, J. F. Desjeux, Quantification of protein transcytosis in the human colon carcinoma cell line CaCo-2. *Journal of Cellular Physiology* **143**, 391 (1990).

94. X. Zhou, M. E. Konkel, D. R. Call, Regulation of type III secretion system 1 gene expression in Vibrio parahaemolyticus is dependent on interactions between ExsA, ExsC, and ExsD. *Virulence* **1**, 260 (2010).

95. X. Zhou, D. H. Shah, M. E. Konkel, D. R. Call, Type III secretion system 1 genes in Vibrio parahaemolyticus are positively regulated by ExsA and negatively regulated by ExsD. *Mol. Microbiol.* **69**, 747 (2008).

96. L. McCarter, Dual Flagellar Systems Enable Motility under Different Circumstances. *Molecular Microbiology and Biotechnology*, 18 (2004).

97. L. McCarter, M. Hilmen, M. Silverman, Flagellar dynamometer controls swarmer cell differentiation of V. parahaemolyticus. *Cell* **54**, 345 (1988).

98. L. McCarter, M. Silverman, Surface-induced swarmer cell differentiation of Vibrio parahaemolyticus. *Mol. Microbiol.* **4**, 1057 (1990).

99. L. L. McCarter, M. E. Wright, Identification of genes encoding components of the swarmer cell flagellar motor and propeller and a sigma factor controlling differentiation of Vibrio parahaemolyticus. *J. Bacteriol.* **175**, 3361 (1993).

100. J. M. Henke, B. L. Bassler, Quorum sensing regulates type III secretion in Vibrio harveyi and Vibrio parahaemolyticus. *J. Bacteriol.* **186**, 3794 (2004).

101. F. Raimondi, J. P. Kao, J. B. Kaper, S. Guandalini, A. Fasano, Calcium-dependent intestinal chloride secretion by Vibrio parahaemolyticus thermostable direct hemolysin in a rabbit model. *Gastroenterology* **109**, 381 (1995).

102. F. B. Abdallah, A. Bakhrouf, A. Ayed, H. Kallel, Alterations of Outer Membrane Proteins and Virulence Genes Expression in Gamma-Irradiated Vibrio parahaemolyticus and Vibrio alginolyticus. *Foodborne. Pathog. Dis.*, (2009).

103. M. L. Chiang, C. C. Chou, Expression of superoxide dismutase, catalase and thermostable direct hemolysin by, and growth in the presence of various nitrogen and carbon sources of heat-shocked and ethanol-shocked Vibrio parahaemolyticus. *Int. J. Food Microbiology* **121**, 268 (2008).

104. S. W. Chiu, S. Y. Chen, H. C. Wong, Localization and expression of MreB in Vibrio parahaemolyticus under different stresses. *Appl. Environ. Microbiol.* **74**, 7016 (2008).

105. F. Coutard, S. Lozach, M. Pommepuy, D. Hervio-Heath, Real-time reverse transcription-PCR for transcriptional expression analysis of virulence and housekeeping genes in viable but nonculturable Vibrio parahaemolyticus after recovery of culturability. *Appl. Environ. Microbiol.* **73**, 5183 (2007).

106. C. J. Gode-Potratz, R. J. Kustusch, P. J. Breheny, D. S. Weiss, L. L. McCarter, Surface sensing in Vibrio parahaemolyticus triggers a programme of gene expression that promotes colonization and virulence. *Mol. Microbiol.* **79**, 240 (2011).

107. Z. Mao, L. Yu, Z. You, Y. Wei, Y. Liu, Cloning, expression and immunogenicty analysis of five outer membrane proteins of Vibrio parahaemolyticus zj2003. *Fish Shellfish Immunology* **23**, 567 (2007).

108. L. L. McCarter, M. Silverman, Phosphate regulation of gene expression in Vibrio parahaemolyticus. *J. Bacteriol.* **169**, 3441 (1987).

109. L. Yang *et al.*, Cold-induced gene expression profiles of Vibrio parahaemolyticus: a time-course analysis. *FEMS Microbiol. Lett.* **291**, 50 (2009).

110. F. L. Thompson, A. A. Neto, O. Santos Ede, K. Izutsu, T. Iida, Effect of N-acetyl-D-glucosamine on gene expression in Vibrio parahaemolyticus. *Microbes and environments* **26**, 61 (2011).

111. D. Wang, S. Yu, W. Chen, D. Zhang, X. Shi, Enumeration of Vibrio parahaemolyticus in oyster tissues following artificial contamination and depuration. *Lett Appl. Microbiol.***51**, 104 (2010).

112. M. J. Chae, D. Cheney, Y. C. Su, Temperature effects on the depuration of Vibrio parahaemolyticus and Vibrio vulnificus from the American oyster (Crassostrea virginica). *J. Food. Sci.* **74**, M62 (2009).

113. L. Croci, E. Suffredini, L. Cozzi, L. Toti, Effects of depuration of molluscs experimentally contaminated with Escherichia coli, Vibrio cholerae 01 and Vibrio parahaemolyticus. *J Appl. Microbiol.***92**, 460 (2002).

114. A. Richardson, S. Fedoroff, *Protocols for Neural Cell Culture 3rd Edition*. (Humana Press, NJ, 1997).

115. Y. Gueguen *et al.*, Immune gene discovery by expressed sequence tags generated from hemocytes of the bacteria-challenged oyster, Crassostrea gigas. *Gene* **303**, 139 (2003).

116. H. Li, M. G. Parisi, M. Toubiana, M. Cammarata, P. Roch, Lysozyme gene expression and hemocyte behaviour in the Mediterranean mussel, Mytilus galloprovincialis, after injection of various bacteria or temperature stresses. *Fish Shellfish Immunology* **25**, 143 (2008).

117. D. A. Foley, T. C. Cheng, A quantitative study of phagocytosis by hemolymph cells of the pelecypods Crassostrea virginica and Mercenaria mercenaria. *J. Invertebr. Pathol.* **25**, 189 (1975).

118. K. Terahara *et al.*, Differences in integrin-dependent phagocytosis among three hemocyte subpopulations of the Pacific oyster "Crassostrea gigas". *Dev. Comp. Immunol.* **30**, 667 (2006).

119. C. Cellura, M. Toubiana, N. Parrinello, P. Roch, Specific expression of antimicrobial peptide and HSP70 genes in response to heat-shock and several bacterial challenges in mussels. *Fish Shellfish Immunology* **22**, 340 (2007).

120. Y. Akeda *et al.*, Dominant-negative Rho, Rac, and Cdc42 facilitate the invasion process of Vibrio parahaemolyticus into Caco-2 cells. *Infect. Immun.* **70**, 970 (2002).

121. Y. Akeda *et al.*, Identification of the Vibrio parahaemolyticus type III secretion system 2-associated chaperone VocC for the T3SS2-specific effector VopC. *FEMS Microbiol. Lett.* **324**, 156 (2011).

122. Y. Akeda, K. Nagayama, K. Yamamoto, T. Honda, Invasive phenotype of Vibrio parahaemolyticus. *J. Infect. Dis.* **176**, 822 (1997).

123. A. Alam, K. A. Miller, M. Chaand, J. S. Butler, M. Dziejman, Identification of Vibrio cholerae type III secretion system effector proteins. *Infect. Immun.* **79**, 1728 (2011).

124. R. N. Bhattacharjee *et al.*, Translocation of VP1686 upregulates RhoB and accelerates phagocytic activity of macrophage through actin remodeling. *J Microbiol. Biotechnol.* **18**, 171 (2008).

125. X. Lian *et al.*, Vibrio parahaemolyticus elevates interferon alpha production in intestinal-like epithelial Caco-2 cells. *Can. J. Microbiol.* **53**, 1084 (2007).

126. T. Shimohata *et al.*, Vibrio parahaemolyticus infection induces modulation of IL-8 secretion through dual pathway via VP1680 in Caco-2 cells. *J. Infect. Dis.* **203**, 537 (2011).

127. T. Tsuchiya, S. Shinoda, Respiration-driven Na+ pump and Na+ circulation in Vibrio parahaemolyticus. *J. Bacteriol.* **162**, 794 (1985).

128. J. V. Holtje, D. Mirelman, N. Sharon, U. Schwarz, Novel type of murein transglycosylase in Escherichia coli. *J. Bacteriol.* **124**, 1067 (1975).

129. T. Tanabe *et al.*, Identification and characterization of genes required for biosynthesis and transport of the siderophore vibrioferrin in Vibrio parahaemolyticus. *J. Bacteriol.* **185**, 6938 (2003).

130. C. N. Peterson, M. J. Mandel, T. J. Silhavy, Escherichia coli starvation diets: essential nutrients weigh in distinctly. *J. Bacteriol.* **187**, 7549 (2005).

131. F. C. Fang *et al.*, The alternative sigma factor katF (rpoS) regulates Salmonella virulence. *Proc. Natl. Acad. Sci. U.S.A.* **89**, 11978 (1992).

132. R. Lange, R. Hengge-Aronis, Identification of a central regulator of stationary-phase gene expression in Escherichia coli. *Mol. Microbiol.* **5**, 49 (1991).

133. T. Atsumi, L. McCarter, Y. Imae, Polar and lateral flagellar motors of marine Vibrio are driven by different ion-motive forces. *Nature* **355**, 182 (1992).

134. C. Xu, H. Ren, S. Wang, X. Peng, Proteomic analysis of salt-sensitive outer membrane proteins of Vibrio parahaemolyticus. *Res Microbiol* **155**, 835 (2004).

135. K. Postle, R. J. Kadner, Touch and go: tying TonB to transport. *Mol. Microbiol.* **49**, 869 (2003).

136. C. J. Gode-Potratz, D. M. Chodur, L. L. McCarter, Calcium and iron regulate swarming and type III secretion in Vibrio parahaemolyticus. *J. Bacteriol.* **192**, 6025 (2010).

137. C. J. Gode-Potratz, L. L. McCarter, Quorum sensing and silencing in Vibrio parahaemolyticus. *J. Bacteriol.* **193**, 4224 (2011).

138. V. Sperandio, J. L. Mellies, W. Nguyen, S. Shin, J. B. Kaper, Quorum sensing controls expression of the type III secretion gene transcription and protein secretion in enterohemorrhagic and enteropathogenic Escherichia coli. *Proc. Natl. Acad. Sci. U.S.A.* **96**, 15196 (1999).

139. J. L. Nordstrom, M. C. Vickery, G. M. Blackstone, S. L. Murray, A. DePaola, Development of a multiplex real-time PCR assay with an internal amplification control for the detection of total and pathogenic Vibrio parahaemolyticus bacteria in oysters. *Appl. Environ. Microbiol.* **73**, 5840 (2007).